

2
0:0

LIBRARY
Michigan State
University

This is to certify that the
dissertation entitled

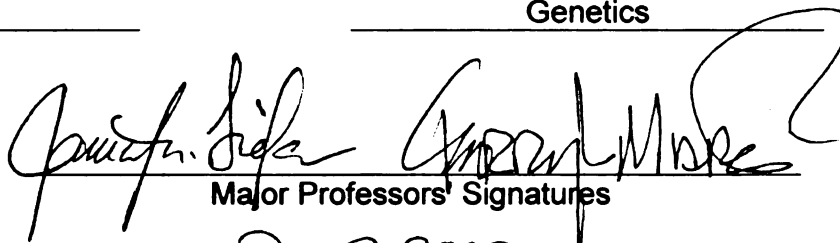
METAL REDUCTION BY
DESULFITOBACTERIUM HAFNIENSE DCB-2

presented by

Christina Lydia Harzman

has been accepted towards fulfillment
of the requirements for the

Ph.D. degree in Microbiology and Molecular
Genetics



Major Professors' Signatures

Dec. 9, 2009

Date

PLACE IN RETURN BOX to remove this checkout from your record.
TO AVOID FINES return on or before date due.
MAY BE RECALLED with earlier due date if requested.

DATE DUE	DATE DUE	DATE DUE

METAL REDUCTION BY
DESULFITOBACTERIUM HAFNIENSE DCB-2

By

Christina Lydia Harzman

A DISSERTATION

Submitted to
Michigan State University
in partial fulfillment of the requirements
for the Degree of

DOCTOR OF PHILOSOPHY

Microbiology and Molecular Genetics

2009

ABSTRACT

METAL REDUCTION BY *DESULFITOBACTERIUM HAFNIENSE* DCB-2

By

Christina Lydia Harzman

I evaluated the ability of the Gram-positive dehalogenator *Desulfitobacterium hafniense* strain DCB-2 to reduce metals and to determine which would support growth as respiratory electron acceptors. Nine metals [As(V), Cd(II), Co(III), Cr(VI), Cu(II), Fe(III), Ni(II), Se(VI and IV), and U(VI)] were used to test growth. Slowed growth was found with 1 mM Cu(II), 1 mM Ni(II), 2.5 mM Se(VI), and 0.5 mM U(VI) and above. While growth was observed with all metals, use of metals as a sole terminal electron acceptor was found only with As(V), Cu(II), and Fe(III), although biomass yield indicated some benefit from Se(VI) and U(VI) as terminal electron acceptors. Valence state analyses detected reduction of As(V to III), Fe(III to II) (provided both as soluble ferric citrate and solid ferric oxide), Se(VI to 0 and IV to 0), and U(VI to IV). While Cu(II) and Co(III) showed the characteristic colors of reduction, changes in their valence state were below detection limits. Extracellular vesicles (containing RNA surrounded by both membrane and cell wall) were produced in response to Se(VI) and Se(IV) by budding from cells. The vesicles but not cells contained reduced Se and appeared to be a protection mechanism from Se toxicity. Both red and black crystalline Se(0) were formed. Microarrays containing probes for *D. hafniense* were used to investigate changes in gene expression when it was grown on nitrate, Fe(III), Se(VI), or U(VI) in comparison

to growth by pyruvate fermentation. Gene expression observed during nitrate reduction can be characterized by two highly induced gene groups annotated for assimilatory sulfate reduction and N₂ fixation-like function by the Nifl operon. The most highly up-regulated genes during Se(VI) reduction were of unknown function. Comparing Fe(III) reduction and U(VI) reduction revealed many genes induced in common, especially those involved with coenzyme metabolism and energy metabolism, e.g. DMSO reductase and NADH dehydrogenase. Genes induced with U(VI) reduction suggested responses to uranium toxicity by rapid replication of DNA and an increase in motility through induction of flagellar genes and chemotaxis. Fe(III) reduction revealed the induction of genes that could produce of large amounts of extracellular material, which was supported by studies that showed Fe(III)-grown cells produced more biofilm on silica and plastic coated beads than cells fermenting pyruvate. Genome analysis and expression studies suggested that this organism may grow as an acetogen, since the acetyl-CoA pathway (Wood-Ljungdahl pathway) was up-regulated during Fe(III) and U(VI) reduction.. Growth studies demonstrated acetogenic growth with 30:30:40 gas combinations of H₂:CO:N₂, H₂:CO₂:N₂ and CO:CO₂:N₂ as the only carbon and energy sources, consistent with using the acetyl-CoA pathway. This pathway is shared with *Moorella thermoacetica*, the closest sequenced acetogenic relative. To test similar physiologies, *D. hafniense* and *M. thermoacetica* were compared for growth and metal reduction. *M. thermoacetica* reduced Se(VI to 0) and As(V to III), but no growth or reduction occurred with soluble Fe(III).

To my parents, Leonard and Barbara

ACKNOWLEDGEMENTS

The author would like to thank her advisors, Professor Terence Marsh and Professor James Tiedje, for support, encouragement and enumerable discussions related to this work. Thanks also go to the other members of the dissertation committee, Professor Julius Jackson for many conversations regarding this research, as well as Professor Robert Britton and Professor David Long. The author also extends her gratitude to Dr. Sang-Hoon Kim and Dr. Shelly Kelly for their collaborations.

TABLE OF CONTENTS

LIST OF TABLES	ix
LIST OF FIGURES.....	x
CHAPTER I	
INTRODUCTION.....	1
OVERVIEW	1
BACKGROUND.....	5
Metals.....	5
Bacterial mediated metal reduction	5
Highly studied systems of bacterial dissimilatory metal reduction.....	7
Desulfitobacteria.....	10
REFERENCES.....	14
CHAPTER II	
Survey of Metal Electron Acceptor Use by <i>Desulfitobacterium hafniense</i> DCB-2	18
ABSTRACT	18
INTRODUCTION.....	19
METHODS	21
Culture conditions	21
Time course measurements.....	22
Yield analyses	23
Calculations.....	24
Metal valence state determination.....	25
RESULTS	26
Fermentative growth with different metals.....	26
Respiration with different metal electron acceptors.....	28
Reduction of metals.....	31
Mineralization of metals by cells	32
Biomass production with different metals	34
Growth yield of cells with metals.....	36
DISCUSSION	38
ACKNOWLEDGEMENTS.....	42
REFERENCES.....	44
CHAPTER III	
Gene Expression of <i>Desulfitobacterium hafniense</i> DCB-2 Exposed to Nitrate, Fe(III), Se(VI), and U(VI) and Proof of Its Acetogenic Growth	46
ABSTRACT	46
INTRODUCTION.....	47
METHODS	49
Bacterial genome sequence	49

Culture conditions	49
RNA extraction, cDNA synthesis and labeling.....	50
Microarray characteristics.....	51
Microarray hybridization and analysis	52
Experimental determination of acetogenic ability.....	53
Culture purity	54
RESULTS and DISCUSSION	55
Pyruvate-fermenting cell metabolism.....	55
Dissimilatory Fe(III)-reducing cell metabolism.....	59
U(VI)-reducing cell metabolism	63
Nitrate-reducing cell metabolism	66
Se(VI)-reducing cell metabolism	69
Nitrogenase activity	72
Determination of an active acetyl-CoA reduction pathway.....	73
Gene expression corresponding to cell morphology differences	76
Conclusions	77
ACKNOWLEDGEMENTS	78
REFERENCES.....	79

CHAPTER IV

Exterior Membrane-Bound Selenium Vesicles Produced by *Desulfitobacterium hafniense*

DCB-2 in Response to Selenate Exposure.....	82
ABSTRACT.....	82
INTRODUCTION.....	83
METHODS	85
Culture conditions	85
Growth	86
Microscopy.....	86
XANES and XRD analyses.....	89
RESULTS	91
Growth in the presence of Se	91
Sphere formation	93
Production of two elemental Se precipitates.....	94
Chronology of spherical, membrane-bound Se vesicles.....	97
DISCUSSION	101
ACKNOWLEDGEMENTS	106
REFERENCES.....	107

CHAPTER V

A Comparison of As(V), Fe(III) and Se(VI) Reduction by the Acetogens

<i>Desulfitobacterium hafniense</i> DCB-2 and <i>Moorella thermoacetica</i>	110
ABSTRACT.....	110
INTRODUCTION.....	110
METHODS	111
Bacterial strains	111
Experimental determination of growth.....	112

Measurements of growth with metals.....	112
RESULTS	113
DISCUSSION	116
ACKNOWLEDGEMENTS.....	117
REFERENCES.....	118
CHAPTER VI	
SUMMARY AND CONCLUSIONS.....	120
APPENDIX A	
Biofilm-Forming Capacities of <i>Desulfitobacterium hafniense</i> DCB-2.....	128
APPENDIX B	
Minimal Medium and Culturing Methods for <i>Desulfitobacterium hafniense</i> DCB-2....	133
APPENDIX C	
Protocols for Selenium Vesicles Isolation from Se-Reducing Cultures of <i>Desulfitobacterium hafniense</i> DCB-2 with RNA and Protein Analyses.....	150

LIST OF TABLES

Table	Page
Chapter I	
Table 1.1. Concentrations of metals used in this study and at NABIR FRC in Oak Ridge, TN.....	12
Chapter II	
Table 2.1. Mineralization of different electron acceptors.....	33
Table 2.2. Effect of electron acceptor concentration and carbon sources on growth yield.....	36
Table 2.3. Effect of different electron acceptor concentrations on growth yield.....	37
Table 2.4. Carbon balance of electron donors (lactate and pyruvate) and yield of cells as C (mMoles).....	38
Chapter III	
Table 3.1. Effect of acetogenic conditions on cell yields of <i>M. thermoacetica</i> and <i>D. hafniense</i>	74
Chapter V	
Table 5.1. Generation times of <i>M. thermoacetica</i> and <i>D. hafniense</i> with metals.....	114
Table 5.2. Se(VI) mineralization ability of <i>M. thermoacetica</i> and <i>D. hafniense</i>	115

LIST OF FIGURES

Images in this dissertation are presented in color.

Figure	Page
Chapter I	
Figure 1.1. Three methods of dissimilatory metal reduction by bacteria (metal shown here is Fe(III) as an example). (A) Direct contact. (B) Extrusion of metal-chelators. (C) Use of electron shuttle type molecules.....	9
Chapter II	
Figure 2.1. Organic acid concentrations in cultures grown fermenting pyruvate in the presence of different metals. Best fit curves and the standard error are shown. All metal concentrations are 1 mM, except Cu(II) at 0.75 mM and U(VI) at 0.5 mM. Cultures were monitored until stationary phase was achieved. (A) Pyruvate consumption over time. (B) Acetate production over time.....	27
Figure 2.2. Generation times of <i>D. hafniense</i> grown with pyruvate under fermentation conditions in the presence of the indicated metals. The generation time with pyruvate fermentation alone (no metal present) is represented as 0.01 mM with each metal. Standard error is shown for all measurements as vertical lines.....	28
Figure 2.3. Organic acid concentrations of cultures incubated with different metal electron acceptors (respiration conditions). Cultures were monitored until stationary phase was achieved. Best fit curves and the standard error are shown. (A) Lactate consumption over time. (B) Acetate production over time.....	30
Figure 2.4. Generation times of <i>D. hafniense</i> during respiration with lactate and different electron acceptors. Standard error is shown for all measurements as vertical lines.....	31

Chapter III

Figure 3.1. Schematic diagram of the key metabolism pathways during fermentation with pyruvate. Menaquinone is abbreviated as “MK”, cytochrome as “cyt”, and phosphoenolpyruvate as “PEP”.....58

Figure 3.2. Schematic diagram of the key metabolism pathways during dissimilatory Fe(III) reduction with lactate. Menaquinone is abbreviated as “MK”, cytochrome as “cyt”, and phosphoenolpyruvate as “PEP”. Green arrows indicate genes similarly expressed as pyruvate fermentation. Red arrows are genes up-regulated (in comparison to pyruvate fermentation) in response to dissimilatory Fe(III) reduction.....62

Figure 3.3. Schematic diagram of the key metabolism pathways during dissimilatory U(VI) reduction with pyruvate. Menaquinone is abbreviated as “MK”, and cytochrome as “cyt”. Green arrows indicate genes similarly expressed as pyruvate fermentation. Red arrows are genes up-regulated (in comparison to pyruvate fermentation) in response to dissimilatory U(VI) reduction.....65

Figure 3.4. Schematic diagram of the key metabolism pathways during nitrate reduction with lactate. Menaquinone is abbreviated as “MK”, cytochrome as “cyt”, adenylyl sulfate as “APS”, and phospho-adenylyl sulfate as “PAPS”. Green arrows indicate genes similarly expressed as pyruvate fermentation. Red arrows are genes up-regulated (in comparison to pyruvate fermentation) in response to nitrate reduction.....68

Figure 3.5. Schematic diagram of the key metabolism pathways during Se(VI) reduction with pyruvate. Menaquinone is abbreviated as “MK”, and cytochrome as “cyt”. Solid green arrows indicate genes similarly expressed as pyruvate fermentation. Red arrows are genes up-regulated (in comparison to pyruvate fermentation) in response to Se(VI) reduction. The vesicle is external in *D. hafniense*, though for simplicity depicted here as internal.....71

Figure 3.6. Induced expression of the genes involved in nitrate reduction and nitrogen fixation (pathways shown at left). Relative induction is shown in grey scales (light to dark; low to high induction). No evidence was found which supports gene expression of nitrate and nitrite reductase genes in pyruvate-fermenting cells. Therefore, relevant cells are shown in white.....72

Figure 3.7. SEM of *D. hafniense* DCB-2 exposed to different electron acceptors. (A) Curved rod morphology during pyruvate fermentation. (B) Curved rod morphology during nitrate respiration. (C) Elongated rod exhibited during U(VI) exposure. (D) Elongated rod with vesicles during growth with Se(VI). (E) Streptobacilli made of shorter rods during Fe(III) respiration. (F) SEM of Fe(III) biomass. White arrow points to cell in G. (G) Backscatter image of Fe(III) biomass from E. White arrow points to cell in F.....76

Chapter IV

Figure 4.1. Growth of *D. hafniense* in sodium selenate medium. (A) Effect of sodium selenate concentration on growth rate: (▲) the zero concentration is displayed as 0.01 to accommodate the log scale. (B) Growth with 1 mM sodium selenate measured by optical density, pyruvate consumption and acetate production. Standard error is shown for all measurements as vertical lines.....92

Figure 4.2. Morphological changes of *D. hafniense* cells when grown under pyruvate fermentation conditions. (A) SEM of a cell grown on pyruvate with no selenium. (B-F) Cells grown with 1 mM selenate. (B) SEM of elongated cells with buds or spheres at 24 h. (C) SEM of cells showing an increase in sphere number and development at 72 h. White arrows in C and E indicate spheres verified to be attached to cells via visible filament connections. (D) SEM of spheres both detached and cell-associated at 72 h. (E) SEM at 72 h of 'beads on a string' (filament with Se spheres). (F) TEM at 72 h of cells surrounded by spheres (very dark circles). Black arrows point to Se spheres where we found Se and lipid-binding osmium predominant around the outer edge. This was confirmed by EDS.....93

Figure 4.3. (A) Se K-edge XANES spectra from sterile selenium medium control (negative control), *D. hafniense* cultures that formed black and red precipitates and the Se metal reference made at the APS at Argonne National Laboratory. The measured spectra for red precipitate are shown as symbols, and the LCF is shown as a line. (B) XRD spectra of red and black selenium precipitates from *D. hafniense* grown in 1 mM sodium selenate compared to the XRD pattern of metallic elemental selenium.....96

Figure 4.4. Representative SEM EDS and TEM EDS mapping of *D. hafniense* cells grown in 1 mM sodium selenate. (A) SEM of Se exposed cell displaying buds and vesicles. (B) SEM backscatter image of A. Arrows indicate regions of the image scanned by EDS. Arrow 1 points to the cell, while arrow 2 points to an associated vesicle. (C) EDS of cell in B at portions indicated by arrows 1 and 2. (D) TEM of hexagonal crystals (cr) and surrounding vesicles (v). (E) TEM backscatter image of hexagonal crystals. (F) TEM of vesicles and cells. Line depicts the TEM EDS line scan through four vesicles and two cells from points 3 to 4. (G) TEM EDS line scan of G illustrating changes in carbon, osmium, and selenium from points 3 to 4 on the line. Locations of the vesicles (v) and cells (c) seen in (F) are represented on the line.....99

Appendix A

Figure A.1. Bright field microscopic images (100× magnification) of beads. (A) Cross-section of a Dupont activated carbon bead showing the thin white plastic surface coating. (B). Side view of a Siran glass bead illustrating its rough surface. (C) Top view of a Siran glass bead showing its deeply pitted surface.....129

Figure A.2. Biofilm cultures with Dupont and Siran beads after 25 medium transfers. (A) Undisturbed (left) and shaken (right) cultures on Siran beads in DCB-1 with pyruvate. (B). Undisturbed (left) and shaken (right) cultures on Dupont beads in DCB-1 with pyruvate. (C) Culture grown on Dupont beads prior to medium transfer (left) and following transfer (right) of fresh ferric citrate medium. (D) Culture grown on Siran beads prior to medium transfer (left) and following transfer of fresh ferric citrate medium. (E) Above view of the biofilm produced by a culture grown on Siran beads in ferric

citrate medium.....	130
---------------------	-----

Appendix B

Figure B.1. Anaerobic inoculation process. (A) The materials necessary for culturing into sterile medium. Only DCB-1 medium is pictured with an anaerobic gas bottle and a bottle dropper of ethanol. The vitamins and carbon source stock bottles are not shown. (B) The position of the hand just prior to removal of the needle from the anaerobic gas bottle is shown. The index finger is on the syringe plunger ready to expel gas to prevent oxygen from coming in the needle. (C) The expelling of the needle contents into a serum bottle. (D) The mixing and measuring of the liquid from a serum bottle for subsequent transfer. The serum bottle is held upside down to obtain the liquid.....145

Figure B.2. Black butyl rubber stoppers with crimped aluminum seals on a specially designed 3-port 1 l flask. These 3-port flasks were used to hold maximally 500 ml anaerobically.....148

Chapter I

INTRODUCTION

OVERVIEW

Metals have played an intimate role in human history from everyday use to technological innovations, arts, communications, and weaponry; however, humans are not the only masters of metallurgy (Nriagu 1996). Long before humans evolved, microbes had found their niche interacting with metals through redox reactions including both oxidative and dissimilatory reduction to gain energy for growth. Presently, there are two dissimilatory metal-reducing model organisms, *Geobacter sulfurreducens* and *Shewanella oniedensis* MR-1 that have been widely studied; however, both are Gram-negative Proteobacteria. Given the central role of the cell membrane in metal reduction, having a model Gram-positive dissimilatory metal-reducing organism is important to further scientific understanding of how energy capture is realized in organisms with a very different cell envelope. This study explores the metal interactions and dissimilatory metal-reducing ability of the Gram-positive bacterium, *Desulfitobacterium hafniense* DCB-2, and its potential role in bioremediation.

The purpose of this research was to investigate the potential of using *D. hafniense* as the first Gram-positive model organism for dissimilatory metal reduction. The guiding hypothesis for this research was that *D. hafniense* is capable of reducing metals for

energy gain through dissimilatory, including respiratory, metal reduction. Additionally, *D. hafniense* is capable of reducing the same metals as have been found to be reduced by model, Gram-negative, metal-reducing organisms.

The main objective of this research was to determine the range of metal-reducing abilities of *Desulfitobacterium hafniense* DCB-2. The specific objectives were:

- to determine the spectrum of metals reduced and which metals support growth by respiratory coupling of metal reduction to energy production.
- to determine whether there are differences in the cell morphology caused by reduction of different metals, and if specific adaptations occurred to aid metal reduction.
- to identify genes and major pathways involved with Fe(III), Se(VI), and U(VI) reduction.

Nine metals were selected for study to represent a broad spectrum of the periodic table with a potential for biological reduction (Chapter 2). Metals surveyed were geochemically diverse and included a pnictogen (i.e. arsenic), a chalcogen (i.e. selenium), an actinide (i.e. uranium), and transition metals (Faure 1991). The nine metals were: the d group metals Cd(II), Co(III), Cr(VI), Cu(II), Fe(III), and Ni(II); the p group metals As(V) and Se(VI); and the f group metal U(VI). These are economically important

metals of concern to human health and to the U.S. Department of Energy for bioremediation (U.S. Geological Survey 2005).

I found that *D. hafniense* reduced As(V), Fe(III), Se(VI), and U(VI), but color change reactions also indicated reduction of Co(III), Cr(VI), and Cu(II) (Chapter 2). Growth with all metals occurred when pyruvate fermentation conditions were provided, but growth did not occur at the same rate. This is consistent with evidence for differing rates of metal reduction by *Shewanella* and *Geobacter* (Liu 2002). Studies on *D. hafniense* and other *Desulfitobacterium* species with As, Fe, Mn, S, and Se had previously reported growth (Christiansen 1996, Venkateswaran 1999, Finneran 2002, Niggemyer 2001, and Shelobolina 2003), but growth via respiratory metal reduction had not been verified. Being able to gain energy from these metal reductions would provide an opportunity for *D. hafniense* to grow specifically on the metal as well as gain energy from fermentation.

I observed morphological differences of cells reducing Fe(III), Se(VI), and U(VI). These cell morphologies were compared to the shape of cells grown by nitrate respiration and pyruvate fermentation (Chapters 3 and 4). The cell morphology observed under dissimilatory metal reduction of U(VI) was an elongation of the cells to 5 μm . This is twice the length of a typical pyruvate-fermenting cell. Dissimilatory metal reduction of Fe(III) produced streptobacilli-type chain growth of short cells. Moreover, Fe was detected in the large amounts of extracellular material produced during Fe(III) reduction (Chapters 2, 3, 4, and Appendix A). Se(VI) reduction yielded elongated cells with extracellular vesicles containing Se. While spheres of Se had been reported previously

(Kessi 1999), I conclusively demonstrated the Se to be in membrane and cell wall-bound vesicles. Negligible amounts of selenium were located in cells and the surrounding matrix; however, the matrix did contain hexagonal crystals of selenium. This is also the first study to demonstrate two different colors of elemental Se precipitate being produced by a single bacterium. The possibility for stages of development in the Se vesicles led to the formulation of a model of Se vesicle development (Chapter 4).

Identifying the genes involved in metal reduction by *D. hafniense* is important as many genes for metal reduction have not yet been identified despite the history of study on the model dissimilatory metal-reducing bacteria *G. sulfurreducens* and *S. oneidensis* MR-1 (Fredrickson 2005). This limitation is in large part due to the fact that most studies involved a gene-by-gene approach (Fredrickson 2005). Only recently have *S. oneidensis* and *G. sulfurreducens* studies transitioned into the whole genome approach, allowing the functional determination of hundreds of genes at once (Beliaev 2005, Bencheikh-Latmani 2005, Gao 2004, and Methé 2004). Moreover, studies of genes involved in metal reduction by Gram-positive organisms are minimal. We found large differences in gene expression amongst pyruvate fermentation, nitrate reduction, and Fe(III) reduction (Chapter 3). U(VI) reduction resulted in similar up-regulated genes as Fe(III) reduction, while in contrast, Se(VI) had many similarities with nitrate reduction. Gene expression supported trends observed in morphology and growth yield studies. To illustrate the functionality of highly expressed genes, the ability of *D. hafniense* to produce biofilm and grow acetogenically were also analyzed (Chapters 3 and Appendix A). Biofilm production was found under all growth conditions presented with varying yields

(Appendix A). Growth of *D. hafniense* as an acetogen was confirmed with combinations of H₂, CO, and CO₂; thus, greatly expanding the breadth of its known metabolic capabilities (Chapter 3). A phylogenetically related organism, *Moorella thermoacetica*, was also tested for reduction of metals under anaerobic growth with lactate, and found to reduce As(V) and Se(VI), but not soluble Fe(III) (Chapter 5).

BACKGROUND

Metals. The terms “metal” and “heavy metal” have been used in a variety of fields to mean different things (e.g. politics, food, health, science, and engineering). For example, these terms can be applied generally to mean elements that are capable of bioaccumulating in plant or animal tissues (Duffus 2002). Elements may also be classified as metals due to causing toxicity effects in organisms, provoking environmental concern, or possessing a specific gravity of at least 4.5 (Duffus 2002). My use of “metals” requires that elements possess a specific gravity greater than 4.5 and fall under the environmentally significant definition of bioaccumulation, toxicity, and human concern. By this definition, both the metalloids As and Se can be included in the term “metals”.

Bacterial mediated metal reduction. Metals may change mobilization potentials (e.g. solubility) by passive or active means. Passive metal mobilization depends upon the physicochemical characteristics surrounding the metal that affects its solubility, such as pH, temperature, water activity, and neighboring materials (physical environment). Passive mobilization does not include environmental influences caused by organisms.

Active metal mobilization requires direct involvement of an organism to mobilize a metal. Active mobilization by bacteria may involve passive or active interactions with metals. Passive interactions of bacteria with metals may include pH, cell wall interactions, ion exchange, or indirect removal associated with exopolysaccharides and H₂S production (Lloyd 2003). Active interactions may include enzymatic reactions, chelation, and metabolism (Lloyd 2003). This metabolism may either oxidize or reduce the metal.

Active metal reduction by bacteria occurs for two reasons. The first is to prevent toxic conditions in the environment surrounding a cell (without energy gain for the cell from the reaction). The second reason is the uptake and transformation of metals to benefit the cell, which occurs via assimilatory and/or dissimilatory metal reduction. Assimilatory metal reduction incorporates metals into a cell, such as to form metalloenzymes. Dissimilatory metal reduction is the use of metals as electron acceptors for energy generation to drive metabolism without the incorporation of the metal. This also includes the use of metals as an electron sink for metabolism. This will prevent a build up of radicals in a cell allowing metabolism to continue.

Three types of dissimilatory metal reduction are known to occur (Luu 2003 and Nevin 2002) (Figure 1.1). The first requires direct contact between the metal and the cell membrane for metal reduction to occur (Figure 1.1A). The second is the production and extrusion of metal-chelating molecules from a cell (Figure 1.1B). These chelated (metal-containing) complexes are then taken up by a cell and the metal is subsequently reduced

within the cell. The third method employs electron shuttle-type molecules (e.g. humic acids) to travel to and indirectly reduce metals (Figure 1.1C). This is the only method that does not involve direct reduction of a metal by a cell. Instead, these electron-shuttle molecules, which are capable of undergoing repetitive oxidation and reduction reactions, provide an intermediate electron acceptor for a cell. These electron shuttle molecules may be environmentally-derived or produced by cells, but they function as an electron intermediate between a metal and a cell.

Highly studied systems of bacterial dissimilatory metal reduction. Studies on dissimilatory metal reduction have centered around two Gram-negatives, *Shewanella* and *Geobacter*. Each genus has more than one member whose genome has been fully sequenced. The focus of research with *Shewanella* has been on *S. oneidensis* MR-1; for *Geobacter* it is *G. sulfurreducens*. Though both are model organisms for dissimilatory metal reduction, most studies have only tested if metals were reduced and not if energy gain occurred. *S. oneidensis* MR-1 (a γ -Proteobacteria) was isolated from sediment at Oneida Lake, New York in 1931 (Venkateswaran 1999). This facultative anaerobe has a polar flagella and reduces a range of compounds, including: fumarate, iodate, nitrate, nitrite, oxygen, sulfite, elemental sulfur, thiosulfate, As(V), Co(III) EDTA, Cr(VI), Fe(III), Mn(IV), Mn(III), Se(VI), Tc(VII), and U(VI) (Venkateswaran 1999). *G. sulfurreducens* (a δ -Proteobacteria) was isolated from an enrichment of iron-reducing bacteria taken from hydrocarbon-contaminated soil near Norman, Oklahoma (Caccavo 1994). This anaerobic rod is non-motile except when expressing flagella in the presence of metal oxides as a chemotactic response to the solid metal (Childers 2002 and Lin

2004). It is capable of reducing elemental sulfur, As(V), Au(III), Cr(VI), Fe(III), Hg(II), Mn(VI), Se(VI), Tc(VII), and U(VI) (Méthé 2003). Neither bacterium ferments sugars or forms spores.

An array of metals are reduced by both *S. oneidensis* and *G. sulfurreducens*; however, they differ in their distinct methods of dissimilatory metal reduction of Fe(III). *G. sulfurreducens* requires direct contact with Fe metals in order to effectively reduce them (Lovley 1993). This is due to the electron shuttle machinery being directly mounted on the cell membrane. Although *S. oneidensis* does also reduce metals via direct membrane contact, it does not require direct contact for Fe reduction as it is able to make use of external electron shuttle-type molecules (e.g. humics) as well as produce electron shuttle-type molecules (e.g. quinones) (Bencharit 2005, Kim 2005, Leang 2003, Lloyd 2003, Luu 2003, Magnuson 2001 and Mehta 2005).

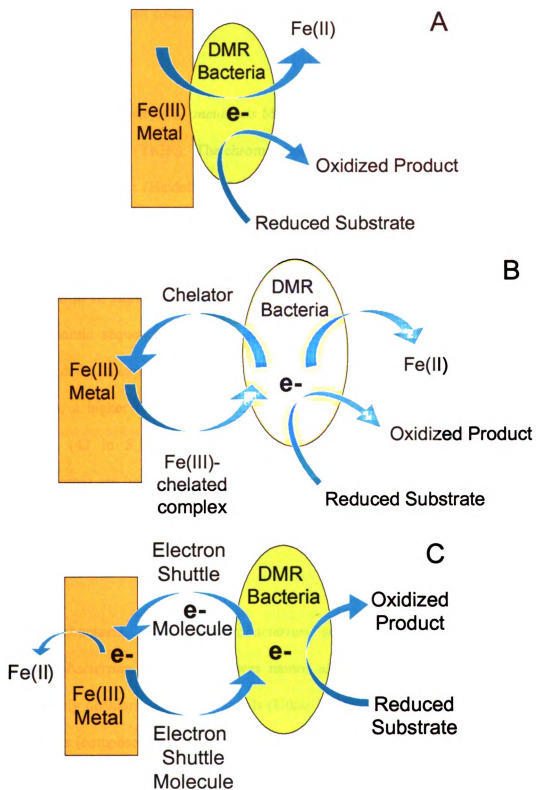


Figure 1.1. Three methods of dissimilatory metal reduction by bacteria (metal shown here is Fe(III) as

an example). (A) Direct contact. (B) Extrusion of metal-chelators. (C) Use of electron shuttle type molecules.

The genome sequence of *S. oneidensis* MR-1 was completed in 2002 by The Institute for Genomic Research (TIGR). The chromosome is 4.97 Mb with a 162 kb plasmid and has 45.9% G-C content (Heidelberg 2002). The *G. sulfurreducens* genome sequence was completed in 2003 by TIGR and contains a 3.81 Mb chromosome with 60.9% G-C content (Methé 2003). There are 4931 predicted protein-encoding genes in *S. oneidensis* and 3466 in *G. sulfurreducens* (Heidelberg 2002 and Methé 2003). Upon obtaining the full genomic sequence for *S. oneidensis* and *G. sulfurreducens*, the genomes were examined for unexplored functions (Fredrickson 2005 and Methé 2003). From these analyses, a higher than expected number of c-type cytochromes were found for both bacteria (42 in *S. oneidensis* and 90 in *G. sulfurreducens*) (Fredrickson 2005). Cytochromes are heme-containing proteins that function as electron carriers in the cell, and are important in shuttling electrons during metal reduction (Beliaev 2001 and Butler 2004).

Desulfitobacteria. The *Desulfitobacterium* genus was established in 1994 when *Desulfitobacterium dehalogenans* was named after being discovered for its ability to reductively dechlorinate chlorophenols (Utkin 1994). Since then, 17 representatives of the genus (composed of six species) have been isolated (Villemur 2006). All members are anaerobic, Gram-positive, slightly curved rods that are motile by one or more flagella (Villemur 2006). Taxonomically falling with the low G-C Clostridia, they reside in the

family Peptococcaceae, order Clostridiales. All desulfitobacteria are capable of fermentative growth using pyruvate to form primarily acetate and CO₂. Desulfitobacteria respire with lactate (electron donor) using nitrate, thiosulfate or sulfite as an electron acceptor to produce ammonia and sulfide. Only *D. chlororespirans* Co23 is unable to respire nitrate (Sanford 1996).

Desulfitobacteria are quite ubiquitous in the environment. They have been found in methanogenic lake sediment (*D. dehalogenans*), tetrachloroethene contaminated soil (*D. hafniense* Y51), compost soil (*D. chlororespirans* Co23), clay soil (*D. hafniense* G-2), and human feces (*D. hafniense* DP-7) (Utkin 1994, Suyama 2001, Sanford 1996, Shelobolina 2003, and van de Pas 2001). A study of soil samples from 44 sites throughout the province of Quebec, Canada found *Desulfitobacterium* species to reside in over 70% of the samples (Lanthier 2001). The *Desulfitobacterium* genus has been documented in Fe(III)-enrichment cultures from rice paddy soil and subsurface sediment as well as in contaminated military base locations (Kostka 2002). One such military site is the aquifer at area 6, Dover Air Force Base, Delaware, which is contaminated with chlorinated solvents such as vinyl chloride and cis-dichloroethene (Davis 2002). *Desulfitobacterium* was also found at the Field Research Center (FRC) at Oak Ridge National Laboratory, Oak Ridge, TN, which is under the jurisdiction of the U.S. Department of Energy (Brooks 2001). It is heavily contaminated with uranium, chromium, technetium, chlorinated solvents such as tetrachloroethylene, and nitric acid (Table 1.1) (Brooks 2001).

Table 1.1. Concentrations of metals used in this study and at NABIR FRC in Oak Ridge, TN

Metal	Abbreviation	Aqueous Phase (mM)	Sludge (ppm or µg/g) dry weight	Study Concentration (mM)
Iron	Fe	1208	92,031	50 mM
Uranium	U	316.57	620	0.5 mM
Nickel	Ni	128	98.8	1 mM
Chromium	Cr	60	163.9	1 mM
Copper	Cu	44	145.3	0.75 mM
Cobalt	Co	1.4	3.3	1 mM
Arsenic	As	0.115	32.5	1 mM
Selenium	Se	0.033	0.02	1 mM
Cadmium	Cd	-	<0.6	1 mM

Source: Brooks 2001.

Two species of *Desulfitobacterium* have been isolated from metal contaminated sites. *D. metallireducens* was cultured from a uranium-contaminated aquifer, which is able to reduce ferric citrate, manganese(IV) oxide, and elemental sulfur (Finneran 2002). However, unlike other members of the genus, *D. metallireducens* does not form spores. *Desulfitobacterium* sp. strain GBFH was enriched from arsenic contaminated lake sediment, and found capable of reducing the metals As(V), Fe(III), Mn(VI), and Se(VI) (Niggemyer 2001). After being isolated from clay soil, *D. hafniense* G-2 was found to reduce Fe(III to II) (Shelobolina 2003).

Since its isolation from municipal sludge in 1992, studies on *Desulfitobacterium hafniense* DCB-2 have largely focused on the spectrum and mechanism of its dehalogenation ability, such as dechlorination of chlorophenols and chloroethenes

(Christiansen 1996 and Madsen 1992). It is an anaerobic, Gram-positive, spore-forming rod, motile by one or two terminal flagella and an optimum growth temperature of 37°C (Christiansen 1996). Besides having been discovered to generate electricity, it is capable of growth by fermentation and respiration with nitrate, nitrite, sulfite, elemental sulfur, thiosulfate, Fe(III), and Mn(IV) (Christiansen 1996, Madsen 1992, and Milliken 2007). Two of my laboratory findings were the ability of *D. hafniense* to grow acetogenically and to produce copious amounts of biofilm under conditions of both pyruvate fermentation and dissimilatory Fe(III) reduction (Chapter 5 and Appendix A).

From sequencing done by the Joint Genome Institute (JGI), *D. hafniense* was found to contain a 5.2 Mb chromosome of 47.5% G-C content with 4715 candidate protein-encoding genes. It is one of only two members to be sequenced from this genus (*D. hafniense* Y-51 has also been sequenced). Scanning the genome for novel functional gene annotations uncovered catalase and superoxide dismutase genes, 43 annotated cytochromes, as well as genes for arsenic reduction, chemotaxis, and bacteriophage. Several genes for membrane transport systems for Co, Cu, Fe, Mn, and Ni were also found.

REFERENCES

- Beliaev, A. S., D. M. Klingeman, J. A. Klappenbach, L. Wu, M. F. Romine, J. M. Tiedje, K. H. Nealson, J. K. Fredrickson, and J. Zhou.** 2005. Global transcriptome analysis of *Shewanella oneidensis* MR-1 exposed to different terminal electron acceptors. *J. Bacteriol.* 187:7138-7145.
- Beliaev, A. S., D. A. Saffarini, J. L. McLaughlin, and D. Hunnicutt.** 2001. MtrC, an outer membrane decahaem c cytochrome required for metal reduction in *Shewanella putrefaciens* MR-1. *Mol. Microbiol.* 39:722-730.
- Bencharit, S. and M. J. Ward.** 2005. Chemotactic responses to metals and anaerobic electron acceptors in *Shewanella oneidensis* MR-1. *J. Bacteriol.* 187:5049-5053.
- Bencheikh-Latmani, R., S. Middleton Williams, L. Haucke, C. S. Criddle, L. Wu, J. Zhou, and B. M. Tebo.** 2005. Global transcriptional profiling of *Shewanella oneidensis* MR-1 during Cr(VI) and U(VI) reduction. *Appl. Environ. Microbiol.* 71:7453-7460.
- Brooks, S. C.** 2001. Waste characteristics of the former S-3 ponds and outline of uranium chemistry relevant to NABIR Field Research Center studies. NBIR Field Research Center, Oak Ridge, TN.
- Butler, J. E., F. Kaufmann, M. V. Coppi, C. Nunez, and D. R. Lovley.** 2004. MacA, a diheme c-type cytochrome involved in Fe(III) reduction by *Geobacter sulfurreducens*. *J. Bacteriol.* 186:4042-4045.
- Caccavo, Jr., F., D. J. Lonergan, D. R. Lovley, M. Davis, J. F. Stoly, and M. J. McInerney.** 1994. *Geobacter sulfurreducens* sp. nov., a hydrogen- and acetate- oxidizing dissimilatory metal-reducing microorganism. *Appl. Environ. Microbiol.* 60:3752-3759.
- Childers, S. E., S. Ciufo, and D. R. Lovley.** 2002. *Geobacter metallireducens* accesses insoluble Fe(III) oxide by chemotaxis. *Nature.* 416:767-769.
- Christiansen, N. and F. K. Ahring.** 1996. *Desulfitobacterium hafniense* sp. nov., anaerobic, reductively dechlorinating bacterium. *Int. J. Syst. Bacteriol.* 46:442-448.
- Davis, J. W., J. M. Odom, K. A. Deweerd, D. A. Stahl, S. S. Fishbain, R. J. West, G. M. Klecka, and J. G. DeCarolis.** 2002. Natural attenuation of chlorinated solvents at Area 6, Dover Air Force Base: characterization of microbial community structure. *J. Contam. Hydrol.* 57:41-59.
- Duffus, J. H.** 2002. "Heavy metal" - a meaningless term? (IUPAC Technical Report). *Pure App. Chem.* 74:793-807.
- Faure, G.** Principles and Applications of Inorganic Geochemistry, MacMillan Publishing Co.: New York, 1991.

Finneran, K. T., H. M. Forbush, C. V. Van Praagh, and D. R. Lovley. 2002. *Desulfitobacterium metallireducens* sp. nov., an anaerobic bacterium that couples growth to the reduction of metals and humic acids as well as chlorinated compounds. *Int. J. Syst. Evol. Microbiol.* 52:1929-1935.

Fredrickson, J. K. and M. F. Romine. 2005. Genome-assisted analysis of dissimilatory metal-reducing bacteria. *Curr. Opin. Microbiol.* 16:1-6.

Gao, H., Y. Wang, X. Liu, T. Yan, L. Wu, E. Alm, A. Arkin, D. K. Thompson, and J. Zhou. 2004. Global transcriptome analysis of the heat shock response of *Shewanella oneidensis*. *J. Bacteriol.* 186:7796-7803.

Heidelberg, J. F., I. T. Paulsen, K. E. Nelson, E. J. Gaidos, W. C. Nelson, T. D. Read, J. A. Eisen, R. Seshadri, N. Ward, B. Methé, R. A. Clayton, T. Meyer, A. Tsapin, J. Scott, M. Beanan, L. Brinkac, S. Daugherty, R. T. DeBoy, R. J. Dodson, A. S. Durkin, D. H. Haft, J. F. Kolonay, R. Madupu, J. D. Peterson, L. A. Umayam, O. White, A. M. Wolf, J. Vamathevan, J. Weidman, M. Impraim, K. Lee, K. Berry, C. Lee, J. Mueller, H. Khouri, J. Gill, T. R. Utterback, L. A. McDonald, T. V. Feldblyum, H. O. Smith, J. C. Venter, K. H. Nealson, and C. M. Fraser. 2002. Genome sequence of the dissimilatory metal ion-reducing bacterium *Shewanella oneidensis*. *Nature Biotech.* 20:1118-1123.

Kessi, J., M. Ramuz, E. Wehrli, M. Spycher, and R. Bachofen. 1999. Reduction of selenite and detoxification of elemental selenium by the phototrophic bacterium *Rhodospirillum rubrum*. *Appl. Environ. Microbiol.* 65:4734-4740.

Kim, B. C., C. Leang, Y. H. Ding, R. H. Glaven, M. V. Coppi, and D. R. Lovley. 2005. OmcF, a putative *c*-type monoheme outer membrane cytochrome required for the expression of other outer membrane cytochromes in *Geobacter sulfurreducens*. *J. Bacteriol.* 187:4505-4513.

Kostka, J. E., D. D. Dalton, H. Skelton, S. Dollhopf, and J. W. Stucki. 2002. Growth of iron(III)-reducing bacteria on clay minerals as the sole electron acceptor and comparison of growth yields on a variety of oxidized iron forms. *Appl. Environ. Microbiol.* 68:6256-6262.

Lanthier, M., R. Villermur, F. Lépine, J. Bisailon, and R. Beaudet. 2001. Geographic distribution of *Desulfitobacterium frappieri* PCP-1 and *Desulfitobacterium* spp. in soils from the province of Quebec, Canada. *FEMS Microbiol Ecol.* 36:185-191.

Leang, C., M. V. Coppi, and D. R. Lovley. 2003. OmcB, a *c*-type polyheme cytochrome, involved in Fe(III) reduction in *Geobacter sulfurreducens*. *J. Bacteriol.* 185:2096-2103.

Lin, W. C., M. V. Coppi, and D. R. Lovley. 2004. *Geobacter sulfurreducens* can grow with oxygen as a terminal electron acceptor. *Appl. Environ. Microbiol.* 70:2525-2528.

Liu, C. Y. A. Gorby., J. M. Zachara, J. K. Fredrickson, and C. F. Brown. 2002. Reduction kinetics of Fe(III), Co(III), U(VI), Cr(VI), and Tc(VII) in cultures of dissimilatory metal-reducing bacteria. *Biotech. Bioengin.* 80:637-649.

Lloyd, J. R. 2003. Microbial reduction of metals and radionuclides. *FEMS. Microbiol. Rev.* 27:411-425.

Lloyd, J. R., C. Leang, A. L. Hodges Myerson, M. V. Coppi, S. Ciuffo, B. Methé, S. J. Sandler, and D. R. Lovley. 2003. Biochemical and genetic characterization of PpcA, a periplasmic *c*-type cytochrome in *Geobacter sulfurreducens*. *Biochem. J.* 369(1):153-161.

Lovley, D. R. 1993. Dissimilatory metal reduction. *Annu. Rev. Microbiol.* 47:263-290.

Luu, Y.-S. and J. A. Ramsay. 2003. Review: microbial mechanisms of accessing insoluble Fe(III) as an energy source. *World J. Microbiol Biotech.* 19:215-225.

Madsen, T. and D. Licht. 1992. Isolation and Characterization of an anaerobic chlorophenol-transforming bacterium. *Appl. Environ. Micro.* 58:2874-2878.

Magnuson, T. S., N. Isoyama, A. L. Hodges-Myerson, G. Davidson, M. J. Maroney, G. G. Geesey, and D. R. Lovley. 2001. Isolation, characterization and gene sequence analysis of a membrane-associated 89 kDa Fe(III)-reducing cytochrome *c* from *Geobacter sulfurreducens*. *Biochem. J.* 359:147-152.

Mehta, T., M. V. Coppi, S. E. Childers, and D. R. Lovley. 2005. Outer membrane protein *c*-type cytochromes required for Fe(III) for Fe(III) and Mn(IV) oxide reduction in *Geobacter sulfurreducens*. *Appl. Environ. Microbiol.* 71:8634-8641.

Methé, B. A., K. Webster, K. P. Nevin, J. E. Butler, and D. R. Lovley. 2004. DNA microarray analysis of nitrogen fixation and Fe(III) reduction in *Geobacter sulfurreducens*. *Appl. Environ. Microbiol.* 71:2530-2538.

Methé, B. A., K. E. Nelson, J. A. Eisen, I. T. Paulsen, W. Nelson, J. F. Heidelberg, D. Wu, M. Wu, N. Ward, M. J. Beanan, R. J. Dodson, R. Madupu, L. M. Brinkac, S. C. Daugherty, R. T. DeBoy, A. S. Durkin, M. Gwinn, J. F. Kolonay, S. A. Sullivan, D. H. Haft, J. Selengut, T. M. Davidsen, N. Zafar, O. White, B. Tran, C. Romero, H. A. Forberger, J. Weidman, H. Khouiri, T. V. Feldblyum, T. R. Utterback, S. E. Van Aken, D. R. Lovley, and C. M. Fraser. 2003. Genome of *Geobacter sulfurreducens*: metal reduction in subsurface environments. *Science.* 302:1967-1969.

Milliken, C. E. and H. D. May. 2007. Sustained generation of electricity by the spore-forming, Gram-positive, *Desulfitobacterium hafniense* strain DCB2. *Appl. Microbiol. Biotechnol.* 73:1180-1189.

Nevin, K. P., and D. R. Lovley. 2002. Mechanisms for accessing insoluble Fe(III) oxide during dissimilatory Fe(III) reduction by *Geothrix fermentans*. Appl. Environ. Microbiol. 68(5):2294-2299.

Niggemyer, A., S. Spring, E. Stackebrandt, and R. F. Rosenzweig. 2001. Isolation and characterization of a novel As(V)-reducing bacterium: implications for arsenic mobilization and the genus *Desulfitobacterium*. Appl. Environ. Microbiol. 67:5568-5580.

Nriagu, J. O. 1996. A history of global metal pollution. Science. 272:223-224.

Posey, J. E. and F. C. Gherardini. 2000. Link of role for iron in the Lyme disease pathogen. Science. 288:1651-1653.

Sanford, R. A., J. R. Cole, F. E. Löffler, and J. M. Tiedje. 1996. Characterization of *Desulfitobacterium chlororespirans* sp. nov., which grows by coupling the oxidation of lactate to the reductive dechlorination of 3-chloro-4-hydroxybenzoate. Appl. Environ. Microbiol. 62:3800-3808.

Shelobolina, E. S., C. G. VanPraagh, and D. R. Lovley. 2003. Use of ferric and ferrous iron containing minerals for respiration by *Desulfitobacterium frappieri*. Geomicrobiol. J. 20:143-156.

Suyama, A., R. Iwakiri, K. Kai, T. Tokunaga, N. Sera, and K. Furukawa. 2001. Isolation and characterization of *Desulfitobacterium* sp. strain Y51 capable of efficient dehalogenation of tetrachloroethene and polychloroethanes. Biosci. Biotechnol. Biochem. 65:1474-1481.

Utkin, I., C. Woese, and J. Wiegel. 1994. Isolation and characterization of *Desulfitobacterium dehalogenans* gen. nov., sp. nov., an anaerobic bacterium which reductively dechlorinates chlorophenolic compounds. Int. J. Syst. Bacteriol. 44:612-619.

U.S. Geological Survey, Mineral Commodities Summaries, January 2005.

van de Pas, B. A., H. J. Harmsen, G. C., Raangs, W. M. de Vos, G. Schraa, and A. J. Stams. 2001. A *Desulfitobacterium* strain isolated from human feces that does not dechlorinate chloroethenes or chlorophenols. Arch. Microbiol. 175:389-394.

Venkateswaran, K., D. P. Moser, M. E. Dollhopf, D. P. Lies, D. A. Saffarini, B. J. MacGregor, D. B. Ringelberg, D. C. White, M. Nishijima, H. Sano, J. Burghardt, E. Stackebrandt, and K. H. Nealson. 1999. Polyphasic taxonomy of the genus *Shewanella* and description of *Shewanella oneidensis* sp. nov. Int. J. Syst. Bacteriol. 49:705-724.

Villemur, R., M. Lanthier, R. Beaudet, and F. Lépine. 2006. The *Desulfitobacterium* genus. FEMS Microbiol. Rev. 30:706-733.

Chapter II

Survey of Metal Electron Acceptor Use by *Desulfitobacterium hafniense* DCB-2

ABSTRACT

Metal reduction has largely been studied in Gram-negative bacteria where reduction pathways are localized in the cell membrane. Here, we report the metal reduction capabilities of a Gram-positive dehalogenator, *Desulfitobacterium hafniense* strain DCB-2. Cultures were grown in liquid media with nine different metals as potential electron acceptors. Growth was unaffected with Cr(VI), Cd(II) and < 1 mM of Cu(II) and Ni(II). Growth rate was enhanced with 0.05 mM Co(III) and all tested concentrations of As(V) as well as concentrations of ≤ 1 mM Se(VI). Growth was depressed in the presence of higher concentrations of Cu(II), Ni(II), Se(VI), and all concentrations of U(VI). Growing cultures reduced soluble Fe(III), U(VI), As(V), and Se(VI) to insoluble products and solubilized solid Fe(III). The growth yield per e^- transferred was highest with Fe(III) followed by U(VI), Se(VI), and As(V), all with cell yields above fermentation alone. The carbon balance of cultures grown with Fe(III) showed much higher carbon in cells and soluble extracellular products than provided from the substrate carbon. *D. hafniense* most likely is using the citrate chelate used to supply the Fe(III) along with some carbon fixation from the acetyl-CoA pathway as the source of the extra carbon. The results show *D. hafniense* can gain energy for growth, i.e. respiration, with reduction of Fe(III), nitrate, and As(V), some energy benefit from U(VI) and Se(VI)

reduction, reduction of Cr(VI), Co(III) and Cu(II) but no significant energy benefit, and no reduction of Cd(II) and Ni(II).

INTRODUCTION

Metals are naturally abundant within the environment, but they can attain toxic concentrations as a result of mining, manufacturing, waste disposal, and other human activities, resulting in potential hazards to human health (Järup 2003). Maximizing bioremediation of environments contaminated with metals may be enhanced by understanding the bacteria performing the desired task. Bacterial interactions with metals have involved both *in vitro* and *in situ* studies (Lovley 1993). Controlled conditions of *in vitro* studies are critical to provide information on basic requirements for the desired reduction under *in situ* conditions.

Determining the spectrum of metal redox ability of a bacterium provides information of how the organism interacts with metals and allows inferences to be made with other related organisms. Bacteria appear to reduce metals for three reasons: to prevent metal toxicity, to assimilate and incorporate a metal into cells for metabolic use, and to obtain energy through dissimilatory metal reduction (Lovley 1993 and Methé 2004). Metal reduction by bacteria has been reported for arsenic, chromium, cobalt, copper, iron, selenium, uranium and other metals (Lloyd 2003, Stolz 2002). Many studies of metal reduction by cultivated bacteria have used media supplemented with yeast extract and other complex nutrients, complicating the interpretation of the impact of metals on bacterial growth. Few metal reduction studies have examined in a comparative study one

bacterium's ability to reduce a spectrum of metals in one publication, and these that have were performed with Gram-negative organisms. As many of these reduction pathways have been found to localize in the membranes of Gram-negative bacteria, here we have chosen to study metal reduction in Gram-positive *Desulfitobacterium hafniense* DCB-2 (Liu 2002, Lovley 2002 and 1993).

D. hafniense possesses many qualities that should prove beneficial to bioremediation, such as the ability to form biofilms and possessing a terminal flagella for responding to chemotactic responses it detects (Appendix A). Having been isolated as a dehalogenator respiring chlorophenol, *D. hafniense* has been traditionally studied for its ability to dehalogenate (Madsen 1992). It is a spore-former able to survive harsh conditions such as acidification that often accompanies metal contamination, and was shown to grow with and reduce Fe(III) and Mn(IV) (Christiansen 1996). The presence of an As(V) reduction pathway and ability to reduce (As) was discovered by Niggemyer (2001), but result interpretation of this study is complicated by the inclusion of yeast extract in the medium. Moreover, the reduction products and the effect on cell growth were not reported in both studies. *D. hafniense* has been found at the Field Research Site, Oak Ridge National Laboratory (Oak Ridge, TN), which is heavily contaminated with U and Cr (Kostka 2002). The full range of contaminating metals that this bacterium is capable of reducing has not been determined. In this report, we explore the ability of *D. hafniense* in minimal media to reduce nine different metals, including whether they enhance or inhibit growth, their valence state and ligand binding. The metals are: As(V), Cd(II), Cr(VI), Co(III), Cu(II), Fe(III), Ni(II), Se(VI), and U(VI). This provides the first broad view of

interactions a Gram-positive bacterium has with a spectrum of metals.

METHODS

Culture conditions. For facilitated electron acceptor and metal toxicity analyses, *D. hafniense* was cultured in a modified DCB-1 medium containing 20 mM sodium pyruvate (pyruvate) (Löffler 1996 and Chapter 4). For dissimilatory metal reduction analyses, a modified carbonate-buffered freshwater (CBF) medium containing 20 mM sodium lactate (lactate) was used with metals provided as the sole electron acceptor. Modified CBF medium consisted of (per liter): 0.25 g NH_4Cl , 0.1 g KCl , 10 ml mineral mix, 0.6 g $\text{NaH}_2\text{PO}_4 \times \text{H}_2\text{O}$, 2.5 g NaHCO_3 (to buffer medium to pH 7), and 0.25 mg resazurin (Lovley 1988). For CBF medium, salts and trace elements were mixed, heated and cooled under $\text{CO}_2:\text{N}_2$ (20:80) (Miller 1974). This medium was then dispensed and autoclaved for 20 min. Modified DCB-1 medium was cooled under a gas mixture of $\text{CO}_2:\text{N}_2$ (5:95). Using strict anaerobic technique, 1 \times Wolin vitamins (Wolin 1963), the carbon source, and a metal electron acceptor from separate sterilized stock solutions were added prior to inoculation (Tschech 1984, Widdel 1983). The following metal salts were each tested separately in DCB-1 and CBF media: sodium arsenate, sodium selenate, sodium selenite, cupric chloride, cupric sulfate, ferric citrate (CBF only), ferric oxide (CBF only), nickel(II) chloride, cobalt(III) chloride, cadmium(II) chloride, and uranyl acetate. Ferric citrate medium was made using CBF medium with 50 mM ferric citrate being added prior to salts, lactate and vitamins as described above (Lovely 1996). The controls were medium with metal without bacteria, medium without metals inoculated

with a live culture, medium with metals and heat-killed bacteria inoculated as a cell pellet, and a heat-killed culture to which metals were then added. None of the controls displayed evidence of metal reduction in any measurement taken.

Time course measurements. Following prescreening for growth in the metal condition, a minimum of 20 biological replicates were measured per condition over time. Inoculated cultures were incubated at 37°C in 1 l anaerobic bottles with side-arm tubes attached to allow for optical density measurements without removing culture. Optical density at 600 nm was obtained by mixing and inverting bottles such that culture in the side-arm tubes could be read using a Spectronic 20D spectrophotometer (Milton Roy, Rochester, NY). Samples were aseptically removed in an anaerobic glove box of H₂:N₂ (4:96) at the start of the experiment and every 12 h thereafter for organic acid analysis as monitored by HPLC, colony counts, color change over time, and microscopy (Chapter 4). Samples from each time point were also frozen at -20°C for further analyses. Samples were no longer taken once the culture reached stationary phase. Time point samples for HPLC were filtered through a 0.45 µm filter prior to run on the HPLC to measure acetate, pyruvate, and lactate as described in Chapter 4. Time point samples of all cultures were inoculated in triplicate onto R2A supplemented with 10 mM pyruvate in an anaerobic glove box of H₂:N₂ (4:96). The plates were incubated at 25°C for 10-12 days prior to counting colonies.

The state of metal reduction was initially inferred (and later confirmed with XANES

data) based on color changes of the cultures. Color change reactions of metal reduction are: clear to red/black for Se, clear to yellow for As, burnt orange to brown to olive green to yellow for Fe, yellow to clear to green/gray to dark brown for U, blue to green to yellow to brown for Cu, purple to pink to clear to brown for Co, clear to bright yellow for Cd, and green to clear to brown for Ni.

Morphology was observed using light microscopy with methylene blue or Gram stain, scanning electron microscopy (SEM), SEM energy dispersive spectroscopy (SEM EDS), transmission electron microscopy (TEM), and TEM energy dispersive spectroscopy (TEM EDS) (Chapter 4). Culture purity was determined throughout the study by fluorescent *in situ* hybridization (FISH) with Cy5-labeled, *D. hafniense*-specific rDNA probe (Lanthier 2001) and DAPI staining (Bloem 1995).

Yield analyses. TOC analysis was performed with all samples on the last time point of the growth curves to determine the mass and carbon balance of the metal reducing reactions. Medium controls without cells were also processed as were additional controls without cells but with metal electron acceptor added. Of the controls with metal electron acceptor added, only the Fe(III) citrate CBF medium control without cells had background levels of organic carbon, and thus is the only metal medium control reported here. Additional replicate cultures in Fe(III) citrate had the initial pellet and supernatant processed separately to aid in biomass analysis.

Prior to submission for TOC analysis, three replicate frozen culture samples were thawed

and pelleted by spinning at 2000 g for 30 min. The supernatant was decanted and mixed with two volumes of 95% ethanol and spun at 2000 g for 30 min to precipitate small soluble extracellular polymeric substances. The two pellets from each sample from the two centrifugations were combined, flash frozen in liquid nitrogen and freeze-dried at -45°C. Tin 5 × 9 mm capsules (Costech, CA) were filled with homogenized freeze-dried culture, compacted, sealed, and shipped for TOC analysis at the UC Davis Stable Isotope Facility (Davis, CA).

ICP-MS was used to determine the solution phase concentrations of As(V), Co(III), Cu(II), Fe(III), Ni(II), Se(VI), and U(VI) (each with five biological replicates) using a PerkinElmer Optima 4300DV inductively coupled plasma optical emission spectrometer (ICP-OES) using the following parameters: air as the shear gas, argon plasma phase at a flow rate of 17 mL min⁻¹, 0.2 mL min⁻¹ auxiliary gas flow, 0.6 mL min⁻¹ nebulizer gas flow, and 1.5 mL min⁻¹ sample aspiration rate. Frozen samples were thawed and spiked with Y as an internal standard, and run in triplicate. Using a CCD detector, metal concentrations were read at 193.696 nm for As, 228.615 nm for Co, 327.394 nm for Cu, 238.201 nm for Fe, 231.604 nm for Ni, 196.026 nm for Se, 385.962 nm for U, and 371.029 nm for Y.

Calculations. Generation time was calculated using cell count data. The slopes of colony counts over time were determined for each sample replicate. Two points in the steepest portion used to calculate doubling time. These doubling times for sample

replicates were then averaged to determine the generation time and standard error for each medium. Confidence intervals of 95% can be determined using: average \pm 1.96 \times standard error.

The rate of organic acids consumption (e.g. pyruvate and lactate) and production (e.g. acetate) were calculated using the slopes of the organic acid concentration over time for each sample replicate. The slope of the line between two points in the steepest portion of the “log phase” slope was calculated. These two point slopes were then averaged to calculate the rate of consumption or production of the organic acids for each sample condition.

Carbon balances were determined based on 20 mM pyruvate or lactate substrate and measured organic acids and biomass produced. The biomass data was obtained by TOC analysis, which was converted to mmol C assuming the biomass is $C_5H_7O_2N$.

Metal valence state determination. The reduction status of the metal in the biomass samples was examined using x-ray absorption near edge structure (XANES) analysis. Samples were prepared in an anaerobic glove box of $N_2:H_2$ (95:5) to prevent metal oxidation (Chapter 4). The K-edge XANES of all metal measurements were made at beamline locations MRCAT 10-ID (Segre 2000) and PNC-CAT 20-BM at the Advanced Photon Source at Argonne National Laboratory (Argonne, IL). At MRCAT, the insertion device was tapered, and the Si(III) double crystal monochromator was slew scanned.

Several EXAFS measurements in transmission mode were averaged for each sample. The incident ionization chamber was filled with N₂, and the transmission ionization chamber was filled with Ar:N₂ (50:50) for metals. A Rh mirror was used to remove harmonic x-rays. The x-ray beam incident on the sample was 1 mm × 1 mm. The beamline parameters were similar at PNC-CAT 20-BM to MRCAT, where the Si(III) monochromator was detuned 15% to enhance harmonic rejection, and scans were collected in step scanning mode in fluorescence using a thirteen element Ge solid state detector. The same elemental metal standard was used for each run of the same element. The XANES spectra were processed using Athena (Ravel 2005) and IFEFFIT software (Newville 2001). The spectra were aligned to each other and the reference spectra. Multiple scans from the same sample were merged to increase the data quality.

RESULTS

Fermentative growth with different metals. *D. hafniense* grew in DCB-1 fermenting pyruvate to acetate in the presence of all eight metals. Greater consumption of pyruvate occurred in the presence of all metals compared to no metal present, except for 1 mM Se(VI) (Figure 2.1A). The fastest consumption of pyruvate occurred with As(V). The acetate production balanced pyruvate consumption for all conditions except with U(VI) (Figure 2.1B). With 0.5 mM U(VI), less acetate was produced over time. As the U(VI) was added as uranyl acetate, this amount of acetate was subtracted. The fastest and highest carbon consumption and production curves were in the presence of 1 mM As(V).

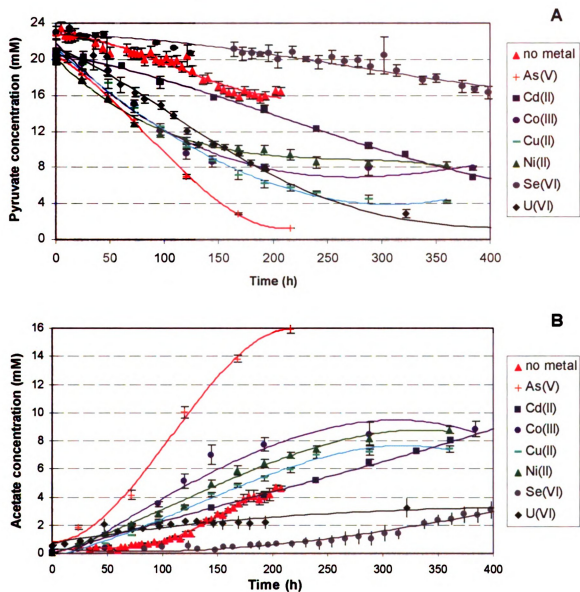


Figure 2.1. Organic acid concentrations in cultures grown fermenting pyruvate in the presence of different metals. Best fit curves and the standard error are shown. All metal concentrations are 1 mM, except Cu(II) at 0.75 mM and U(VI) at 0.5 mM. Cultures were monitored until stationary phase was achieved. (A) Pyruvate consumption over time. (B) Acetate production over time.

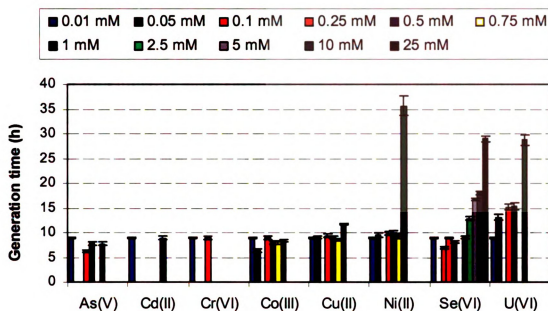


Figure 2.2. Generation times of *D. hafniense* grown with pyruvate under fermentation conditions in the presence of the indicated metals. The generation time with pyruvate fermentation alone (no metal present) is represented as 0.01 mM with each metal. Standard error is shown for all measurements as vertical lines.

The time required for *D. hafniense* to double was 8.9 h when grown with pyruvate alone (Figure 2.2 -shown as 0.01). This generation time was unaffected in the presence of Cd(II), Cr(VI), or Co(III), except with 0.05 mM Co(III) it was faster. At all concentrations, As(V) provided for a faster generation time, 6 to 7.8 h. Generation time was unaffected with increasing concentrations of Cu(II) or Ni(II) up to 1 mM, after which the generation time increased significantly to 12 and 36 h respectively. This may be due to concentration dependent metal toxicity effects on the cells. Concentrations of Se(VI) at 0.1 mM decreased generation time, but concentrations of 2.5 mM Se(VI) and above caused a significantly increased generation time to 13 h or more. Longer generation times than pyruvate alone were also found in the presence of all concentrations of U(VI)

tested.

Respiration with different metal electron acceptors. Lactate can not be fermented by *D. hafniense*, but it can serve as an electron donor for respiration that produces acetate (Christiansen 1996). As cultures incubated with lactate alone have no change in the amount of lactate (20 mM) consumed or acetate produced over time, cultures with a non-metal electron acceptor (nitrate) and lactate were monitored as a respiration control to which Fe(III), As(V) or Cu(II) with lactate were compared (Fig 2.3A). Growth was visible in all these conditions. Lactate consumption rates were fastest in the medium with Fe(III); however, acetate production rates were similar for both Fe(III) and nitrate over time. Lactate consumption decreased in the presence of As(V) (1:2.5) and Cu(II) (1:3.6) compared to nitrate. Acetate production mirrored lactate consumption for nitrate, Fe(III) and Cu(II). An increased lag in acetate production was present with As(V) (Figure 2.3B). These trends were reflected in the generation time with each metal (Figure 2.4). Fe(III) and nitrate provided similar generation times at 4.5 and 4.6 h respectively. A marked increase in generation time occurred with As(V) (7 h) and Cu(II) (27 h).

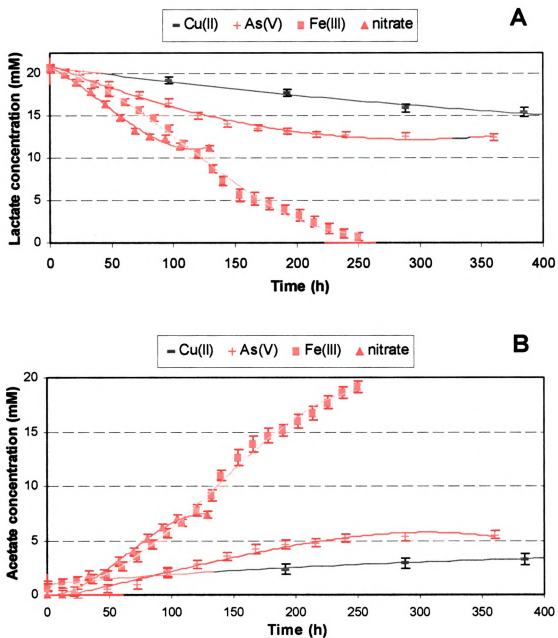


Figure 2.3. Organic acid concentrations of cultures incubated with different metal electron acceptors (respiration conditions). Cultures were monitored until stationary phase was achieved. Best fit curves and the standard error are shown. (A) Lactate consumption over time. (B) Acetate production over time.

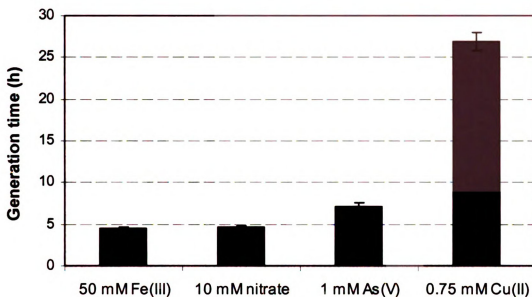


Figure 2.4. Generation times of *D. hafniense* during respiration with lactate and different electron acceptors. Standard error is shown for all measurements as vertical lines.

Reduction of metals. Change in the oxidation state of metals after growth in DCB-1 and CBF media was determined by XAS (data not shown). While reduction of Cd(II), Co(III), Cu(II) and Ni(II) was not found with either medium, the ligand bound to the metal was altered, producing color changes of precipitate [Ni(II), green turned clear; Co(III), purple to clear; Cd(II), clear to yellow; Cu(II), blue to green to clear]. Although reduction was below detection limits with XAS, the change in color observed in cultures with Co(III) is characteristic of conversion to Co(II) in previous studies (Roh 2002). Reduction in both media of U(VI to IV), As(V to III), and Se(VI to 0) was detected by XAS. Solid Fe(III) oxide and soluble Fe(III) citrate were also reduced [Fe(III to II)] by cells in CBF medium with lactate. Reduction of Cr(VI) was not assayed by XAS because reduction of the metal was observed by color and occurred within minutes of addition to

cultures, a character noted in other studies (Roh 2002).

Mineralization of metals by cells. Mineralization (removal of metals from solution) was determined by ICP-MS in the presence of live and heat-killed cells for both media, reported as means of five biological replicates (Table 2.1). When presented with a solid Fe(III) oxide, live cultures solubilized Fe, likely to more easily make use of it as an electron acceptor. An increasing mineralization of soluble Fe(III) citrate was found as further reduction occurred simultaneously with the color changing process of Fe(III to II) reduction by cells (Table 2.1). Passive metal interactions were not observed for cultures with Fe. Cells did not appear to influence mineralization for Cu or Co regardless of medium as all changes were within the margin of error (Table 2.1). Cultures with Ni(II), regardless of medium produced passive mineralization of Ni by cells; similar results were found for live and heat-killed cultures. Live cultures demonstrated substantial mineralization with As and Se with little passive effect by heat-killed cultures. Similar to Se, U was virtually eliminated from solution by active cell cultures; however, passive interactions by heat-killed cultures may account for nearly half of the loss of soluble U.

Table 2.1. Mineralization of different electron acceptors.

Electron acceptor	Medium	EA concentration (mM)	EA in solution (ppm)	% EA in solution versus nc
As (V) nc	DCB-1	1	70.6	100
As (V) hk	DCB-1	1	66.2	93.9
As (V) cells	DCB-1	1	26.2	37.1
As (V) nc	CBF	1	68.6	100
As (V) cells	CBF	1	34.7	50.6
Co (III) nc	DCB-1	1	18	100
Co (III) cells	DCB-1	1	17.4	96.7
Cu (II) chloride nc	CBF	0.75	3.25	100
Cu (II) chloride cells	CBF	0.75	3.38	104
Cu (II) sulfate nc	CBF	0.75	7.34	100
Cu (II) sulfate cells	CBF	0.75	8.16	111
Fe (III) oxide nc	CBF	50	0.874	100
Fe (III) oxide cells	CBF	50	32	3660
Fe (III) citrate nc	CBF	50	2790	100
Fe (III) citrate cells (brown)	CBF	50	968	34.7
Fe (III) citrate cells (black)	CBF	50	823	29.5
Fe (III) citrate cells (olive)	CBF	50	788	28.2
Fe (III) citrate cells (yellow)	CBF	50	760	27.2
Ni (II) nc	DCB-1	1	24.4	100
Ni (II) hk	DCB-1	1	18.2	74.6
Ni (II) cells	DCB-1	1	16.9	69.3
Ni (II) nc	CBF	1	7.5	100
Ni (II) cells	CBF	1	4.92	65.6
Se (VI) nc	DCB-1	1	78.1	100
Se (VI) hk	DCB-1	1	76.5	97.9
Se (VI) cells	DCB-1	1	0.18	0.23
U (VI) (acetate) nc	DCB-1	0.5	92	100
U (VI) (acetate) hk	DCB-1	0.5	52.80	57.4
U (VI) (acetate) cells	DCB-1	0.5	0.41	0.446

nc = negative control (metal present without cells)

hk = heat-killed cells

cells = live cultures

Biomass production with different metals. Total organic carbon (TOC) was reported as a mean of 18 measurements for all culture conditions in order to determine the effect of metals on biomass yield (Table 2.2). Fermentation of pyruvate alone produced equivalent amounts of biomass as in the presence of Cd(II), indicating that Cd had no influence on growth of cells. Increased biomass was found with both Cu(II) and Co(III); however, Ni(II) dramatically decreased biomass production. Increasing amounts of Se(VI) in the culture resulted in increased biomass production by cells. Similar yields were found with addition of either 1 mM Se(VI) or 1 mM Se(IV). The presence of 1 mM As(V) nearly doubled biomass production by cells. *D. hafniense* was previously determined to be unable to ferment acetate (Christiansen 1996). Here, we report growth with acetate alone, which yields 72% less biomass than pyruvate fermentation (Table 2.2). This is further exemplified by an increase in biomass yield with pyruvate fermentation supplemented with acetate compared to pyruvate. To determine if the acetate in cultures with U(VI) was potentially enhancing growth, uranyl acetate was provided as the sole carbon source. Significant biomass production was found with uranyl acetate alone (8.36 mg/L), which was 40% and 13.5% the amount of biomass produced when uranyl acetate was with lactate and pyruvate respectively (Table 2.2).

Unable to ferment lactate, background biomass levels of culture inocula could be determined in CBF medium with lactate alone (Table 2.2) (Christiansen 1996). Significant biomass production was found in the presence of all metals tested: Fe(III), As(V), Co(III), Cu(II), and U(VI) (Table 2.2). Dramatic increases in biomass were seen with 1 mM Cu(II), 1 mM As(V), 50 mM Fe(III), and 0.5 mM and higher U(VI). Only

Fe(III) citrate CBF medium without cells produced complexes with ethanol. This background was quite high at 12.9% of the total biomass produced when Fe(III) citrate medium was inoculated. The amount of biomass produced by growth with Fe(III) was 1330 mg/ L, which is 38 fold higher than the next highest biomass in CBF medium [10 mM U(VI)]. However, only 17% \pm 1% of that biomass is from the pelleted sample.

Growth yield of cells with metals. Growth yield was determined with six metals [U(VI), Fe(III), Ni(II), Co(III), As(V), and Se(VI)] (Table 2.3). Fe(III) was the most efficiently mineralized metal for the amount of carbon produced with an 8-fold higher growth yield per e^- . Growth yields per e^- were similar for pyruvate with Se(VI) and U(VI) in DCB-1, and As(V) in CBF with lactate. These were 20% or higher yields than with pyruvate fermentation alone, which was 0.97 M of carbon per e^- . In contrast, cultures in DCB-1 with pyruvate and As(V) or Co(III) had 20% less growth yield than pyruvate alone (Table 2.3). The measured difference in cultures with As(V) and pyruvate or lactate appears to indicate a change in metal mineralization efficiency and biomass dependent not only on the number of e^- available, but also on the electron donor source.

Table 2.2. Effect of electron acceptor concentration and carbon sources on biomass yield.

Electron Acceptor	EA concentration (mM)	Medium	Carbon source (20 mM)	Biomass produced mg/ L
-	-	DCB-1	pyruvate	15.1
As (V)	1	DCB-1	pyruvate	28.3
Cd (II)	1	DCB-1	pyruvate	15.1
Co (III)	1	DCB-1	pyruvate	19.4
Cu(II) Cl	1	DCB-1	pyruvate	17.1
Ni (II)	1	DCB-1	pyruvate	6.74
Se (VI)	0.5	DCB-1	pyruvate	16.4
Se (VI)	1	DCB-1	pyruvate	18.8
Se (VI)	5	DCB-1	pyruvate	22.2
Se (VI)	10	DCB-1	pyruvate	37.1
Se (IV)	1	DCB-1	pyruvate	18.5
-	-	CBF	lactate	0.295
As (V)	1	CBF	lactate	32.1
Co (III)	1	CBF	lactate	2.25
Cu(II) Cl	0.5	CBF	lactate	3.75
Cu(II) Cl	1	CBF	lactate	22.9
Fe (III) (citrate) nc*	50	CBF	lactate	198
Fe (III) (citrate)	50	CBF	lactate	1530
-	-	DCB-1	pyruvate	15.1
-	-	DCB-1	pyruvate + acetate	18.3
-	-	DCB-1	acetate	4.22
U (VI) (acetate)	0.5	DCB-1	-	8.36
U (VI) (acetate)	0.05	DCB-1	pyruvate	21.2
U (VI) (acetate)	0.5	DCB-1	pyruvate	61.7
-	-	CBF	lactate	0.295
U (VI) (acetate)	0.25	CBF	lactate	4.65
U (VI) (acetate)	0.5	CBF	lactate	21.2
U (VI) (acetate)	1	CBF	lactate	21.8
U (VI) (acetate)	5	CBF	lactate	40.6
U (VI) (acetate)	10	CBF	lactate	35.3

nc = no cells

* control condition to account for C complexes formed with Fe(III) citrate and ethanol

Table 2.3. Effect of different culture conditions and electron acceptor concentrations on growth yield

Electron Acceptor (EA)	Medium	Initial EA amount (mM)	EA in solution (ppm)	EA solution/ control %	Carbon source (20 mM)	Biomass produced mg C / L	Biomass/ metal in solution (ppm) ratio	Carbon source consumption (mM)	Acetate production (mM)	EA loss/ C consumption %	Growth yield biomass/ C provided (g/mol)	Growth yield C/ H+ provided (M)
As (V)	DCB-1	1	26.2	37.1	pyruvate	28.3	1.080	18.5	15.4	2.4	1.51	0.76
As (V)	CBF	1	34.7	50.6	lactate	47.2	1.36	7.6	3.8	4.46	6.21	1.24
Co (III)	DCB-1	1	17.4	96.7	pyruvate	19.4	1.12	12.3	8.7	0.049	1.58	0.79
Fe (III) citrate	CBF	50	760	27.2	lactate	1330*	1.75	19.95	18.5	102	66.7	13.3**
Ni (II)	DCB-1	1	16.9	69.3	pyruvate	6.74	0.399	11.7	8.1	0.64	0.58	0.29
Se (VI)	DCB-1	1	0.18	0.23	pyruvate	18.8	104	7	4.4	11.1	2.68	1.34
U (VI) (acetate)	DCB-1	0.5	0.41	0.446	pyruvate	61.7	151	19.6	3.1	4.67	3.15	1.58

*This is the biomass produced by cultures only. As Fe(III) citrate medium forms precipitating complexes upon ethanol addition, this has been accounted for here.

**Over 70% of growth yield has conclusively been determined to be soluble biomass.

Table 2.4. Carbon balance of electron donors (lactate and pyruvate) and yield of cells as C (mMoles)

Electron acceptor	Substrate/ electron donor	C from substrate equivalent	Yield of C (mMoles)				
			Lactate	Pyruvate	Acetate	Cell biomass	Additional Carbon
no metal	pyruvate	60	0	49.5	9.29	1.26	-0.05
Fe(III)	lactate	60*	2.22	0	38.2	111	-94.4
Se(VI)	pyruvate	60	0	49.2	9.28	1.56	-0.04

*Citrate is also a possible weak substrate, though not measured in a our studies.

The calculated carbon balances show that 99.9% of all carbon can be accounted for during pyruvate fermentation without metals and pyruvate fermentation with Se(VI) reduction (Table 2.4). Table 2.4 data are derived from means of eighteen biological replicates for organic acids and 5 biological replicates for cell biomass per condition. The bulk of carbon remains as pyruvate in these conditions. However, growth in CBF medium with lactate and Fe(III) citrate demonstrated a severe lack of carbon substrate to account for the carbon yield (Table 2.4).

DISCUSSION

The ability of *D. hafniense* to remove soluble metal electron acceptors was determined in cultures fermenting pyruvate or with lactate as the substrate which could require respiration of the metal for growth. Growth in the presence of all metals was achieved; however, depressed generation times were found with 1 mM Cu(II) and 1 mM Ni(II), which is illustrated in the lowered biomass yields and growth rates with Ni(II). This is surprising as weak respiration of Cu(II) with lactate was observed as well as characteristic color changes though Cu(II) was not detected to be reduced by XAS. These longer generation times may be due to concentration dependent metal toxicity

effects on cells. In contrast, Co(III) addition to pyruvate fermenting cultures produced more biomass and a faster generation time than pyruvate fermentation alone. Weak biomass production was also detected during respiration with Co(III). While reduction of Co(III) EDTA has been reported previously (Gorby 1998), reduction of Co(III) chloride was not detected by XAS in this study. Cd(II) was not reduced by pyruvate-fermenting cultures nor did the metal appear to significantly impact growth; this is similar to previously observed results with *M. thermoacetica* (Cunningham 1993).

Metals that were reduced included U(VI), Se(VI), As(V), and Fe(III). Despite reducing Se(VI to 0) and U(VI to IV), 2.5 mM and above Se(VI), and all concentrations of U(VI) significantly slowed generation times of pyruvate fermenting cultures. Disproportionate production of extracellular organic carbon or rapid, incomplete cell division may explain the larger biomass yields accompanying the slowed generation times.

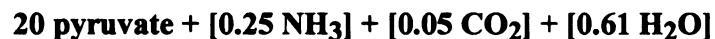
A larger amount of biomass was produced and mineralization efficiency was enhanced consistently in cultures respiring metals with lactate. The largest biomass production by 38 fold was measured during Fe(III) citrate respiration. Previous reports have also found large productions of biomass in response to soluble Fe(III) reduction, such as with the thermophilic, Fe-oxidizing bacteria (Bridge 1998). However, the provided lactate substrate is not enough carbon to account for the large carbon yield. This carbon can easily be accounted for if only a third of the citrate from Fe(III) citrate is used as a carbon source. However, as no previous reports found citrate as a carbon source for *D. hafniense* despite its use in medium (Christiansen 1996), citrate is not likely a strong carbon source.

We also found evidence of growth with acetate, a substrate also not reported to suggest growth (Table 2.2). As the amount of acetate is so high in the Fe(III) citrate condition, it may serve as a carbon source. Recent work demonstrating acetogenic ability by *D. hafniense* has been observed in cultures containing 30% CO₂ (Chapter 3). In this study, 20% CO₂ was present in respiration conditions, so CO₂ fixation is a potential source for carbon substrate. But the biomass contribution of CO₂ fixation is not sufficient to cover the negative net carbon yield, as we found the biomass produced by acetogenically growing *D. hafniense* to be over 300 fold less than what we found here with Fe(III) citrate and lactate (Chapter 3). Further studies would be necessary to determine that it is a combination of carbon resources (lactate, citrate, carbon dioxide, and possibly an increasing acetate pool) that greatly enable biomass production by *D. hafniense* with Fe(III). While the growth yield from citrate provided as Fe(III) citrate should also be measured to determine its role, a combination of carbon resources likely account for the carbon balance discrepancy found.

Large production of soluble extracellular polymeric substances was also found with Fe(III) citrate cultures. High amounts of soluble extracellular organic carbon production have also been reported to occur during halo-respiration of trichloroethene (Ayala-del-Río, 2002). Contributing over 70% of the biomass in *D. hafniense* with Fe(III) citrate, this soluble fraction may facilitate Fe(III) reduction; however, further tests will need to be done to determine the role of such significant soluble biomass production.

Enhanced growth yield and a faster generation time were observed in the presence of As(V). This study confirms that previously discovered As(V) reduction genes in *D. hafniense* are functional with the ability to reduce As(V to III) and use it as a sole terminal electron acceptor (Niggemyer 2001). Genes for the full reduction of As(V to 0) in *D. hafniense* are present and the reaction has a higher energy yield; however, here we found a preference for only partial reduction. This is important for bioremediation as As(III) is more mobile than As(V), unless bound to sulfide (Laverman 1995).

Clear evidence exists of the ability of *D. hafniense* to grow using metal electron acceptors. Lactate alone can not be fermented, but in the presence of metals it was readily respired to acetate, showing that the metals must be serving as the terminal electron acceptors. Even during fermentation with pyruvate faster growth rates and enhanced biomass production were seen with most metals. The carbon balances during pyruvate fermentation and pyruvate fermentation during Se(VI) reduction account for virtually all carbon. Assuming the biomass as C₅H₇O₂N, the equation for the carbon balance of pyruvate fermentation without metal can be written as (things not measure in brackets):



This is the first large study on a Gram-positive species exposed to a broad array of metal

electron acceptors. *D. hafniense* is capable of obtaining energy through fermentation and respiration, including both halorespiration and metalorespiration (Madsen 1992 and Christiansen 1996). Electron acceptors for respiration include: sulfite (not sulfate), thiosulfite, nitrate, nitrite, arsenate, selenate, selenite, Fe(III), U(VI), and halogenated compounds, such as chlorophenols and tetrachloroethene (Villemur 2006). This organism is also able to tolerate high concentrations of potentially toxic metals before exhibiting declining growth. Determining an array of usable metal electron acceptors for an organism is of importance to furthering knowledge of the organism's role not only in the environment in which it was found but for applications, such as in bioremediation through mineralization and reduction of compounds toxic to plants and animals. The ability of *D. hafniense* to grow in the presence of Cr(VI) and reduce U(VI) with large biomass production present the possibility of its niche at Oak Ridge National Laboratory (Oak Ridge, TN) as a desired metal-reducer. This study also not only provides a new organism to study the various pathways of metal reduction, but this organism is Gram-positive. Many of these pathways have been extensively studied in Gram-negative organisms, and many proteins have been found to localize to the cell membrane (Lovley 1993 and Schröder 1997). Due to the difference in outer membrane, it is possible that having a Gram-positive model organism for metal reduction may lead to the discovery of different redox proteins and pathways involved in metal reduction.

ACKNOWLEDGEMENTS

Funding for this study was provided by the U.S. Department of Energy, Office of Science, Environmental Remediation Science and Genomes to Life Programs. Research

at the Advanced Photon Source at Argonne National Laboratory (Argonne, IL) was supported by the U.S. Department of Energy, Office of Science, Office of Basic Energy Sciences, under Contract No DE-AC02-06CH11357. The assistance of Dr. Shelly Kelly was greatly appreciated during beamline studies and performing XAS analyses at Argonne National Laboratory. The equipment operation and collection of ICP-MS data was performed by Dr. Ed O'Loughlin of the Molecular Environmental Science Group in the Biosciences Division at Argonne National Laboratory for which we are grateful.

REFERENCES

- Ayala-del-Río, H. L.** 2002. Long-term effects of phenol and phenol plus trichloroethene application on microbial communities in aerobic sequencing batch reactors. Ph.D. dissertation. Michigan State University, East Lansing.
- Bloem, J.** 1995. Fluorescent staining of microbes for total counts. In: Akkermans A.D.L., Elsas J.D., Bruijn F.J. (eds), *Molecular Microbial Ecology Manual*. Kluwer Academic Press, Dordrecht, The Netherlands, pp. 1-12.
- Bridge, T. and D. B. Johnson.** 1998. Reduction of soluble iron and reductive dissolution of ferric iron-containing minerals by moderately thermophilic iron-oxidizing bacteria. *Appl. Environ. Microbiol.* 64:2181-2186.
- Christiansen, N. and F. K. Ahring.** 1996. *Desulfitobacterium hafniense* sp. nov., anaerobic, reductively dechlorinating bacterium. *Int. J. Syst. Bacteriol.* 46:442-448.
- Cunningham, D. P. and L. L. Lundie Jr.** 1993. Precipitation of cadmium by *Clostridium thermoaceticum*. *Appl. Environ. Microbiol.* 59:7-14.
- Gorby, Y., F. Caccavo, Jr., and H. Bolton, Jr.** 1998. Microbial Reduction of cobalt^{III} EDTA⁻ in the presence and absence of manganese(VI) oxide. *Environ. Sci. Technol.* 32:244-250.
- Järup, L.** 2003. Hazards of heavy metal contamination. *Brit. Med. Bull.* 68:167-182.
- Kostka, J. E., D. D. Dalton, H. Skelton, S. Dollhopf, and J. W. Stucki.** 2002. Growth of iron(III)-reducing bacteria on clay minerals as the sole electron acceptor and comparison of growth yields on a variety of oxidized iron forms. *Appl. Environ. Microbiol.* 68:6256-6262.
- Lanthier, M., R. Villemur, F. Lepine, J-G. Bisailon, and R. Beaudet.** 2001. Geographic distribution of *Desulfitobacterium frappieri* PCP-1 and *Desulfitobacterium* spp. in soils from the province of Quebec, Canada. *FEMS Micro. Ecol.* 36:185-191.
- Laverman, A. M., J. S. Blum, J. K. Schaefer, E. J. P. Phillips, D. R. Lovley, and R. S. Oremland.** 1995. Growth of strain SES-3 with arsenate and other diverse electron acceptors. *Appl. Environ. Microbiol.* 61:3556-3561.
- Liu, C. Y., A. Gorby, J. M. Zachara, J. K. Fredrickson, and C. F. Brown.** 2002. Reduction kinetics of Fe(III), Co(III), U(VI), Cr(VI), and Tc(VII) in cultures of dissimilatory metal-reducing bacteria. *Biotech. Bioeng.* 80:637-649.
- Löffler, F. E., R. A. Sanford, and J. M. Tiedje.** 1996. Initial characterization of a reductive dehalogenase from *Desulfitobacterium chlororespirans* Co23. *Appl. Environ. Microbiol.* 62:4982-4985.

- Lovley, D. R.** 2002. Dissimilatory metal reduction: from early life to bioremediation. *Amer. Soc. Microbiol. News.* 68:231-237.
- Lovley, D. R.** 1993. Dissimilatory metal reduction. *Annu. Rev. Microbiol.* 47:263-290.
- Lovley, D. R. and E. J. P. Phillips.** 1988. Novel mode of microbial energy metabolism: organic carbon oxidation coupled to dissimilatory reduction of iron or manganese. *Appl. Environ. Microbiol.* 54:1472-1480.
- Madsen, T. and D. Licht.** 1992. Isolation and characterization of an anaerobic chlorophenol-transforming bacterium. *Appl. Environ. Microbiol.* 58:2874-2878.
- Méthé, B. and C. M. Fraser.** 2004. Roll with the flow: microbial masters of redox chemistry. *Trends in Microbiol.* 12:439-441.
- Miller, T. L. and W. J. Wolin.** 1974. A serum bottle modification of the Hungate technique for cultivating obligate anaerobes. *Appl. Microbiol.* 27:985-987.
- Niggemyer, A., S. Spring, E. Stackebrandt, and R. F. Rosenzweig.** 2001. Isolation and characterization of a novel As(V)-reducing bacterium: implications for arsenic mobilization and the genus *Desulfitobacterium*. *Appl. Environ. Microbiol.* 67:5568-5580.
- Ravel, B. and M. Newville.** 2005. ATHENA, ARTEMIS, HEPHAESTUS: data analysis for X-ray absorption spectroscopy using IFEFFIT. *J. Synch. Rad.* 12:537-541.
- Roh, Y., S. V. Liu, G. Li, H. Huang, T. J. Phelps, and J. Zhou.** 2002. Isolation and characterization of metal-reducing *Thermoanaerobacter* strains from deep subsurface environments of the Piceance Basin, Colorado. *Appl. Environ. Microbiol.* 68:6013-6020.
- Schröder, I., S. Rech, T. Kralft, and J. M. Macy.** 1997. Purification and characterization of the selenate reductase from *Thauera selenatis*. *J. Biol. Chem.* 272:23765-23768.
- Segre, C. U., N. E. Leyarovska, L. D. W. M. Lavender, P. W. Plag, A. S. King, A. J. Kropf, B. A. Bunker, K. M. Kemner, P. Dutta, R. S. Druan, and J. Kaduk.** 2000. The MRCAT insertion device beamline at the advanced photon source. *Synch. Rad. Inst. CP521*:419-422.
- Stolz, J. F., P. Basu, and R. S. Oremland.** 2002. Microbial transformation of elements: the case of arsenic and selenium. *Int. Microbiol.* 5:201-207.
- Villemur, R., M. Lanthier, R. Beaudet, and F. Lépine.** 2006. The *Desulfitobacterium* genus. *FEMS Microbiol. Rev.* 30:706-733.
- Wolin, E. A., R. S. Wolfe, and M. J. Wolin.** 1963. Viologen dye inhibition of methane formation by *Methanobacillus omelianskii*. *J. Bacteriol.* 87:993-998.

Chapter III

Gene Expression of *Desulfitobacterium hafniense* DCB-2 Exposed to Nitrate, Fe(III), Se(VI), and U(VI) and Proof of Its Acetogenic Growth

ABSTRACT

The ability of the Gram-positive, dehalogenator *Desulfitobacterium hafniense* DCB-2 to reduce a broad spectrum of metals has only recently been discovered. Despite extensive research, pathways responsible for metal reduction remain poorly understood. Gram-negatives have been the primary focus of these gene studies, with results indicating much of the metal-reduction is membrane associated. The genome sequence of *D. hafniense* has recently been completed lending itself to gene expression studies with microarrays. To better understand metal-reduction by *D. hafniense*, analysis of the genome, transcriptome and physiology were combined. Metal-reducing conditions of Fe(III), Se(VI) and U(VI) were compared to pyruvate fermentation and NO_3^- respiration. Results show that *D. hafniense* can greatly shift its metabolism in response to these metals. Interestingly, nitrate reducing-conditions did not induce the annotated nitrate reduction pathway in *D. hafniense* above levels during pyruvate fermentation. Instead, despite the large amount of available nitrate, the annotated nitrogen fixation pathway was induced. Three general patterns of expression appear when similarities in gene expression and the number of electrons available for reduction were compared. These similarities were:

Fe(III to II) and U(VI to IV); NO_3^- (to NH_4) and Se(VI to 0); and pyruvate fermentation with a unique pattern of expression. Morphological observations reflect gene expression, such as the short rods in chains surrounded by copious amounts of extracellular biomass exhibited during Fe(III) reduction. The data also supports the presence of an active acetyl-CoA reduction pathway (Wood-Ljungdahl pathway) in *D. hafniense* DCB-2. The three patterns of expression differ in their induction levels of the acetyl-CoA reduction pathway with Fe and U inducing the pathway most. This is likely due to the necessity of cells to rid themselves of excess electrons, and the decreased electron accepting capacity with Fe and U compared to the other groups. Studies *in vitro* with *D. hafniense* in mixtures of H_2 , CO_2 , and CO confirm it can grow as an acetogen.

INTRODUCTION

The use of bacteria to immobilize or degrade toxic compounds, such as metals, radionuclides and chlorinated solvents, through bioremediation has been proposed and put into practice at several U.S. Department of Energy sites (Gorby 1994, Rilely 1992, Rooney-Varga 1999). At these sites, genomic studies through phylogenetic and functional genome arrays *in situ* have compiled an immense amount of data, but it is difficult to decipher which organisms (other than the target study organism) are performing the desired redox tasks for remediation within the given environment. Only a few representative bacteria have been studied for their ability to reduce desired contaminants, making optimization of a desired bioremediation difficult.

Controlled *in vitro* studies to determine reduction capabilities of different bacteria and their gene expression is one method to solve this problem. Gene expression studies of a greater diversity of bacterial species allows for better comparisons to *in situ* conditions and provides more opportunity for detailed monitoring and optimization of the desired bioremediation. Genomic studies of whole-genome microarray expression profiles on a single bacterial species grown with different electron acceptors, such as metals, have focused largely on Gram-negative organisms. Much of their redox machinery has been found to be membrane associated, thus a study of the gene expression profile of a Gram-positive bacterium is warranted (Lovley 1993a).

Desulfitobacterium hafniense DCB-2 is a recently sequenced anaerobic Gram-positive dehalogenator also capable of metal reduction (Christiansen 1996, Madsen 1992, Chapter 2). Using molecular analyses, *D. hafniense* has been found in both pristine environments and environments highly contaminated with uranium, chromium, and nitrate (Kostka 2002, Lanthier 2001). Current studies have found that besides iron and manganese, this bacterial species is capable of reducing arsenic, selenium, and uranium (Madsen 1992, Niggemyer 2001, Chapter 2). Here we performed expression studies with *D. hafniense* in the presence of different potential electron acceptors, including NO_3^- , Fe(III), Se(VI), and U(VI). Toxicity and redox pathways of the anaerobic organism were examined for each electron acceptor. Following expression analysis, gene studies confirmed the presence of an active acetyl-CoA reduction pathway (Wood-Ljungdahl pathway).

METHODS

Bacterial genome sequence. *D. hafniense* strain DCB-2 was originally isolated from municipal sludge in Copenhagen, Denmark, using a chlorophenol enrichment (Madsen 1992). Its genome has been sequenced by the U.S. Department of Energy's Joint Genome Institute and annotated by the automated pipeline operated by Oak Ridge National Laboratory's Computational Genomics Group, but at the time of microarray development for this paper the genome was at 10× coverage (August 11, 2005). The latest sequence and annotation analysis for *D. hafniense* DCB-2 may be found at http://genome.jgi-psf.org/draft_microbes/desha/desha.home.html.

Culture conditions. For all studies, *D. hafniense* was inoculated into medium following autoclave sterilization and addition of 1× Wolin vitamins (Wolin 1963), the test compound, and a carbon source. Iron reduction studies used modified ferric citrate medium containing 50 mM ferric citrate (Lovely 1988, Chapter 2) with 20 mM sodium lactate (lactate) added. Modified DCB-1 medium (Löffler 1996, Chapter 4) was used for selenium and uranium studies with 1 mM sodium selenate, and 500 µM uranyl acetate, added with vitamins and a sole carbon source of 20 mM sodium pyruvate (pyruvate). Carbonate-buffered freshwater medium (CBF) (Lovely 1988, Chapter 2) was made with 10 mM nitrate, Wolin vitamins, and 20 mM lactate as the sole carbon source. As a positive control, *D. hafniense* was also grown in modified DCB-1 medium with only 20 mM pyruvate and Wolin vitamins to which all cultures were compared during hybridization and microarray analyses.

Cultures were incubated at 37°C to mid-logarithmic phase as monitored by HPLC and optical density, correlating data to a previously derived standard curve of growth that monitored total colony forming units, HPLC, color change, and optical density (Chapters 2 and 4). While both black and red precipitates were produced by *D. hafniense* in the presence of sodium selenate (Chapter 4), only red precipitate-producing cultures were examined in this study. Scanning electron microscopy (SEM) and transmission electron microscopy (TEM) were used to observe differences in cell morphology among culture conditions with a minimum of 20,000 cells viewed per condition (Chapter 4).

RNA extraction, cDNA synthesis and labeling. In triplicate, cell cultures were harvested at mid-log phase by centrifugation under anaerobic conditions with the pellet suspended in RNA Protect (QIAGEN, Valencia, CA) at room temperature with a 45 min lysozyme digestion. RNA was extracted from the cell pellet using an RNeasy RNA extraction kit (QIAGEN) according to the manufacturer's instructions with the DNase digestion step included. RNA quality was tested by running a 1× FA gel containing 0.74% formaldehyde and 1.2% agarose, and RNA concentration was determined using a UV-spectrophotometer at OD₂₆₀.

Direct amino-allyl labeling was performed as according to a protocol of The Institute for Genomic Research (TIGR) <http://www.tigr.org/tdb/microarray/protocolsTIGR.shtml>. Total RNA (5 µg) was denatured by incubation at 70°C for 10 min in the presence of 0.4 mM Random Hexamer Primers (Invitrogen, Carlsbad, CA) and snap-cooled 10 min on ice. cDNA was synthesized at 42°C overnight using the RNA-primers mix, 3 µl 0.1 M

dithiothreitol, 1.2 μ l 25 \times deoxynucleoside triphosphates (3:2 ratio of amino-allyl dUTP to dTTP), 6 μ l 5 \times First Strand synthesis buffer, and 2 μ l Superscript II reverse transcriptase (Invitrogen). Amino-allyl dUTP was purchased from Ambion (Austin, TX). RNA was hydrolyzed through addition of 10 μ l 1 M NaOH, 10 μ l 0.5 M EDTA and incubation at 65°C for 15 min. The reaction was neutralized with 10 μ l of 1 M HCl. Purification of cDNA was performed following amino-allyl label incorporation and chemical dye coupling using the Qiaquick PCR purification system (QIAGEN) according to the TIGR protocol. Dyes were incorporated at 25°C for 1.5 h with 4.5 μ l amino-allyl labeled cDNA in 0.1 M sodium carbonate (pH 9) and 4.5 μ l reactive Cy5 and Cy3 N-hydroxysuccinamide ester fluorophores (Amersham, Piscataway, NJ) in dimethyl sulfoxide (GE Biosciences, Piscataway, NJ). Amino-allyl labeled cDNA quantity and fluorophore incorporation efficiency were determined using UV-visible spectrophotometry.

Microarray characteristics. Glass slide arrays were made by the Institute for Environmental Genomics (IEG) at Oklahoma State University (Dr. Jizhong Zhou, Norman, OK) from the *D. hafniense* DCB-2 draft sequence with 10 \times coverage (August 11, 2005) at which time *D. hafniense* was believed to have a 5.2 Mb chromosome. The probe design was performed by IEG (He 2005, Li 2005) with on average one probe per predicted open reading frame. A total of 4,667 probes were present in duplicate for a total of 9,984 spots present on the array including positive and negative controls. Negative controls included 10 human and 10 Arabidopsis probes. Positive controls consisted of probes to detect six different quantities (5~300 ng μ l⁻¹) of genomic DNA

spotted four times in duplicate per slide.

Microarray hybridization and analysis. Microarray slides were incubated at 49°C for 1 h in prehybridization solution containing 5× SSC buffer, 0.1% sodium dodecyl sulfate (SDS), and 0.1 mg/ml bovine serum albumin. A series of room temperature washing steps followed, including: two washes in 0.1× SSC buffer for 5 min and two washes in sterile water for 30 sec. Slides were then dried by centrifugation at 1800 rpm for 2 min using a Sorvall RT 6000D centrifuge with an H1000B hanging basket rotor. LifterSlips® (22 by 60 mm; Erie Scientific, Portsmouth, NH) were prepared by washing once in water and once in 95% ethanol and drying with filtered forced air. LifterSlips® were placed over the microarray on the slide.

Equivalent concentrations of Cy dye labeled cDNA from the metal sample and the alternate Cy dye labeled positive control (pyruvate fermentation without additional electron acceptor) were then mixed, dried in a SpeedVac, and resuspended in 50 µl of hybridization buffer (5× SSC buffer, 0.1% SDS, 25% formamide, 0.1 mg/ml salmon testis DNA [Sigma-Aldrich]). This mixture was heated to 95°C for 10 min, spin-cooled, reheated to 70°C, and applied to the array using capillary action. Microarray slides were then sealed in a hybridization chamber (CMT Hybridization Chamber; Corning Incorporated, Corning, NY) and incubated for 18 h in a 49°C shaking water bath (30 rpm).

Microarray hybridizations were performed with a dye swap and 3 biological replicates for

a total of 6 slides per comparison. LifterSlips® were removed from hybridized microarray slides carefully in a wash of 1× SSC buffer and 0.1% SDS at 49°C. Slides were then washed in a shaking water bath (50 rpm) for 5 min in 1× SSC buffer and 0.1% SDS at 49°C, twice for 5 min in 0.1× SSC buffer and 0.1% SDS at room temperature, four times for 1 min in 0.1× SSC buffer at room temperature, and once for 10 s in 0.01× SSC buffer. Washed slides were spun dry at 1800 rpm for 2 min.

Slides were immediately scanned on an Axon 4000B laser scanner (Axon Laboratories, Molecular Devices, Sunnyvale, CA) using histogram verification in GenPix Pro 5.1 (Axon Laboratories) for raw data production followed by gene identifier alignment. Correction for background was made by background subtraction of the median value. Median signal intensities for each channel (Cy5 and Cy3) were imported into GeneSpring 6.0 (Silicon Genetics, Redwood City, CA) and normalized by dye swapping and (per chip and per gene) using Lowess intensity-dependent normalization. Only spots with more than 80% of pixels above background with P-values less than 0.01, and 2 standard deviations in either Cy5 or Cy3 channel were considered differentially expressed genes and used for further analysis. Our analyses further focused on operons containing genes of similar expression to determine important metabolic pathways.

Experimental determination of acetogenic ability. When testing *D. hafniense* DCB-2 for the ability to grow as an acetogen, *Moorella thermoacetica* served as the positive acetogen control. *D. hafniense* and *M. thermoacetica* were originally grown in modified DCB-1 medium fermenting pyruvate with a head space of CO₂:N₂ (5:95) (Brumm 1988,

Löffler 1996, Chapter 4). Cultures were incubated at 37°C for *D. hafniense* and 55°C for *M. thermoacetica*. These fermenting cultures served as the initial inocula for testing for CO₂ fixation. The medium was 20 ml of modified DCB-1 medium with five different gas mixtures [CO₂:N₂ (40:60), CO:N₂ (40:60), CO:CO₂:N₂ (30:30:40), H₂:CO:N₂ (30:30:40), and H₂:CO₂:N₂ (30:30:40)] in 120 ml serum bottles (Löffler 1996, Miller 1974, Chapter 4). Wolin vitamins (1×) and cysteine were the only other potential sources for carbon in this medium (Wolin 1963). Cultures were transferred following a 14 d incubation. The cultures were shaken daily at the time visible growth was noted. Four serial transfers into new media were performed prior to measuring growth by optical density at 600 nm and total biomass production (TOC) (Chapter 4). Samples for TOC were collected as a pellet by centrifugation. The supernatant was then combined with ethanol (2:3) to precipitate soluble organic carbon, centrifuged, and the new pellet was combined with the first and sent for TOC analysis at UC Davis Stable Isotope Facility (Davis, CA). Eight biological replicates were performed for all samples and submitted for TOC analysis. Controls consisted of all media conditions without cells, cultures without electron acceptor addition, and cultures with heat-killed cells.

Culture purity. Culture purity was tested throughout this study in duplicate using fluorescent *in situ* hybridization (FISH) on all samples with DAPI, a Cy3-labeled universal eubacterial rDNA probe, and a Cy5-labeled *D. hafniense*-specific rDNA probe (Bloem 1995, Lanthier 2001). *Escherichia coli* was used as a positive control for DAPI and the Cy3-labeled probe and as a negative control for the Cy5-labeled probe. Slides

were observed on a Nikon epifluorescent microscope equipped with a 50 W mercury lamp.

RESULTS and DISCUSSION

In this study, total genome transcriptomic profiles were obtained from *D. hafniense* DCB-2 cells growing with four different electron acceptors: Fe(III), NO_3^- , U(VI), and Se(VI). Microarray studies on these culture conditions have not only provided valuable information about key genes/metabolic pathways that respond to each redox condition, but also offered an opportunity to view the previously inaccessible global metabolism of pyruvate fermentation by *D. hafniense* DCB-2. This was possible because transcripts obtained from each culture were compared against pyruvate-fermenting cultures. The resulting down-regulated genes from each microarray were then used to deduce and unravel some of underlying metabolic events in pyruvate-fermenting cells.

Pyruvate-fermenting cell metabolism. From the analysis of the down-regulated gene lists [623 genes from Fe(III), 643 genes from NO_3^- , 857 genes from U(VI), 371 genes from Se(VI)] and the *D. hafniense* DCB-2 genome sequence archived in JGI, some key metabolic features in pyruvate-fermenting *D. hafniense* DCB-2 were deduced (Figure 3.1).

Carbon cycling. Carbon flow in the cell was determined relative to biogenesis of cell material and up-regulation of genes under dissimilatory Fe(III) reduction. During

pyruvate-fermenting conditions, the tricarboxylic acid cycle (TCA) seemed discontinuous. Like many strict anaerobes, it lacked genes of the 2-oxoglutarate dehydrogenase complex. Pyruvate-fermenting cells may instead use bidirectional citrate to 2-oxoglutarate and oxaloacetate or succinyl-CoA routes. Moreover, the glyoxylate pathway to replenish oxaloacetate is absent. Instead, citrate lyase, which converts citrate to oxaloacetate and acetate, appeared active in the cell. Even in pyruvate-fermenting conditions cells were fixing CO₂ via the reductive acetyl-CoA pathway (Wood-Ljungdahl pathway) since the downstream NAD-dependent formate dehydrogenase operon (Dhaf_4268-4271) was induced (Figure 3.1).

Electron flow. Cells appeared to use anaerobic respiration to gain additional energy. It is evident that some fumarate reductase and DMSO reductase genes are constitutively expressed. Also, a cytochrome-dependent formate dehydrogenase operon (Dhaf_4616-4621) seems to provide electrons for energy. There are three putative N₂-fixing nitrogenase operons in the genome that contain a complete *nifHDK* gene unit (Figure 3.6). Apparently, cells are actively using these operons to fix N₂ (Dhaf_1350-1360, Dhaf_1047-1059, and Dhaf_1810-1818). However, it is not clear whether both nitrate reductase genes and nitrite reductase genes are expressed in pyruvate-fermenting cells. Ammonia formation through N₂-fixation rather than nitrate ammonification seems to be preferred by *D. hafniense* under all tested conditions (Figure 3.6). Nitrate could be reduced to nitrite by periplasmic Nap nitrate reductase (Dhaf_1289), but genes encoding membrane-bound Nar nitrate reductases are absent in the *D. hafniense* genome.

Although not differentially expressed during pyruvate-fermenting conditions, genes for direct ammonification of nitrite are present consisting of two nitrite reductase (Nrf) operons (Dhaf_3630-3631, Dhaf_4234-4235). Also, putative genes for nitric oxide reductase (Dhaf_2253-2254) and nitrous oxide reductase (Dhaf_1205) of the denitrification pathway were found, which may potentially convert nitric oxide to N₂.

Pyruvate

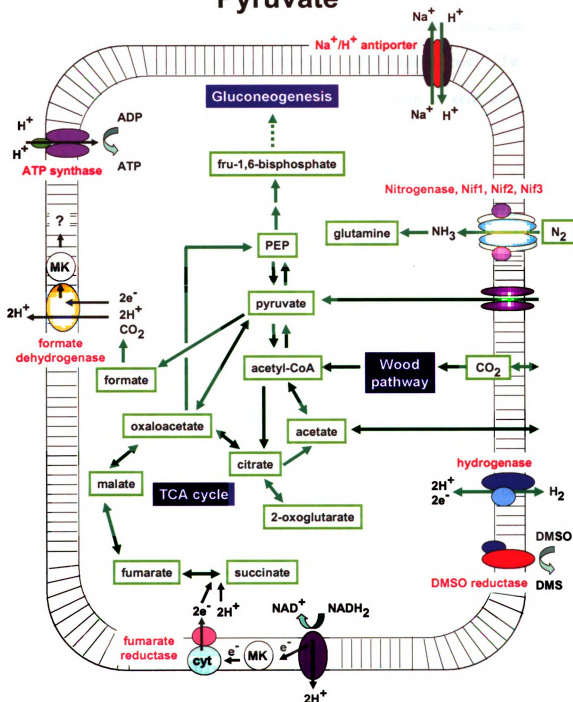


Figure 3.1. Schematic diagram of the key metabolism pathways during fermentation with pyruvate.

Menaquinone is abbreviated as "MK", cytochrome as "cyt", and phosphoenolpyruvate as "PEP".

Dissimilatory Fe(III)-reducing cell metabolism. Microarray experiments with Fe(III)-respiring cells resulted in 655 up-regulated genes and 523 down-regulated genes (>2 and <0.5 fold cutoff) against pyruvate-fermenting cell transcriptomes. Fe-reducing conditions proved to have the largest differential expression in cells of the major pathways compared to pyruvate fermentation (Figure 3.2).

Carbon cycling. Among the highly induced gene groups (at least >5 fold) were CO dehydrogenase catalytic genes (induced 50-60 fold). These gene products are part of the reductive acetyl-CoA pathway (Wood-Ljungdahl pathway) which is the major mechanism of CO₂ fixation under anaerobic conditions. Other genes that are involved in the same pathway were also highly induced (20-45 fold). When we consider that pyruvate-fermenting cells are already actively utilizing this pathway, an additional 50-60 fold induction appears to be extraordinarily high. Although CO₂ fixation is an energy demanding process, it could provide a redox balance by consuming excess electrons by using them to assimilate more reduced cellular material. In fact, under nitrate-reducing conditions, which also used lactate as the substrate, the CO₂ fixation pathway was slightly repressed. This is likely because nitrate can take up eight electrons to form NH₃ while Fe(III) reduction to Fe(II) can only accept one electron; giving NO₃⁻-reducing cells less of a burden to deal with excess intracellular electrons.

Many of the other up-regulated genes are associated with central metabolism. These

were the genes coding for pyruvate carboxyltransferase, acetaldehyde dehydrogenase, fumarate reductases, malic enzyme, pyruvate formate-lyase, and fructose-1,6-bisphosphatase. Both pyruvate carboxyltransferase and fructose-1,6-bisphosphatase are involved in gluconeogenesis, mediating the carboxylation of pyruvate to oxaloacetate and the dephosphorylation of fructose-1,6-bisphosphate to fructose-6-phosphate. Five fumarate reductase genes located at different loci were moderately induced (2-6 fold) and a gene putatively encoding NADH:flavin oxidoreductase/fumarate reductase was highly induced by ~20 fold. *D. hafniense* may use the reverse TCA cycle to fix CO₂ and generate energy via fumarate reduction to succinate. Since the genome lacks 2-oxoglutarate dehydrogenase complex genes, which convert 2-oxoglutarate to succinyl-CoA in the TCA cycle, succinate formed by fumarate reduction can be either converted to succinyl-CoA (succinyl-CoA synthetase gene, 9-fold induction) or excreted through the TRAP dicarboxylate transporter (10-fold induction) for future recycling.

Electron flow. Under Fe(III)-respiring conditions, *D. hafniense* exhibited increased transcriptional activities on many oxidoreductase, transporter, flavoprotein, and coenzyme biosynthesis genes. Formate dehydrogenase (Fdh) appears to be a key enzyme in both carbon and energy flows. Two classes of this enzyme system exist in *D. hafniense* (cytochrome-dependent and NAD-dependent). Cytochrome-dependent formate dehydrogenase (Fdh1) (Dhaf_4616-4621 induced ~7 fold) acts on formate to produce CO₂, 2H⁺, and two electrons. These electrons are used in the electron transport chain to reduce a terminal electron acceptor, and the released protons are used to generate energy.

Interestingly, under NO_3^- -, U(VI)-, and Se(VI)-reducing conditions, Fdh1 transcription activity was down-regulated. NAD-dependent formate dehydrogenase (Fdh2a) directs carbon fixation by catalyzing CO_2 to produce formate, which is subsequently used in the Wood-Ljungdahl pathway to generate acetyl-CoA. Expression of Fdh2a-encoding operon (Dhaf_4268-4271) under Fe(III)-reducing conditions was, to our surprise, significantly decreased (~8 fold down-regulation). BLAST search for another potential NAD-dependent formate dehydrogenase operon has identified a second operon (Fdh2b, Dhaf_1508-1513), which was highly induced (~50 fold) under Fe(III)-reduction. Induction and repression of this operon seems to be highly specific since under no other conditions examined were significant changes in its expression detected.

Consistent with our predictions, genes encoding a ferric uptake regulator (Dhaf_1359, ~3 fold) and a ferrous iron transporter (Dhaf_2887, ~8 fold) were up-regulated, as were lactate dehydrogenase gene and lactate transporter genes. Many such examples have strengthened the integrity of our microarray results. At this stage, it is too early to identify the terminal reductase genes involved in dissimilatory Fe(III) reduction. Potential candidates may be obtained from more extensive analysis of microarray data and targeted experimentation.

Fe(III) + Lactate

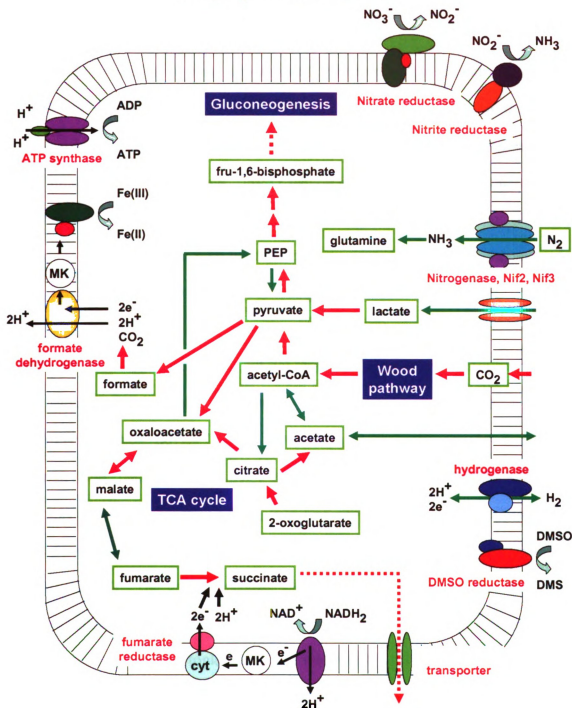


Figure 3.2. Schematic diagram of the key metabolism pathways during dissimilatory Fe(III) reduction with lactate. Menaquinone is abbreviated as "MK", cytochrome as "cyt", and phosphoenolpyruvate as "PEP". Green arrows indicate genes similarly expressed as pyruvate fermentation. Red arrows are genes

up-regulated (in comparison to pyruvate fermentation) in response to dissimilatory Fe(III) reduction.

U(VI)-reducing cell metabolism. First examination of the U(VI) microarray data immediately revealed that many up-regulated genes were shared with those of the dissimilatory Fe(III) reduction microarray (Figure 3.3). This is especially true for the genes involved in coenzyme metabolism and energy metabolism. Examples are the genes for cobalamin biosynthesis, DMSO reductases, FAD dependent oxidoreductase, coenzyme F390 synthetase, NiFe hydrogenase, and NADH dehydrogenase. However, the wide range of induction seen with Fe-respiration (oxidoreductase genes and redox protein genes) was not observed in U(VI)-reducing conditions.

In other studies of U(VI)-reduction (but not respiring), *Desulfovibrio desulfuricans* G20 and *D. vulgaris*, a periplasmic cytochrome c3 was implicated in direct reduction of U(VI) to U(IV) (Payne 2004, Lovley 1993b). However, insoluble U(IV) was also found in the cytoplasm (Sani 2006), suggesting that a secondary mode of U(VI) reduction was present in the cytoplasm. Recently, transposon-mediated mutagenesis of *Desulfovibrio desulfuricans* G20 identified an operon which was implicated in cytoplasmic reduction of U(VI) (Li 2009). The operon-encoded oxidoreductase, thioredoxin, and thioredoxin reductase added NADPH and was shown to reduce both U(VI) and Cr(VI) *in vitro*. One such operon similar to the cytoplasmic U(VI) reductase of *D. desulfuricans* G20 is found in *D. hafniense* with moderate levels of induction with U(VI) reduction (Dhaf_476-484, 3-7 fold).

Cells in the presence of U(VI) had induced transcriptional activities on other gene groups whose functions include; chemotaxis, flagella biosynthesis, cell wall biosynthesis, DNA replication, DNA repair, and cell division. While CO₂-fixing gene activity had increased, N₂-fixing gene activity had decreased. The acetyl-CoA pool appeared to be provided from pyruvate (by pyruvate-formate lyase), acetate (by acetyl-CoA synthase), and the Wood-Ljungdahl pathway. Acetyl-CoA formation from lipid breakdown (β -oxidation by acetyl-CoA acetyltransferase and others) was severely inhibited, suggesting that cells were preserving the lipid pool. Furthermore, heavy-metal efflux pump (P-type ATPase) genes were significantly induced.

All of these activities suggest that cells were highly stressed, accelerated cell division while fixing damaged DNA trying to prevent toxicity. There was no indication of sporulation initiation, demonstrating that cells could tolerate U(VI) and were trying to adapt to these less favorable conditions. High induction of DNA repair genes (*radC* and *recF*) and different classes of DNA helicase genes suggest that DNA damage had occurred either by chemicals, radiation, or possibly by intracellular insoluble U(IV) species. This accelerated cell division attempt, regardless of whether division was successful, is likely to provide *D. hafniense* with a better chance of adaptation to U(VI)-rich environments, through the creation of mutations and recombination events occurring with DNA replication and repair.

U(VI) + Pyruvate

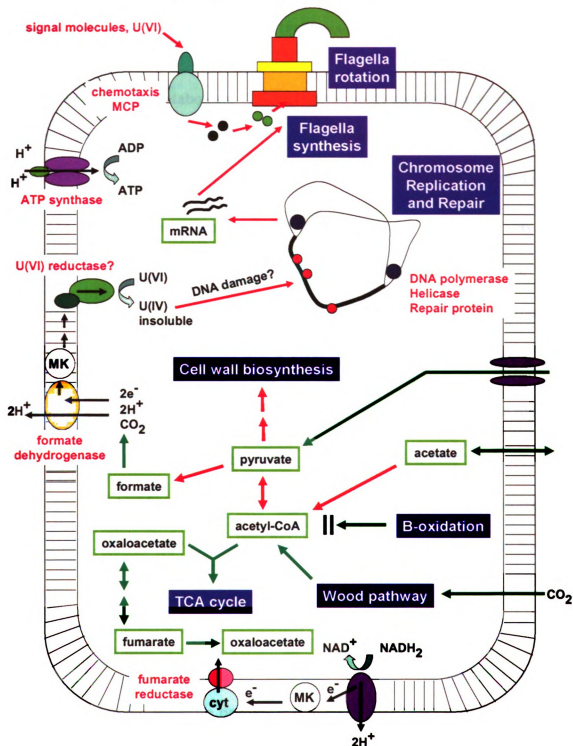


Figure 3.3. Schematic diagram of the key metabolism pathways during dissimilatory U(VI) reduction

with pyruvate. Menaquinone is abbreviated as “MK”, and cytochrome as “cyt”. Green arrows indicate genes similarly expressed as pyruvate fermentation. Red arrows are genes up-regulated (in comparison to pyruvate fermentation) in response to dissimilatory U(VI) reduction.

Nitrate-reducing cell metabolism. The microarray study on nitrate-reducing cells can be characterized by two highly induced gene groups that are each involved in assimilatory sulfate reduction and N₂ fixation-like function by the *Nifl* operon (Figure 3.4). The 13 gene operon involved in the formation of H₂S from SO₄²⁻ was highly induced (8-33 fold). Among these genes, four genes encoded ABC-type sulfate transporter components: two genes for activation of SO₄²⁻ by adenylation and phosphorylation, a thioredoxin gene (*Dhaf_4113*, ~8 fold) for SO₄²⁻ reduction to sulfite (SO₃²⁻), three genes for molybdopterin/thiamine biosynthesis, and two genes for sulfite reductase (*Dhaf_4107*, 33 fold), which catalyzes H₂S formation from SO₃²⁻. The *Nifl* operon was also highly induced (5-26 fold) including a molybdopterin oxidoreductase gene (*Dhaf_1350*, 16 fold) which is located immediately upstream of the N₂-fixing *NifHDK* genes and the nitrate (NO₃⁻) transporter genes.

No significant induction was observed in the *Nap* nitrate reductase operon (*Dhaf_1289*) or the two *Nrf* nitrite reductase operons (*Dhaf_3630-3631*, *Dhaf_4234-4235*). Nitrate reduction is preferred when the ratio of electron donor to nitrate is high. Therefore, under a nitrate-rich environment, the two operons are not likely to be significantly up-regulated.

Because the Nap nitrate reductase is located in the periplasm, this system may be used for the reduction of external nitrate. During this process, ATP-generating proton accumulation across the membrane may not be possible since protons released are likely to be used immediately for H₂O production. Together with the periplasmic Nrf nitrite reductase, the Nap nitrate reductase system in *D. hafniense* may function as an electron sink as well as produce NH₃. These two operons were significantly induced (4-7 fold) under Fe(III)-reducing conditions, where excess amounts of electrons were predicted to form intracellularly because of the use of lactate substrate and the low electron-accepting capacity of Fe(III).

Nitrate + Lactate

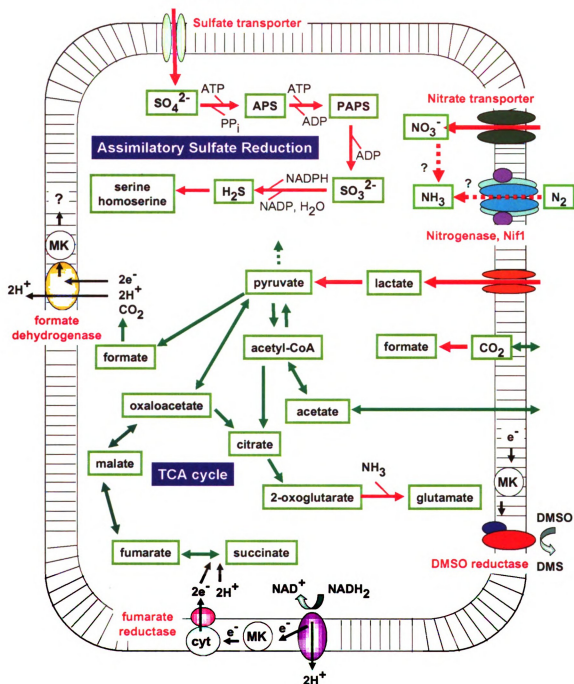


Figure 3.4. Schematic diagram of the key metabolism pathways during nitrate reduction with lactate. Menaquinone is abbreviated as “MK”, cytochrome as “cyt”, adenylyl sulfate as “APS”, and phospho-adenylyl sulfate as “PAPS”. Green arrows indicate genes similarly expressed as pyruvate fermentation.

Red arrows are genes up-regulated (in comparison to pyruvate fermentation) in response to nitrate reduction.

Se(VI)-reducing cell metabolism. Out of 305 genes that were up-regulated during Se(VI)-reducing conditions, 122 genes were of unknown functions. These unknown genes were, in many cases, among the most highly induced genes. Since Se(VI) cultures were provided pyruvate as the carbon and energy source, the numbers of genes that were up-regulated and the overall induction rates were relatively low compared to pyruvate fermentation (Figure 3.5).

Genes showing significant induction include the genes for a specialized RNA polymerase sigma-E factor (9 fold), transcriptional regulators, ABC transporters, N₂-fixing nitrogenase operon Nif3 (3 fold), fumarate reductases (3 fold), glutamine synthase (6 fold), and PBSX prophage genes (2-8 fold). Whereas, genes showing transcription reduction encoded succinyl-CoA synthetase (0.1 fold), CO₂-fixation (0.2 fold), flagella biosynthesis (0.2 fold), NADH dehydrogenase (0.3 fold), menaquinone biosynthesis (0.3 fold), sulfite reductase (0.4 fold) and sulfate transporter (0.4 fold). These results may indicate that cells no longer had to fix as much CO₂ in order to balance their internal redox state since Se(VI) has a large electron-accepting capacity. It is evident that the dependency on NADH-mediated energy generation decreased. Cells also appeared to fix cellular nitrogen through N₂-fixation and glutamine synthesis.

Escherichia coli K-12 carries a putative oxidoreductase gene, *YgfK*, required for selenate reduction (Bébian 2002), and the YgfK enzyme has three distinct domains: a N-terminal NAD-binding domain, a central pyridine nucleotide-disulfide redox domain, and a C-terminal [4Fe-4S]-binding domain. Two other genes in the same operon, YgfMN were predicted to encode proteins with a FAD-binding domain and a [2Fe-2S]-binding domain, respectively. The anaerobic bacterium *Thauera selenatis* contains the *serABC* operon encoding a periplasmic heterotrimeric selenate reductase which shows high substrate specificity unable to reduce nitrate, chlorate or sulfate (Krafft 2000). The *SerABC* genes encode subunits with Mo active site, Fe-S clusters, and b-type cytochrome, respectively. The Se(VI) reductase in a Gram-negative facultative anaerobe, *Enterobacter cloacae* SLD1a-1, is a membrane-bound heterotrimeric complex that faces the periplasm, and contains Mo, heme, and nonheme iron as prosthetic groups and a b-type cytochrome in the active complex (Ridley 2006, Watts 2003). The membrane-bound Se(VI) reductase showed broader substrate specificity. In *D. hafniense* cultures grown with Se(VI), a potential candidate gene encoding the b-type cytochrome protein was not identified. However, three oxidoreductase genes that were up-regulated by 2-3 fold were found (Dhaf_313, 480, 2375).

Se(VI) + Pyruvate

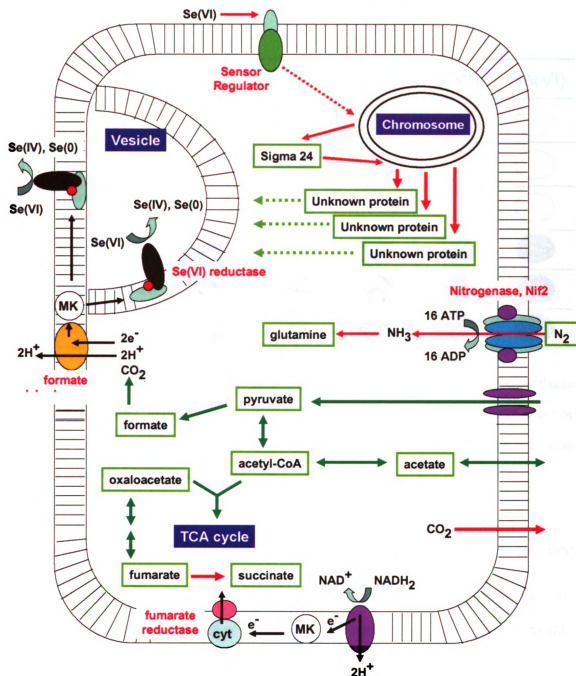


Figure 3.5. Schematic diagram of the key metabolism pathways during Se(VI) reduction with pyruvate. Menaquinone is abbreviated as “MK”, and cytochrome as “cyt”. Solid green arrows indicate genes similarly expressed as pyruvate fermentation. Red arrows are genes up-regulated (in comparison to

pyruvate fermentation) in response to Se(VI) reduction. The vesicle is external in *D. hafniense*, though for simplicity depicted here as internal.

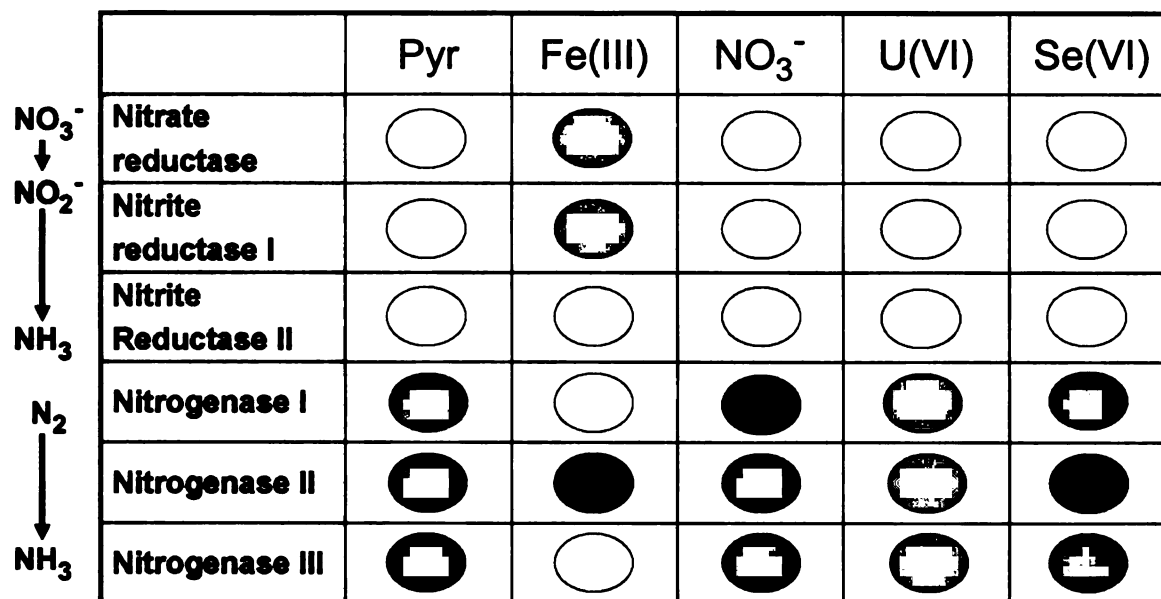


Figure 3.6. Induced expression of the genes involved in nitrate reduction and nitrogen fixation (pathways shown at left). Relative induction is shown in grey scales (light to dark; low to high induction). No evidence was found which supports gene expression of nitrate and nitrite reductase genes in pyruvate-fermenting cells. Therefore, relevant cells are shown in white.

Nitrogenase activity. As mentioned briefly, *D. hafniense* can fix N₂, and three nitrogenase operons are present in the genome, Nif1 (Dhaf_1350-1360), Nif2 (Dhaf_1047-1059), and Nif3 (Dhaf_1810-1818). These operons all contain a *NifHDK* catalytic gene unit, but they differ in other genes residing in each operon. All of these operons appeared to be expressed in pyruvate-fermenting cells. The eight-gene operon, Nif1, which contains three ABC-type nitrate transporter genes, was strongly repressed under Fe(III)-respiring conditions (Figure 3.6). The remaining two operons stayed at

similar levels of expression (slightly lower with Nif3 and slightly higher with Nif2). The presence of nitrate transporter genes in the Nif1 operon suggests that Nif1 nitrogenase system may be positively regulated by NO_3^- . This is supported by the fact that under NO_3^- -reducing conditions, the Nif1 operon was highly up-regulated (5-26 fold). Also, under NO_3^- -reducing conditions, neither the Nap nitrate reductase system nor Nrf nitrite reductase system were induced above the cutoff level (>2). In this respect, it is possible that the Nif1 operon has evolved for nitrate-reduction utilization, and not for the true N_2 -fixing pathway.

Determination of an active acetyl-CoA reduction pathway. Turbid growth was observed with *M. thermoacetica*, the positive acetogen control, consistently within 7 days in all 30:30:40 headspace combinations. Growth of *D. hafniense* under these same headspace conditions was undetectable until cultures were shaken, revealing light growth. The biomass produced was 25 to 50% less than that by *M. thermoacetica* (Table 3.1). The vast majority of the *D. hafniense* biomass appeared to be extracellular soluble organic carbon because very large amounts of precipitate formed following ethanol addition during TOC sample processing. Growth of either species in carbonate-buffered freshwater medium (CBF) with lactate was undetectable by all methods other than TOC, which was used to determine the amount of growth attributable to inoculum alone. This was selected as both *D. hafniense* and *M. thermoacetica* are reportedly unable to ferment lactate alone, thus any biomass production above this indicated the organism was making use of the provided terminal electron acceptor (Christiansen 1996, Brum 1988). Ten-fold

Table 3.1. Effect of acetogenic conditions
of cell yields of *M. thermoacetica* and *D. hafniense*

Organism	Gas mixture	Gas ratio	Medium	Carbon source (20 mM)	Biomass produced (mg/L)
<i>D. hafniense</i>	CO ₂ :N ₂	5:95	DCB-1	pyruvate	15.1
<i>D. hafniense</i>	CO ₂ :N ₂	20:80	CBF	lactate	0.295
<i>D. hafniense</i>	CO:N ₂	40:60	DCB-1	-	1.44
<i>D. hafniense</i>	CO:CO ₂ :N ₂	30:30:40	DCB-1	-	13.9
<i>D. hafniense</i>	H ₂ :CO:N ₂	30:30:40	DCB-1	-	33.1
<i>D. hafniense</i>	H ₂ :CO ₂ :N ₂	30:30:40	DCB-1	-	13.3
<i>D. hafniense</i>	CO ₂ :N ₂	40:60	DCB-1	-	1.00
<i>M. thermoacetica</i>	CO ₂ :N ₂	5:95	DCB-1	pyruvate	34.3
<i>M. thermoacetica</i>	CO ₂ :N ₂	20:80	CBF	lactate	3.19
<i>M. thermoacetica</i>	CO:N ₂	40:60	DCB-1	-	4.10
<i>M. thermoacetica</i>	CO:CO ₂ :N ₂	30:30:40	DCB-1	-	46.5
<i>M. thermoacetica</i>	H ₂ :CO:N ₂	30:30:40	DCB-1	-	54.5
<i>M. thermoacetica</i>	H ₂ :CO ₂ :N ₂	30:30:40	DCB-1	-	24.7
<i>M. thermoacetica</i>	CO ₂ :N ₂	40:60	DCB-1	-	3.16

more biomass was produced in CBF with lactate alone for *M. thermoacetica* than with *D. hafniense* (Table 3.1), revealing that either *M. thermoacetica* possessed more residual nutrient carry-over from inoculation, or more likely that it was better able to use the components present in the CBF medium (e.g. vitamins, 20% CO₂, etc.) to yield low amounts of growth. Moreover, *M. thermoacetica* produced twice as much biomass with pyruvate fermentation alone as did *D. hafniense* (Table 3.1).

All gas combinations for both species produced more biomass than CBF with lactate (the amount of biomass attributable to inoculation) (Table 3.1). It is thought that even in the absence of a typical electron donor, e.g. hydrogen gas, *D. hafniense* may utilize CO₂ and CO as electron donors and acceptors for growth. The amount of gaseous carbon was

twice the amount in CBF medium with CO₂:N₂ (20:80). A 5-fold increase in biomass was observed in CO:N₂, and a 3-fold increase in CO₂:N₂ (Table 3.1). *M. thermoacetica* remained unchanged with CO₂:N₂, and increased by 33% with CO:N₂. In the presence of H₂:CO:N₂, both species produced the most cell material, followed by CO:CO₂:N₂ and H₂:CO₂:N₂. The CO:CO₂:N₂ yields are considerably less than those found by Daniels (1993) (146 mg/L); however, those studies were performed with an undefined medium containing yeast extract. The low amount of growth from CO:N₂ for either *D. hafniense* or *M. thermoacetica* is not surprising. When *M. thermoacetica* was previously cultured in CO:N₂, glucose and yeast extract were provided, and when glucose was removed, cultures did not grow reproducibly (Kerby 1983). It was an unexpected result that CO:CO₂:N₂ would facilitate more significant biomass production than H₂:CO₂:N₂ [when compared to results found by Daniel (1990)], which indicates a preference for CO as both the electron donor and acceptor for acetogenesis. Controls of media alone did not produce detectable biomass, thus all biomass was produced by the bacteria. Some biomass production by *D. hafniense* and *M. thermoacetica* was observed in cultures with only CO:N₂ or CO₂:N₂. These findings indicate that CO and CO₂ might be used both as electron acceptors and donors but with better biomass yields when H₂ and CO are provided for the electron donor and acceptor (30:30:40 combination). This evidence strongly suggests *D. hafniense* is capable of growth as an acetogen, though this may be weak acetogenic growth due to the bulk of its fixed carbon forming from small soluble

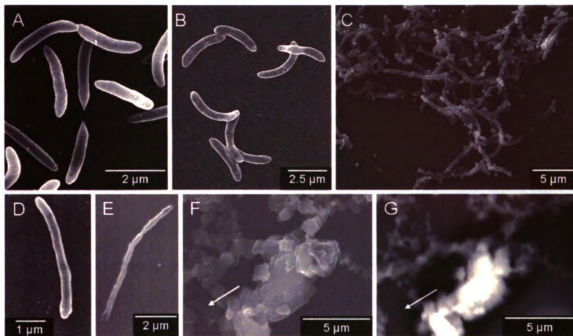


Figure 3.7. SEM of *D. hafniense* DCB-2 exposed to different electron acceptors. (A) Curved rod morphology during pyruvate fermentation. (B) Curved rod morphology during nitrate respiration. (C) Elongated rod exhibited during U(VI) exposure. (D) Elongated rod with vesicles during growth with Se(VI). (E) Streptobacilli made of shorter rods during Fe(III) respiration. (F) SEM of Fe(III) biomass. White arrow points to cell in G. (G) Backscatter image of Fe(III) biomass from E. White arrow points to cell in F.

extracellular polymeric substances rather than cells.

Gene expression corresponding to cell morphology differences. Cell morphology observed during metal reduction appears to mirror changes in gene expression. In the absence of metal-reducing conditions, similar curved rods were found (2.5 μm with both pyruvate fermentation and nitrate respiration) (Figure 3.3A and B). The presence of both Se(VI) and U(VI) in medium with pyruvate resulted in cells elongating to nearly twice

their normal cell length (averaging 4.7 and 4.8 μm per cell respectively) (Figure 3.3C and D). This observation seems to correlate with the gene expression of cells trying to limit exposure to toxic U(VI). While further investigation would be required to determine if this was the case for Se(VI)-reducing conditions, repressed growth has been found with Se(VI) (Chapter 2). Se(VI) exposed cells also produced extracellular vesicles of selenium (Chapter 4). Perhaps the genes responsible for this adaptation are in the 122 genes of unknown function. The highly expressed RelB antitoxin-like gene (Dhaf_0577) might function in part of these processes. Shorter cells in a streptobacilli formation were present with Fe(III) (Fig 3.3E). Surrounding these chains of cells was large amounts of biomass containing elements of high atomic weight (Figure 3.3F and G). Upon investigation with EDS, bound iron was determined to be the cause of the heavy elements detected in the biomass (data not shown). This high amount of extracellular material production reflects the large induction of the Wood-Ljungdahl pathway and gluconeogenesis (Figure 3.2). A large number of oxidoreductases and a ferrous transporter gene were highly expressed, this along with the induction of the carbon-fixation pathway provide evidence for the Fe(II)-bound in biomass as seen in Figure 3.3G.

Conclusions. In summary, the largest contrast in gene expression existed between pyruvate fermentation and Fe(III) reduction. Genes expressed with U(VI)-reducing conditions were similar to those of Fe(III)-reducing conditions, while Se(VI)-reducing conditions had many highly expressed genes in common with NO_3^- -reducing conditions, though most were of unknown function. This difference may be in part due to the

number of electrons reduced per molecule of metal; however, further research would be required to verify this interpretation.

The physiology of *D. hafniense* DCB-2 has been expanded to such diverse growth as fermentation, halorespiration, metalorespiration, and now acetogenesis. The growth of *D. hafniense* in conditions providing only a gaseous electron donor, electron acceptor, and carbon source have shown that it is an acetogen; however, this growth was weak compared to the profuse cell material produced by *M. thermoacetica*. Moreover, CO was found to be the preferred carbon source for cell material production during acetogenesis. Further studies of metal-reduction supported by gaseous carbon may be of interest, as bioremediation with *D. hafniense* may be less expensive using gaseous carbon to support growth.

ACKNOWLEDGEMENTS

Research was supported by the U.S. Department of Energy, Office of Science, Environmental Remediation Science and Genomes to Life Programs. The collaboration of Dr. Sang-Hoon Kim of Michigan State University (East Lansing, MI) was greatly appreciated in operon expression analyses and creation of figures within this chapter.

REFERENCES

- Bébian, M., J. Kirsch, V. Me'jean, and A. Verméglio.** 2002. Involvement of a putative molybdenum enzyme in the reduction of selenate by *Escherichia coli*. *Microbiology* 148:3865-3872.
- Bloem, J.** 1995. Fluorescent staining of microbes for total counts. In: Akkermans A.D.L., Elsas J.D., Bruijn F.J. (eds), *Molecular Microbial Ecology Manual*. Kluwer Academic Press, Dordrecht, The Netherlands, pp. 1-12.
- Brumm, P. J.** 1988. Fermentation of single and mixed substrates by the parent and an acid-tolerant mutant strain of *Clostridium thermoaceticum*. *Biotech. Bioeng.* 32:444-450.
- Christiansen, N. and F. K. Ahring.** 1996. *Desulfitobacterium hafniense* sp. nov., anaerobic, reductively dechlorinating bacterium. *Int. J. Syst. Bacteriol.* 46:442-448.
- Daniel, S. L. and H. L. Drake.** 1990. Characterization of the H₂- and CO-dependent chemolithotrophic potentials of the acetogens *Clostridium thermoaceticum* and *Acetogenium kivui*. *J. Bacteriol.* 172:4464-4471.
- Gorby, Y. A., T. J. Beveridge, and R. P. Blakemore.** 1988. Characterization of the bacterial magnetosome membrane. *J. Bacteriol.* 170:834-841.
- He, Z., L. Wu, X. Li, M. W. Fields, and J. Zhou.** 2005. Empirical establishment of oligonucleotide probe design criteria. *Appl. Environ. Microbiol.* 71:3753-3760.
- Kerby, R. and J. G. Zeikus.** 1983. Growth of *Clostridium thermoaceticum* on H₂/CO₂ or CO as energy source. *Curr. Microbiol.* 8:27-30.
- Kostka, J. E., D. D. Dalton, H. Skelton, S. Dollhopf, and J. W. Stucki.** 2002. Growth of iron(III)-reducing bacteria on clay minerals as the sole electron acceptor and comparison of growth yields on a variety of oxidized iron forms. *Appl. Environ. Microbiol.* 68:6256-6262.
- Krafft, T., A. Bowen, F. Theis, and J. M. Macy.** 2000. Cloning and sequencing of the genes encoding the periplasmic-cytochrome B-containing selenate reductase for *Thauera selenatis*. *DNA Sequence* 10:365-377.
- Lanthier, M., R. Villemur, F. Lepine, J-G. Bisaillon, and R. Beaudet.** 2001. Geographic distribution of *Desulfitobacterium frappieri* PCP-1 and *Desulfitobacterium* spp. in soils from the province of Quebec, Canada. *FEMS Micro. Ecol.* 36:185-191.
- Li, X., Z. He, and J. Zhou.** 2005. Selection of optimal oligonucleotide probes for microarrays using multiple criteria, global alignment and parameter estimation. *Nucleic Acids Res.* 33:6114-6123.

- Li, X and L. Krumholz.** 2009. Thioredoxin is Involved in U(VI) and Cr(VI) Reduction in *Desulfovibrio desulfuricans* G20. J. Bacteriol. published online ahead of print.
- Löffler, F. E., R. A. Sanford, and J. M. Tiedje.** 1996. Initial characterization of a reductive dehalogenase from *Desulfitobacterium chlororespirans* Co23. Appl. Environ. Microbiol. 62:4982-4985.
- Lovley, D. R.** 1993a. Dissimilatory metal reduction. Annu. Rev. Microbiol. 47:263-290.
- Lovley, D. R., P. K. Widman, J. C. Woodward and E. J. Phillips.** 1993b. Reduction of uranium by cytochrome c3 of *Desulfovibrio vulgaris*. Appl. Environ. Microbiol. 59:3572-3576.
- Lovley, D. R. and E. J. P. Phillips.** 1988. Novel mode of microbial energy metabolism: organic carbon oxidation coupled to dissimilatory reduction of iron or manganese. Appl. Environ. Microbiol. 54:1472-1480.
- Madsen, T. and D. Licht.** 1992. Isolation and characterization of an anaerobic chlorophenol-transforming bacterium. Appl. Environ. Microbiol. 58:2874-2878.
- Miller, T. L. and W. J. Wolin.** 1974. A serum bottle modification of the Hungate technique for cultivating obligate anaerobes. Appl. Microbiol. 27:985-987.
- Niggemyer, A., S. Spring, E. Stackebrandt, and R. F. Rosenzweig.** 2001. Isolation and characterization of a novel As(V)-reducing bacterium: implications for arsenic mobilization and the genus *Desulfitobacterium*. Appl. Environ. Microbiol. 67:5568-5580.
- Payne, R. B., L. Casalot, T. Rivere, J. H. Terry, L. Larsen, B. J. Giles and J. D. Wall.** 2004. Interaction between uranium and the cytochrome c3 of *Desulfovibrio desulfuricans* strain G20. Arch. Microbiol. 181:398-406.
- Ridley, H., C. A. Watts, D. J. Richardson, and C. S. Butler.** 2006. Resolution of distinct membrane-bound enzymes from *Enterobacter cloacae* SLD1a-1 that are responsible for selective reduction of nitrate and selenate oxyanions. Appl. Environ. Microbiol. 72:5173-5180.
- Riley, R.G., J. M. Zachara, and F. J. Wobber.** 1992. Chemical contaminants on DOE lands and selection of contaminant mixtures for subsurface science research. DOE/ER-0547T. U.S. Dept. of Energy. Subsurface Science Program, Washington, DC.
- Rooney-Varga, J. N., R. T. Anderson, J. L. Fraga, D. Ringelberg, and D. R. Lovley.** 1999. Microbial communities associated with anaerobic benzene degradation in a petroleum-contaminated aquifer. Appl. Environ. Microbiol. 65:3056-3064.
- Sani, R. K., B. M. Peyton and A. Dohnalkova.** 2006. Toxic effects of uranium on *Desulfovibrio desulfuricans* G20. Environ. Toxicol. Chem. 25:1231-1238.

Watts, C. A., H. Ridley, K. L. Condie, J. T. Leaver, D. J. Richardson, and C. S. Butler. 2003. Selenate reduction by *Enterobacter cloacae* SLD1a-1 is catalyzed by a molybdenum-dependent membrane-bound nitrate reductase. FEMS Microbiol. Lett. 228:273-279.

Wolin, E. A., R. S. Wolfe, and M. J. Wolin. 1963. Viologen dye inhibition of methane formation by *Methanobacillus omelianskii*. J. Bacteriol. 87:993-998.

Chapter IV

Exterior Membrane-Bound Selenium Vesicles Produced by *Desulfitobacterium hafniense* DCB-2 in Response to Selenate Exposure.

ABSTRACT

Desulfitobacterium hafniense DCB-2, a Gram-positive bacterium with abilities to reduce N, S, Fe, Mn and chlorinated compounds, grew in minimal medium with selenate concentrations up to 25 mM, and reduced both selenate and selenite to insoluble Se(0) forms. When grown with selenate, the cells produced extracellular vesicles containing the selenium, while the cells contained no detectable selenium. Gram, lipophilic, live/dead® and DAPI stains confirmed that the Se-containing vesicles possessed membranes with cell wall but lacked detectable DNA. Red and black selenium precipitates were produced when grown with selenate, while only a red precipitate was produced from growth with 1 mM selenite. Se XANES established that both red and black precipitates were elemental selenium, and XRD showed that the red precipitates are XRD amorphous and the black precipitates are slightly more ordered with several small broad peaks consistent with elemental selenium. Extrusion of membrane vesicles that bind the reduced selenium appears to be a mechanism to protect cells from selenium toxicity as well as results in insoluble selenium.

INTRODUCTION

Selenium is found in four oxidation states in nature: Se(-II) (sodium selenide and hydrogen selenide), Se(0) (colloidal, elemental selenium), Se(IV) (selenite, selenium dioxide and selenious acid), and Se(VI) (selenate and selenic acid). Although an essential trace element, selenium is toxic at only three to five times its required concentration for nutrition, producing clinical symptoms such as “blind staggers”, hair loss, and nail disfigurement (Diplock 1981, NAS 1976, Young 1981). Elemental selenium is neither absorbed by the intestine nor taken up by plants; however, selenite and selenate are soluble and taken up by plants. Soils elevated in these ions can cause elevated Se concentrations in plants and toxicity in organisms ingesting them. Distribution of selenium in soil varies regionally, ranging from 0.1 to 4.3 ppm in US soils with a mean of 0.3 ppm (Shacklette 1974). Selenate is the most bioavailable form and predominates in most soils above pH 5.5 (Elrashidi and Adriano 1987, Neal 1987 and 1989, Shamberger 1981).

Bioreduction to insoluble Se(0) using bacteria has been proposed as a means of selenate and selenite bioremediation from sites with toxic levels; thereby decreasing the risk to humans, plants, and animals (Losi 1997). Bacterial species capable of reducing selenate have been identified in many phylogenetic groups. Some can use selenium reduction to support growth as a terminal electron acceptor, while others reduce selenium without supporting growth (Stolz 1999). Microorganisms capable of reducing selenate for respiratory growth include some Crenarcheota, β -, γ -, δ -, ϵ - Proteobacteria, and both low and high G+C Gram-positive bacteria (Stolz 2002, Narasingarao 2007, Huber 2000).

However, the processes by which bacteria reduce selenium are poorly understood.

Several bacterial genera have been studied to gain insight into bioreduction of selenate. In *Sulfospirillum barnesii*, selenate reduction is localized in the membrane fraction, while a soluble selenate reductase has been isolated from *Thauera selenatis* (Stolz 2002). There is no consistent pattern as to where bacteria localize reduced (insoluble) selenium since it is found in the cytoplasm, cell wall, or the surrounding medium, and in various combinations of these three in different species (Milne 1998). Whole cells and cell-free extracts of *Clostridium pasteurianum* reduce selenate to elemental selenium, but cell-associated selenium was not found (Harrison 1980). Oremland (2004) reported *Bacillus selenitireducens*, *S. barnesii*, and *Sulfospirillum shriftii* produce uniform nanospheres of elemental selenium following selenium reduction, which were located both internal and external to the cell. These elemental selenium spheres were either red or black, indicative of reduction state, for each bacterial species, but were never both colors. Sulfate and nitrate reduction pathways have been shown to also reduce selenate in some bacteria (Milne 1998). In *S. barnesii*, however, selenate and nitrate induced different reduction pathways, though both pathways could reduce selenite and nitrite (Oremland 1994). The dissimilatory sulfur reduction pathway was also proposed to reduce selenite, but not selenate.

We studied selenium reduction in *Desulfitobacterium hafniense* DCB-2, a Gram-positive, spore-forming anaerobe with a broad capacity for using inorganic electron acceptors for growth, including iron, manganese, arsenic, nitrate, sulfite, but not sulfate (unpublished

data and Christiansen 1996). Here we focus on its selenium reducing abilities, its reduction products, and the selenium-containing vesicles it produces when grown with selenate. We then propose a morphologically-based model of selenate reduction in which external vesicles play a key role.

METHODS

Culture conditions. *Desulfitobacterium hafniense* DCB-2 was cultivated using strict anaerobic technique at 37°C in a modified DCB-1 medium: (per liter) 1 g NaCl, 0.5 g MgCl₂, 0.2 g KH₂PO₄, 0.3 g KCl, 0.3 g NH₄Cl, 15 mg CaCl₂, with 1 ml trace elements solution SL-10, 1 ml selenite tungstate solution, 0.25 mg resazurin, and 10 mM HEPES, pH 7.0 (Löffler 1996, Tschech 1984, Widdel 1983). Salts and trace elements were mixed, heated and cooled under a gas mixture of N₂:CO₂ (95:5) (Miller 1974). Cysteine (0.08 g) was added, and the medium was buffered to pH 7.0 with NaHCO₃. The medium was then dispensed into 25 ml Balch tubes, 120 ml or 1 L serum bottles; all sealed with butyl-rubber stoppers and aluminum crimp tops, and autoclaved for 40 min. Prior to inoculation, Wolin vitamins, (Wolin 1963), sodium pyruvate (pyruvate), and sodium selenate were added from separate sterilized stocks to yield final concentrations of 1 ml/L, 20 mM and 1 mM, respectively. Sodium selenate concentrations up to 25 mM and sodium selenite concentrations up to 1 mM were tested, but 1 mM sodium selenate was used in this study unless otherwise stated. The controls were medium without selenium inoculated with a live culture, medium with selenium but without inoculation, medium with selenium and heat-killed cells inoculated as a cell pellet, and a heat-killed culture to

which selenium was then added. Neither selenium precipitate nor any evidence of selenate or selenite reduction was observed in any of the controls.

Growth. Cultures were grown at 37°C without shaking. Samples were removed aseptically from cultures and controls using syringes in an anaerobic glove box containing N₂:H₂ (95:5) at time 0 and every 6 h, for 126 h. Portions of the samples were used immediately for optical density, organic acid analysis, colony counts, and microscopy. The remainder of the sample was frozen at -20°C for further analyses. All culture manipulations were performed in an anaerobic glove box.

Bacterial growth was monitored by optical density at 600 nm and by consumption and production of organic acids as monitored by HPLC. Samples for HPLC were collected and filtered through a 0.45 µm membrane under anaerobic conditions. Organic acids were quantified at 210 nm on a Hewlett-Packard 1050 HPLC system equipped with a heated C18 column using 0.013 N sulfuric acid as the solvent pumped at a rate of 0.6 ml/min. Standard curves of pyruvate, acetate, lactate and combinations of these were made from 40 mM down to 0.1 mM without loss of detection sensitivity. Colony counts were determined on R2A medium with 10 mM pyruvate after anaerobic incubation for 10 days in a N₂:H₂ (95:5) atmosphere at 30°C.

Microscopy. Gram stains of vesicles sampled over the time course were observed on two replicate slides per time point with each slide consisting of two replicate samples and

one control mixture of *Escherichia coli* and *Staphylococcus aureus*. Cells of wet mounts and Gram stains were observed under bright field on a Nikon epifluorescent microscope. The *E. coli* and *S. aureus* control consistently showed Gram-negative and Gram-positive staining, respectively. Portions of the same samples were used for DAPI staining, scanning electron microscopy (SEM), transmission electron microscopy (TEM), and energy dispersive spectroscopy (EDS). Duplicate samples were stained for DNA using the DAPI protocol of Bloem (1995) and viewed on a Nikon epifluorescent microscope.

Culture purity was tested in duplicate by comparing fluorescent *in situ* hybridization (FISH) staining on all samples using a Cy3-labeled universal eubacterial rDNA probe, Cy5-labeled *D. hafniense* specific rDNA probe (Lanthier 2001), and DAPI staining (Bloem 1995). *E. coli* was used as a quality control for all dyes and as a negative control for the *D. hafniense*-specific rDNA probe. Slides were observed on a Nikon epifluorescent microscope equipped with a 50 W mercury lamp.

For the live/dead® stain, propidium iodide and SYTO 9 (Molecular Probes, Eugene, Oregon) were used, while N-(3-triethylammoniumpropyl)-4- (p-diethylaminophenyl)-hexatrienyl pyridinium dibromide (FM 4-64) was used as the lipophilic dye (Molecular Probes). Live/dead® staining, lipophilic staining, SEM, TEM, and EDS were done on samples taken at 24, 48 and 72 h. Stained cultures were viewed using an Olympus FluoView 1000 laser scanning confocal microscope (Olympus America Inc., Center Valley, PA). Bright field microscopy provided target confirmation. For viewing membrane disruption in the presence of dyes, 33% formamide (Sigma Aldrich, St. Louis,

MO) was applied to avoid compromising dye fluorescence.

Three samples were prepared with gold coating for SEM and three with carbon coating for EDS. Samples were fixed in 2.5% paraformaldehyde, 2.5% glutaraldehyde and 0.1 M cacodylate buffer, pH 7.4 (Electron Microscopy Sciences, Hatfield, PA). A drop of sample was added to 1% poly-L-lysine (Sigma Aldrich) coated, 12 mm, circular cover slips and left to adhere for 5 min prior to being gently rinsed with sterile H₂O. Slow dehydration was achieved through an ethanol series of 1 min in each of 10%, 25%, 50%, 75%, 85%, 90%, 95%, and twice in 100%. A Balzers critical point dryer (Balzers, Lichtenstein) was used for drying before mounting the cover slips on aluminum stubs and coating for viewing. Gold was sputter coated using an EMSCOPE SC500 sputter coater (Ashford, Kent, Great Britain), and the carbon was coated using a carbon string evaporator (EFFA MkII Carbon Coater, Ernest F. Fullam Inc., Latham, New York). Samples were viewed on a JEOL 6400V (Japan Electron Optics Laboratories, Tokyo, Japan) microscope with a LaB6 emitter (Noran EDS). The average number of cells per stub viewed at 24 and 72 h of selenium exposure was 1,960 and 3,570 respectively, for a total of over 11,000 and 21,000 cells. At least 20 photos per stub were acquired for documentation.

Three sample replicates per time point were prepared for TEM. Each fixed sample was embedded in 2% agarose and secondarily stained with 1% osmium tetroxide (Sigma Aldrich) in 0.1 M cacodylate buffer. An acetone series of 1 min in each of 10%, 25%, 50%, 75%, 85%, 90%, 95%, and twice in 100% was used for sample dehydration. The

sample was then embedded in the epoxy resin Poly/Bed 812, cut using a MTX ultramicrotome (RMC, Tucson, AZ), and sections were placed on formvar-coated copper grids. These sections were then stained with 1% uranyl acetate followed by lead citrate with sodium hydroxide pellets present (Venable 1965). The grids were imaged on a JEOL 2200FS 200 keV emission TEM EDS (Japan Electron Optics Laboratories, Tokyo, Japan). The number of cells viewed averaged 1,790 per copper grid at 72 h of selenium exposure for a total of over 5,370 cells viewed. A minimum of 20 photos per condition were acquired for documentation.

XANES and XRD analyses. For x-ray absorption near edge structure (XANES) analysis, biomass samples containing selenium were prepared in an anaerobic glove box of N₂:H₂ (95:5). The biomass was captured on a 0.2 µm filter (Millipore, Bedford, MA), wrapped with Kapton film, and sealed air tight with Kapton tape. The x-ray measurements were made on the moist biomass paste within 24 h of preparation to prevent sample dehydration and oxygen exposure. The samples were kept in the anoxic chamber until a few hours before measurement and then transferred to the beamline in a Mason jar sealed under anoxic conditions. The Kapton sealed samples were exposed to the atmosphere during the x-ray measurement for 1 to 2 h. The Se K-edge XANES measurements were made at beamline locations MRCAT 10-ID (Segre 2000) and PNC-CAT 20-BM at the Advanced Photon Source at Argonne National Laboratory. At MRCAT, the insertion device was tapered, and the Si(III) double crystal monochromator was slew scanned. Several quick EXAFS measurements in transmission mode were

averaged for each sample. The incident ionization chamber was filled with N₂, and the transmission ionization chamber was filled with Ar:N₂ (50:50). A Rh mirror was used to remove harmonic x-rays. The x-ray beam size of 1 mm × 1 mm was incident on the sample. The beamline parameters were similar at PNC-CAT 20-BM, where the Si(III) monochromator was detuned 15% to enhance harmonic rejection, and scans were collected in step scanning mode in fluorescence with a thirteen element Ge solid state detector. The same selenium metal standard was measured with each scan and used to align the sample scans to each other.

The XANES spectra were processed using Athena (Ravel 2005) and IFEFFIT software (Newville 2001). The spectra were aligned to each other and the reference spectra. Multiple scans from the same sample were merged to increase the data quality. Linear combinations of the control sample and the sample showing the most reduction (*D. hafniense* black precipitate) were used to estimate the amount of Se in the initial oxidation state that was not reduced. The Se(0) standard was not used because of the differences measured in the white line shape and intensity, the strong peak in the spectra at the absorption edge, as compared to the samples. This measured difference may indicate small particle size within the samples compared to the standard and/or more disorder in the measured samples as compared to the standard.

X-ray diffraction (XRD) was performed on the filtered samples from synchrotron analysis of the red and black precipitates from *D. hafniense* in DCB-1 medium using a

Rigaku Miniflex x-ray diffractometer with a Cu anode with step size of 0.02° and a 2theta range from 5 to 90°. Spectra lines were compared with the lines from selenium standard ICSD-40016.

RESULTS

Growth in the presence of Se. *Desulfitobacterium hafniense* grew when incubated with sodium selenate at concentrations up to 25 mM, the highest concentration tested, but the doubling time increased with concentrations greater than 1 mM (Figure 4.1A). A red precipitate was produced when grown with all concentrations of sodium selenate and with 1 mM sodium selenite. More red precipitate was produced over time at all selenium concentrations. This particle formation accounted for the increased standard error in the optical density measurement (Figure 4.1B). Cell counts more accurately reflect cell growth and were used to calculate doubling times (Figure 4.1A). Pyruvate was consumed by *D. hafniense* to produce acetate (Figure 4.1B) similar to cells were grown without selenium. No precipitate was produced in any of the controls.

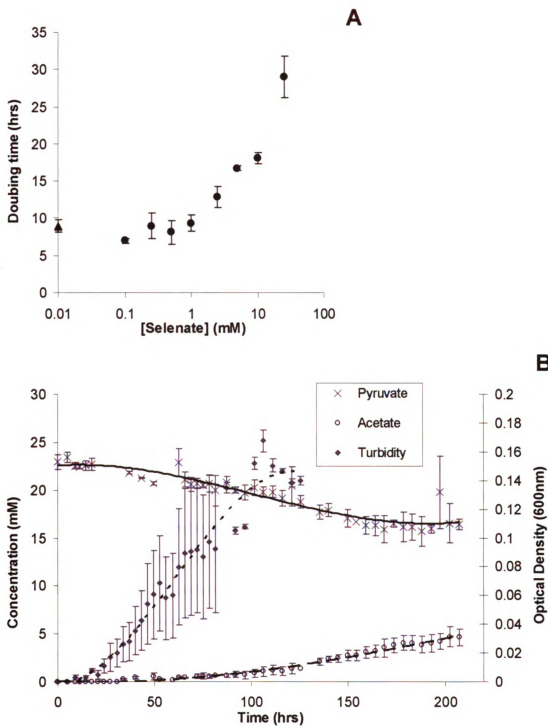


Figure 4.1. Growth of *D. hafniense* in sodium selenate medium. (A) Effect of sodium selenate concentration on growth rate: (▲) the zero concentration is displayed as 0.01 to accommodate the log scale. (B) Growth with 1 mM sodium selenate measured by optical density, pyruvate consumption and

acetate production. Standard error is shown for all measurements as vertical lines.

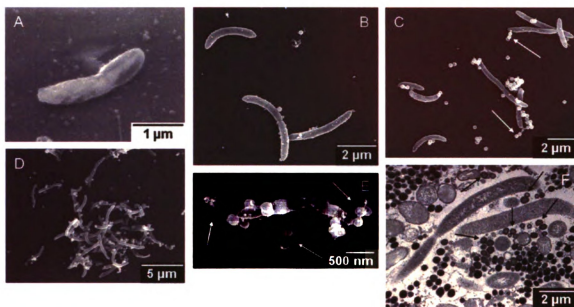


Figure 4.2. Morphological changes of *D. hafniense* cells when grown under pyruvate fermentation conditions. (A) SEM of a cell grown on pyruvate with no selenium. (B-F) Cells grown with 1 mM selenate. (B) SEM of elongated cells with buds or spheres at 24 h. (C) SEM of cells showing an increase in sphere number and development at 72 h. White arrows in C and E indicate spheres verified to be attached to cells via visible filament connections. (D) SEM of spheres both detached and cell-associated at 72 h. (E) SEM at 72 h of 'beads on a string' (filament with Se spheres). (F) TEM at 72 h of cells surrounded by spheres (very dark circles). Black arrows point to Se spheres where we found Se and lipid-binding osmium predominant around the outer edge. This was confirmed by EDS.

Sphere formation. Bright field microscopy of *D. hafniense* cells revealed an abundance of refractive spheres on and around the cells (Figure 4.2) but only when grown with sodium selenate. Images of cells taken over time during growth with 1 mM sodium selenate were viewed under SEM and TEM to determine patterns of morphological

change, including sphere production. Under SEM, selenium-grown cells were elongated (Figure 4.2B) compared to cells not exposed to selenate (Figure 4.2A). At 24 h, small raised buds, or potential spheres, were visible on the cell surface (Figure 4.2B). After 48 h, spherical structures appeared on the surface of cells or were protruding on elongated filament structures away from the cell where further buds were observed. Detached spheres were approximately 200 nm in diameter as measured by SEM. At 72 h of exposure, cells had multiple 200 nm spheres both attached and detached from the cells (Figure 4.2C and D). Electron microscopy showed filament connections between cells and spheres. New spheres appeared to repeatedly form in localized spots producing 'beads on a string' (Figure 4.2E). Selenium as determined by TEM EDS was found only associated with spheres and was not detectable in cells (detection limit 0.01%) (Figure 4.2F). Moreover, the spheres were found only external to the elongated cell. The selenium signal intensity of spheres was highest at sphere edges with different degrees of intensity internally. The majority of spheres; however, possessed strong selenium signal intensity throughout the sphere as determined by TEM EDS and shown by their dark pigmentation (Figure 4.2F).

Production of two elemental Se precipitates. In *D. hafniense* cultures grown with selenate, two different colored precipitates were noted, red and black, with red being the most predominant form. When the red and black precipitates were found together, the red precipitate formed prior to the black. In rare cases, cultures appeared to exclusively produce black precipitates, but upon closer observation, red precipitate was present. All precipitates were produced with the same medium under identical conditions. Parallel

experiments using a separate basal medium in which only the trace elements and the gaseous head space varied produced only red precipitate (data not shown), suggesting that subtle differences influence the precipitate form. In all cultures, no organism other than *D. hafniense* was found.

The Se reduction state was investigated from Se XANES spectra of the red and black precipitates along with a control sample of medium with selenium but without inoculation (negative control) and a Se metal standard (reference) (Figure 4.3A). The negative control spectrum has a strong white line, which is a strong peak in the spectra at the absorption edge. The white line was not visible in the *D. hafniense* black precipitate; this sample was used as the fully reduced standard for the linear combination fit (LCF). The white line from the negative control spectrum is barely apparent in the *D. hafniense* red precipitate spectrum. From LCF calculations, the oxidation state of Se in the red precipitate is $2 \pm 10\%$.

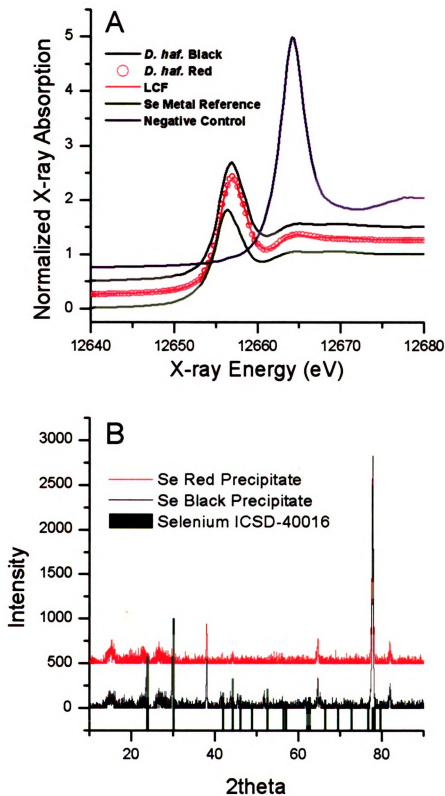


Figure 4.3. (A) Se K-edge XANES spectra from sterile selenium medium control (negative control), *D.*

hafniense cultures that formed black and red precipitates and the Se metal reference made at the APS at Argonne National Laboratory. The measured spectra for red precipitate are shown as symbols, and the LCF is shown as a line. (B) XRD spectra of red and black selenium precipitates from *D. hafniense* grown in 1 mM sodium selenate compared to the XRD pattern of metallic elemental selenium.

The structure of both precipitates was determined by XRD (Figure 4.3B). Large particles of metallic selenium did not form in the red or black precipitates, as evidenced by the absence of strong diffraction peaks in the measured XRD spectra based on the calculated pattern of metallic selenium. This occurred even though the Se XANES spectra indicate predominately elemental Se (Figure 4.3A). Instead, the red precipitates are almost XRD amorphous as no XRD signal was detected (defined by the absence of any strong diffraction peaks) (Fig 4.3B). For the black precipitates, some of the predicted lines are visible as small broad peaks indicating that some limited ordering of selenium metal particles may have occurred in this sample (Figure 4.3B). Moreover, as different XRD patterns were observed (i.e. no signal from the red precipitates, and small broad signals from the black precipitates), we suggest that the increased ordering in the precipitates is responsible for the color shift from red (XRD amorphous elemental selenium) to black (slightly crystalline elemental selenium).

Chronology of spherical, membrane-bound Se vesicles. Spherical bodies were visible on the outer surface of elongated cells exposed to selenate (Figure 4.4A). Higher atomic weights were present where spherical precipitates were located when imaged using SEM backscatter (Figure 4.4B). SEM EDS showed the selenium was concentrated in the spheres (Figure 4.4C -arrow 2), and was not detected in the cell itself (Figure 4.4C -arrow

1). The detached spheres, more prominent at 72 h, surrounded hexagonal crystals (Figure 4.4D). The crystals appeared to be composed of 200 nm spherical components that were of similar intensity in TEM backscatter (Figure 4.4E). TEM EDS (data not shown) confirmed that the hexagonal crystals were selenium. A TEM EDS line scan (Figure 4.4F and G) shows that selenium was below the detection limit in cells, but produced the highest Se signals in locations corresponding to the spheres. Osmium, which binds to lipids, was elevated not only at the edges of the cells, but also along edges of the spheres. This provides evidence that a membrane was surrounding the spheres, indicating they can be termed vesicles (Fig 4.2F and 4.4F). The carbon signal remained high throughout the cells and at regions around the vesicles, evidence consistent with lipids surrounding the vesicles. Similar results were found on eight separate TEM EDS scans that sampled 265 vesicles, 9 cells, and 14 hexagonal crystals. All evidence pointed to selenium sequestered inside the membrane bound vesicles and not in the cells.

To further discern if the selenium spheres were membrane-bound selenium vesicles, 1 mM selenate grown cultures were stained with a fluorescent lipophilic dye (FM-464). Under the confocal microscope, the dye was concentrated at the perimeter of selenium spheres and cells indicating the presence of a membrane structure also surrounding the selenium spheres (vesicles). A loss over time of the fluorescence surrounding cells, cell-associated vesicles, and detached vesicles following formamide addition demonstrated the vesicles were membrane-bound as formamide disrupts membranes. Gram stains of Se vesicle-producing cultures over time showed that both cells and vesicles stained Gram-positive, suggesting that the Gram-positive envelope also surrounded the

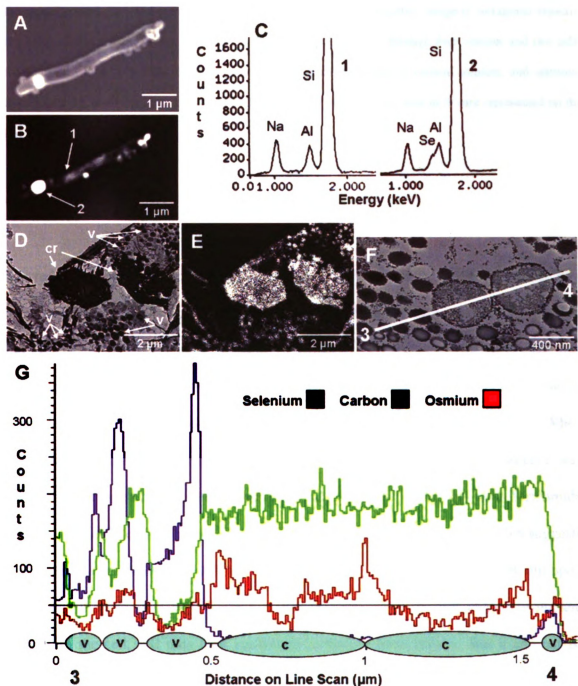


Figure 4.4. Representative SEM EDS and TEM EDS mapping of *D. hafniense* cells grown in 1 mM sodium selenate. (A) SEM of Se exposed cell displaying buds and vesicles. (B) SEM backscatter image of A. Arrows indicate regions of the image scanned by EDS. Arrow 1 points to the cell, while arrow 2 points to an associated vesicle. (C) EDS of cell in B at portions indicated by arrows 1 and 2. (D) TEM of

hexagonal crystals (cr) and surrounding vesicles (v). (E) TEM backscatter image of hexagonal crystals. (F) TEM of vesicles and cells. Line depicts the TEM EDS line scan through four vesicles and two cells from points 3 to 4. (G) TEM EDS line scan of G illustrating changes in carbon, osmium, and selenium from points 3 to 4 on the line. Locations of the vesicles (v) and cells (c) seen in (F) are represented on the line.

vesicles. Gram-negative structures were not found.

The red fluorescence of propidium iodide of the live/dead® stain provided evidence of a once living structure. Active transport across a membrane was indicated by green fluorescence of SYTO 9 dye. Green fluorescence after staining with both dyes was observed in vesicles attached to cells or cell debris, however, unattached vesicles possessed no fluorescence indicating active transport was functional in the former. When formamide was added, cells lost their green fluorescence and only red fluorescence was visible indicative of nucleic acids. All vesicles lost green fluorescence upon formamide addition, but only cell-associated vesicles showed some red fluorescence. This suggests that unattached vesicles may still possess nucleic acids, which may readily leak out upon membrane disruption with formamide. Attached vesicles may still exchange nucleic acids with the cell, and thus their nucleotide content is more stable. But it can not be ruled out that this is due to the reflecting red fluorescence of cells and not due to vesicles. *D. hafniense* cells not exposed to selenate, which do not produce vesicles, exhibited similar cellular responses to the dyes and formamide, indicating that in general nucleic acid and membrane function of the cell are not changing their reactivity with the dyes.

Since the vesicles stained with the live/dead® stain, nucleic acids must be present. Whether the vesicles contained DNA and were perhaps mini-cells was investigated using DAPI on duplicate samples taken at 20 time points. For all preparations, DAPI was only detected in the cell and not in detached vesicles. Whether DAPI stained cell-associated vesicles was unclear due to the fluorescence intensity of the cells. As the DAPI fluorescence faded; however, fluorescence was seen solely in cells and not in associated vesicles regardless of proximity. Presence of RNA was later confirmed (data not shown).

DISCUSSION

Oremland (2004) reported that some Gram-negative and Gram-positive bacteria are capable of reducing both selenate and selenite, producing spheres of elemental selenium as well as precipitates of reduced selenium inside or on the surface of bacterial cells. Here we show that *D. hafniense* DCB-2, a Gram-positive bacterium, produced extracellular vesicles in the presence of selenate and selenite, and EDS and XANES data show that these vesicles contained the reduced selenium produced by the culture. Bacterial growth is not inhibited by selenium until concentrations exceed 1 mM selenate (Figure 4.1). No selenium was detected in the cells. Hence, vesicle production and selenium fate are closely linked.

D. hafniense could not have reduced selenate and selenite by the sulfate reduction pathway since it is incapable of sulfate reduction (Christiansen 1996). Although, *D. hafniense* can reduce nitrate, nitrate-reduction, which is inducible by nitrate in this strain, was not induced in this study. In previous studies, *T. selenatis* was found unable to

reduce selenite without the presence of nitrate (Milne 1994). Thus, the absence of nitrate in the medium with *D. hafniense* likely eliminated the potential for facilitated or passive reduction by the nitrate reduction pathway. Moreover, vesicles were not observed under any of the control growth conditions or during growth with nitrate where nitrate reduction was induced (data not shown). Thus, selenium reduction is likely by a non-sulfate and non-nitrate pathway and in concordance with vesicle production, perhaps as a detoxification mechanism.

Previous work demonstrated that only one type of elemental selenium precipitate was generated for each bacterial species capable of Se reduction (Oremland 2004). Here we show that *D. hafniense* is capable of reducing selenate to two different colored elemental selenium precipitates, red and black, with red more abundant than the black. Most pure cultures of selenium-reducing bacteria, as well as a sediment slurry, produce only the red precipitate (Oremland 1989). Selenium reduction rates were previously reported to change due to differences in temperature, media, carbon source, and substrate (Lortie 1992); however, these factors were held constant in our experiments. The ability of *D. hafniense* to also produce black selenium precipitate may be due to altered metabolism or minor differences in trace elements or gaseous head space of the medium.

Spheres of elemental selenium were produced by *D. hafniense* during the reduction of sodium selenate. Moreover, selenium-grown cells were elongated with an increasing number of spherical selenium vesicles exterior to the cell over time. Interior selenium vesicles were never found. As we determined these exterior selenium spheres were

membrane bound, the term vesicles was applied. While it had been speculated previously by Oremland (2004) that selenium nanospheres were membrane bound, conclusive evidence was missing until now.

Moreover, the vesicles produced outside the cell by *D. hafniense* were found to be bound by a membrane that was attached to the cell by a filament. Unless selenium metal is capable of interacting with crystal violet, which has not been shown previously, results indicate the vesicles likely contain cell wall and are formed by a budding event. We propose that selenium-reducing membrane proteins are present in regions of vesicle formation since the ‘bead on a string’ vesicle formations were preferentially localized, ‘hot spots’, on the cell surface. The periplasmic associated selenate reductase of *Thauera selenatis* and the presence of selenate reductase activity pointedly in the membrane of *Sulfospirillum barnesii* give precedence to this hypothesis (Schröder 1997, Stolz 1997).

We tested whether the vesicles were created for the purposes of selenium sequestration and reduction. The high abundance of only selenium spectroscopic patterns in the vesicles and the lack of vesicles in selenium-free cultures suggest that vesicles resulted in protecting the cell from selenium toxicity. The lack of DAPI and propidium iodide in detached vesicles and in protruding attached vesicles indicates no functional DNA was present in these vesicles. We speculate that DNA is also not present in vesicles closely associated with the cell membrane as a fading DAPI fluorescence signal was only detected to emanate from the cell and not from any attached structure. The red fluorescence of detached vesicles stained with the lipophilic dye indicates the presence of

a vesicle membrane. SYTO-9 and propidium iodide of the live/dead® stain binds DNA and RNA to produce green and red fluorescence. Green fluorescence was observed in vesicles attached to cells or cell debris, but upon formamide addition the green fluorescence quickly became red from propidium iodide and then was lost entirely. Thus, these vesicles likely contain some RNA, which upon disruption of the vesicle membrane by formamide is lost to the surrounding matrix. Presence of active transport across the vesicle membrane may also be supported by the presence of green fluorescence inside vesicles. The lack of fluorescence in completely detached vesicles still possessing membrane supports the breakdown of the RNA without replenishment. Thus, we conclude the main purpose of the vesicles is to sequester and subsequently reduce selenium.

Previous studies have found bacteria, such as *Bacillus selenitireducens* and *Selenihalanaerobacter shriftii*, capable of producing both external and internal selenium spheres. However, only extracellular selenium vesicles were produced by *D. hafniense* cultures. Since selenium levels were below EDS detection limits in cells, it was not sequestered in cells, but selenium molecules may still induce the vesicle response. Based on our observations of *D. hafniense* growth in the presence of selenate, we propose a model describing external vesicle formation and their fate. First, the cell detects selenium in the environment and in response begins manufacturing a pool of membrane associated selenium influx pumps, reductases, and other specialized proteins. These selenium-reducing proteins flock to locales on the cell envelope which initiates bud formation. In an effort to separate the potentially toxic selenium area, the cell completely

surrounds the selenium with membrane, forming a vesicle. To make room for further reduction structures, a fully developed vesicle is then pushed away from the cell leaving a thin filament connection between the vesicle and cell. A new bud forms at the site of the filament and develops into a vesicle that has high concentrations of selenium-reducing proteins. These 'hot spots' for vesicle formation result in the 'beads on a string' morphology of multiple attached vesicles. At some point the filament and associated vesicles break away from the cell. The detached vesicles may continue to reduce selenium as long as there is reductant and functional reductase. The vesicles eventually slough off the inactive membrane, and with proper conditions the selenium coalesces into larger hexagonal selenium crystals.

Vesicles have been produced by other bacteria in response to a variety of stimuli, such as iron, e.g. the production of internal magnetosomes for magnetotaxis (Gorby 1988). Here the metal response appears to be a detoxification reducing the selenium to an insoluble form. Determining the amount of reduction a vesicle performs remains to be answered. Do the vesicles remain active until their potential is exhausted, until a vesicle has reached capacity, or until a vesicle is released from a filament connection to the cell? With respect to the final question, our confocal microscopy data of the live/dead® stain and TEM EDS supports the continued presence of selenium-reducing activity in vesicles even after separation from the cell. Moreover, if these vesicles are capable of reducing selenium when detached from the cell, the potential remains for sustained and dispersed remediation of selenium in the environment.

This research may prove of interest to those in selenium bioremediation for bioreduction of mobile selenium in the environment. The nano-scale selenium vesicle product also lends itself to nanotechnology. The electronics and glass industries in particular, which require high purities of selenium and comprise 10% and 30% of the US selenium market, respectively (Butterman 2004), may be interested in the potential of vesicles to reduce selenium when detached from the microbial cell. As the global selenium demand is projected to continually increase (Backman 2008), perhaps bioreduction will prove useful in selenium recovery and purification.

ACKNOWLEDGEMENTS

Research was supported by the U.S. Department of Energy, Office of Science, Environmental Remediation Science and Genomes to Life Programs. I am grateful to the beamline staff at Argonne National Laboratory (Argonne, IL), in particular Dr. Mali Balasubramanian at Pacific Northwest Consortium Collaborative Access Team (PNC-CAT) Sector 20-BM and Dr. Soma Chattopadhyay at Material Research Collaborative Access Team (MR-CAT) Sector 10-ID for their assistance with the x-ray measurements. MRCAT operations are supported by the Department of Energy and the MR-CAT member institutions. Use of the Advanced Photon Source was supported by the U.S. Department of Energy, Office of Science, Office of Basic Energy Sciences, under Contract No DE-AC02-06CH11357. The author would especially like to thank Dr. Shelly Kelly for assistance at Argonne National Laboratory performing beamline and XRD studies, evaluating XANES data, and providing Figure 4.3.

REFERENCES

- Backman, C-M.** 2008. Global supply and demand of metals in the future. *J. Tox. Env. Health.* 71:1244-1253.
- Bloem, J.** 1995. Fluorescent staining of microbes for total counts. In: Akkermans A.D.L., Elsas J.D., Bruijn F.J. (eds), *Molecular Microbial Ecology Manual*. Kluwer Academic Press, Dordrecht, The Netherlands, pp. 1-12.
- Butterman, W. C. and R. D. Brown Jr.** 2004. Mineral commodity profile: selenium. US Geological Survey. Open file report 03-018.
- Christiansen, N. and F. K. Ahring.** 1996. *Desulfitobacterium hafniense* sp. nov., anaerobic, reductively dechlorinating bacterium. *Int. J. Syst. Bacteriol.* 46:442-448.
- Diplock, A. T.** 1981. Metabolic and Functional Defects in Selenium Deficiency. *Philos. Trans. R. Soc. London Ser. B* 294:105-117.
- Elrashidi, M. A., and D. C. Adriano.** 1987. Effect of redox potential and pH on chemical speciation of inorganic selenium in soils. Sixth International Conference on Heavy Metals in the Environment, New Orleans. Proceedings Vol. 1, pp. 107-109. CEP Consultants Ltd., Edinburgh.
- Gorby, Y. A., T. J. Beveridge, and R. P. Blakemore.** 1988. Characterization of the bacterial magnetosome membrane. *J. Bacteriol.* 170:834-841.
- Harrison, G. I., E. J. Laishley, and H. R. Krouse.** 1980. Stable isotope fractionation by *Clostridium pasteurianum*. 3. effect of SeO_3^{2-} on the physiology and associated sulfur isotope fractionation during SO_3^{2-} and SO_4^{2-} reductions. *Can. J. Microbiol.* 26:952-958.
- Huber, R., M. Sacher, A. Vollmann, H. Huber, and D. Rose.** 2000. Respiration of arsenate and selenate by hyperthermophilic archaea. *Syst. Appl. Microbiol.* 23:305-14.
- Lanthier, M., R. Villemur, F. Lepine, J-G. Bisailon, and R. Beaudet.** 2001. Geographic distribution of *Desulfitobacterium frappieri* PCP-1 and *Desulfitobacterium* spp. in soils from the province of Quebec, Canada. *FEMS Micro. Ecol.* 36:185-191.
- Löffler, F. E., R. A. Sanford, and J. M. Tiedje.** 1996. Initial characterization of a reductive dehalogenase from *Desulfitobacterium chlororespirans* Co23. *Appl. Environ. Microbiol.* 62:4982-4985.
- Lortie, L., W. D. Gould, S. Rajan, R. G. L. McCready, and K.-J. Cheng.** 1992. Reduction of selenate and selenite to elemental selenium by a *Pseudomonas stutzeri* isolate. *Appl. Environ. Microbiol.* 58:4042-4044.
- Losi, M. E., and W. T. Frankenberger Jr.** 1997. Bioremediation of selenium in soil and water. *Soil. Sci.* 162:692-702.

Miller, T. L. and W. J. Wolin. 1974. A serum bottle modification of the Hungate technique for cultivating obligate anaerobes. *Appl. Microbiol.* 27:985-987.

Milne, J. B. 1998. The uptake and metabolism of inorganic selenium species. In: W. T. Frankenberger and R. A. Engberg. (eds), *Environmental Chemistry of Selenium*. Marcel Dekker, New York, pp. 459-478.

Narasingarao, P., and M. M. Häggblom. 2007. *Pelobacter seleniigenes* sp. nov., a selenate-respiring bacterium. *Int. J. Syst. Evol. Microbiol.* 57:1937-1942.

NAS. 1976. Medical and biological effects of environmental pollutants - selenium. National Academy of Sciences, Washington, D.C.

Neal R. H., and G. Sposito. 1989. Selenate adsorption on alluvial soils. *Soil Sci. Soc. Am. J.* 53:70-74.

Neal, R. H., G. Sposito, K. M. Holtzclaw, and S. J. Traina. 1987. Selenite adsorption on alluvial soils: I. Soil composition and pH effects. *Soil Sci. Soc. Am. J.* 51:1161-1165.

Newville, M. 2001. IFEFFIT: interactive XAFS analysis and FEFF fitting. *J. Synch. Rad.* 8:322-324.

Oremland, R. S., J. T. Hollibaugh, A. S. Maest, T. S. Presser, L. G. Miller, C. W. Culbertson. 1989. Selenate reduction to elemental selenium by anaerobic bacteria in sediments and culture: biogeochemical significance of a novel, sulfate independent respiration. *Appl. Environ. Microbiol.* 55:2333-2343.

Oremland, R. S. J. Switzer Blum, C. W. Culbertson, P. T. Visscher, L. G. Miller, P. Dowdle, and F. E. Strohmaier. 1994 Isolation, growth, and metabolism of an obligately anaerobic, selenate-respiring bacterium, strain SES-3. *Appl. Environ. Microbiol.* 60:3011-3019.

Oremland, R. S., M. J. Herbel, J. Switzer Blum, S. Langley, T. J. Beveridge, P. M. Ajayan, T. Sutto, A. V. Ellis, and S. Curran. 2004. Structural and spectral features of selenium nanospheres produced by Se-respiring bacteria. *Appl. Environ. Microbiol.* 70:52-60.

Ravel, B., and M. Newville. 2005. ATHENA, ARTEMIS, HEPHAESTUS: data analysis for X-ray absorption spectroscopy using IFEFFIT. *J. Synch. Rad.* 12:537-541.

Schröder, I., S. Rech, T. Kralft, and J. M. Macy. 1997. Purification and characterization of the selenate reductase from *Thauera selenatis*. *J. Biol. Chem.* 272:23765-23768.

Segre, C. U., N. E. Leyarovska, L. D. Chapman, W. M. Lavender, P. W. Plag, A. S. King, A. J. Kropf, B. A. Bunker, K. M. Kemner, P. Dutta, R. S. Druan, J. Kaduk. 2000. The MRCAT insertion device beamline at the advanced photon source. Synchrotron Rad. Inst. CP521:419-422.

Shacklette, H. T., J. G. Boerngen, and J. R. Keith. 1974. Survey Circular 692. US Department of Interior, Washington, D.C.

Shamberger, R. J. 1981. Selenium in the environment. Sci Total Environ. 17:59-74.

Stolz, J. F., T. Gugliuzza, J. Switzer Blum, R. Oremland, and F. M. Murillo. 1997. Differential cytochrome content and reductase activity in *Geospirillum barnesii* strain SES-3. Arch. Microbiol. 167:1-5.

Stolz, J. F., P. Basu, and R. S. Oremland. 2002. Microbial transformation of elements: the case of arsenic and selenium. Int. Microbiol. 5:201-207.

Tschech, A., and N. Pfennig. 1984. Growth yield increase linked to caffeate reduction in *Acetobacterium woodii*. Arch. Microbiol. 137:163-167.

Venable, J. H., and R. Coggeshall. 1965. A simplified lead citrate stain for use in electron microscopy. J. Cell. Bio. 25:407-408.

Widdel, F., G.-W. Kohrin, and F. Mayer F. 1983. Studies on dissimilatory sulfate-reducing bacteria that decompose fatty acids. Arch. Microbiol. 134:286-294.

Wolin, E. A., R. S. Wolfe, and M. J. Wolin. 1963. Viologen dye inhibition of methane formation by *Methanobacillus omelianskii*. J. Bact. 87:993-998.

Young, V. R. 1981. Selenium: a case for its essentiality. N. Eng. J. Med. 304:1228-1230.

Chapter V

A Comparison of As(V), Fe(III) and Se(VI) Reduction by the Acetogens

Desulfitobacterium hafniense DCB-2 and *Moorella thermoacetica*

ABSTRACT

Two bacterial species, *Desulfitobacterium hafniense* DCB-2 and *Moorella thermoacetica*, were compared for growth in minimal media with metal-reducing conditions. *M. thermoacetica* was capable of growth in the presence of Cd(II), As(V) and Se(VI) but, unlike *D. hafniense*, it did not grow with lactate and soluble Fe(III) as the sole electron acceptor. It also reduced As(V to III) and Se(VI to 0) similar to *D. hafniense*, although less selenium was mineralized.

INTRODUCTION

Bacteria are capable of utilizing a large variety of electron acceptors for growth. Acetogens possess the unique ability to fix carbon to create biomass during which the carbon serves as the electron acceptor for respiration. This process has been heavily studied in thermophilic, Gram-positive *Moorella thermoacetica* (previously known as *Clostridium thermoaceticum*) with both CO₂ and CO as carbon sources and electron acceptors (Daniel 1990, Kerby 1983). Metals have never been tested as terminal electron acceptors for *M. thermoacetica*; however, functional cytochromes and menaquinone have been found as well as its ability to use nitrate, nitrite and thiosulfate as terminal electron

acceptors (Gottwald 1975, Drake 2004). Studies with metals in trace amounts for growth determined that Fe(II) was required for growth. Though Se(IV) was not required, it did enhance production of formate dehydrogenase (Andreesen 1973).

Recently, microarray data of *Desulfitobacterium hafniense* DCB-2 has detected the Wood-Ljungdahl carbon fixation pathway to be highly expressed and functional with genes similar to *M. thermoacetica* (Chapter 3). In fact, *D. hafniense* resides in the same phylogenetic family as *M. thermoacetica*. *D. hafniense* and *M. thermoacetica* are both spore-formers that were isolated from excrement and have been found in soils (Fontaine 1942, Madsen 1992, Lanthier 2004). *D. hafniense* is a Gram-positive, dehalogenator that has been found to reduce many different electron acceptors, including metals. Both species grow well fermenting pyruvate, but unlike *D. hafniense*, *M. thermoacetica* is unable to ferment fumarate (Andreesen 1973, Christiansen 1996). The phylogenetic similarities between these two organisms suggested the possibility that *M. thermoacetica* might be capable of metal reductions as well. We tested the ability of the long studied acetogen (*M. thermoacetica*) to grow with and respire Cd(II), As(V), Se(VI), and Fe(III) and compared these results to *D. hafniense*.

METHODS

Bacterial strains. *M. thermoacetica* and *D. hafniense* DCB-2 were originally grown in modified DCB-1 medium fermenting sodium pyruvate (pyruvate) with a head space of CO₂:N₂ (5:95) (Brumm 1988, Löffler 1996, Chapter 4). Cultures were incubated at 37°C for *D. hafniense* and 55°C for *M. thermoacetica*. These fermenting cultures served

as inocula for growth with metals. Culture purity was checked using microscopy and growth on R2A plates supplemented with 10 mM pyruvate in an anoxic chamber of H₂:N₂ (4:96) (Chapter 4).

Experimental determination of growth. Growth was determined by cell counts, optical density at 600 nm, HPLC of organic acids, and total biomass production (TOC) (Chapters 2, 3 and 4). Two replicate samples were sent for TOC analysis at UC Davis Stable Isotope Facility (Davis, CA) following freeze-drying of combined sample pellets from initial centrifugation and centrifugation of ethanol (2:3) precipitated sample supernatants. Controls consisted of media conditions without cells, cultures without electron acceptor addition, and culture conditions with heat-killed cells. When testing *M. thermoacetica* for growth with metals and metal reduction abilities, *D. hafniense* served as the positive control.

Measurements of growth with metals. Both strains were grown with Cd(II), As(V), Se(VI), and Fe(III) in two different media: modified DCB-1 with 20 mM pyruvate and Wolin vitamins (1×) in CO₂:N₂ (5:95) and carbonate-buffered freshwater medium (CBF) with 20 mM sodium lactate (lactate) in CO₂:N₂ (20:80) (Löffler 1996, Lovley 1996, Wolin 1963, and Chapters 2 and 4). The electron acceptors were presented as 50 mM ferric citrate, 1 mM sodium arsenate, and 1 mM sodium selenate. Mineralization of selenium was measured by inductively coupled plasma mass spectrometry (ICP-MS) (Chapter 2). Upon precipitate production in cultures, reduction of the electron acceptors

was determined using x-ray absorption spectroscopy (XAS) (Chapter 2).

RESULTS

The ability of *M. thermoacetica* to grow with Cd(II), As(V), Se(VI), and Fe(III) were compared to cultures unexposed to metals (Table 5.1). Cultures grown in DCB-1 with As(V) produced 38% more biomass than unexposed cultures. Growth with As(V) as the sole electron acceptor (CBF medium with lactate) was found with twice the amount of cell material being produced compared to the amount attributable to inoculation (CBF with lactate alone). However, this growth with As(V) in CBF had only 17% (5-fold less) the amount of biomass as growth in DCB-1 with As(V). Similar biomass production levels were found in DCB-1 medium with pyruvate for both Cd(II) and Se(VI), which were about 33% less than pyruvate-fermenting cultures alone. Although previously found to grow and affect precipitation of Cd(II) in complex media (Cunningham 1993), *M. thermoacetica* demonstrated repressed growth in our study with Cd(II). Growth did not occur using Fe(III) as a sole terminal electron acceptor in CBF medium with lactate.

The generation times for *M. thermoacetica* DCB-1 medium with and without metal were all within 30 min of each other (Table 5.1). Fermentative growth without metal had the fastest generation time of 3.5 h, followed by As(V), Cd(II), and Se(VI). No growth was detected when grown in CBF medium with lactate alone or with Fe(III) and lactate. The change in time between DCB-1 and CBF media with As(V) was nearly 3-fold. This

Table 5.1. Generation times and cell yields of *M. thermoacetica* and *D. hafniense* with metals

Metal	Metal concentration (mM)	Organism	Medium	Carbon source (20 mM)	Biomass produced (mg/L)	Generation time (h)
-	-	<i>M. thermoacetica</i>	DCB-1	pyruvate	34.3	3.47
Se (VI)	1	<i>M. thermoacetica</i>	DCB-1	pyruvate	22.4	3.88
Cd (II)	1	<i>M. thermoacetica</i>	DCB-1	pyruvate	24.1	3.85
As (V)	1	<i>M. thermoacetica</i>	DCB-1	pyruvate	47.2	3.63
-	-	<i>D. hafniense</i>	DCB-1	pyruvate	15.1	8.95
Se (VI)	1	<i>D. hafniense</i>	DCB-1	pyruvate	18.8	9.01
Cd (II)	1	<i>D. hafniense</i>	DCB-1	pyruvate	15.1	8.9
As (V)	1	<i>D. hafniense</i>	DCB-1	pyruvate	28.30	7.78
-	-	<i>M. thermoacetica</i>	CBF	lactate	3.19	unable to determine
Fe (III)	50	<i>M. thermoacetica</i>	CBF	lactate	..**	unable to determine
As (V)	1	<i>M. thermoacetica</i>	CBF	lactate	8.30	10.2
-	-	<i>D. hafniense</i>	CBF	lactate	0.295	unable to determine
Fe (III)	50	<i>D. hafniense</i>	CBF	lactate	1330	4.49
As (V)	1	<i>D. hafniense</i>	CBF	lactate	32.1	7.08

* Generation time could not be determined for these conditions due to lack of measureable cell growth

** Biomass was undetectable for *M. thermoacetica* in CBF with Fe (III) above background

along with the biomass production data suggest that growth is considerably more strained with lactate and As(V) as the sole electron acceptor (Table 5.1).

This contrasted growth in DCB-1 by *D. hafniense* which had an equal amount of biomass production with Cd(II) (15.1 mg/L) and greater amount with Se(VI) (18.1 mg/L) than pyruvate fermentation alone, while growth with As(V) produced 46% more biomass (Table 5.1). While *M. thermoacetica*, which had longer generation times in all cultures with metals, *D. hafniense* had similar generation times with Cd(II) and Se(VI) to cultures unexposed to metal. Moreover, the generation time for *D. hafniense* with As(V) was faster in DCB-1 medium than unexposed cultures. In CBF medium, *D. hafniense* had a considerably faster generation time with As(V) (21% faster) and Fe(III) (2-fold increase) and As(V) (21% faster), while *M. thermoacetica* grew 2.9-fold slower with As(V) and had no growth with Fe(III).

Table 5.2. Se (VI) mineralization ability of *M. thermoacetica* and *D. hafniense*

Organism	Medium	Metal concentration (mM)	Metal in solution (ppm)	Percent metal in solution relative to "no cells" (ppm/ppm)
No cells	DCB-1	1 mM Se (VI)	78.1	100
<i>M. thermoacetica</i>	DCB-1	1 mM Se (VI)	16.3	20.9
<i>D. hafniense</i>	DCB-1	1 mM Se (VI)	0.18	0.230

Reduction analyses using XAS for precipitates in cultures with Cd(II), As(V), or Se(IV) showed Cd(II) was not reduced, while As(V to III) and Se(VI to 0) were reduced (data not shown). These results are similar to those found with *D. hafniense*. Cd(II) was previously shown to be precipitated as CdS by *M. thermoacetica*; however, these experiments were performed in undefined medium (Cunningham 1993). Unlike *D. hafniense*, which produced both red and black precipitates with Se(VI), *M. thermoacetica* produced only red precipitates (Chapters 2 and 4). Extracellular vesicles on *M. thermoacetica* were observed and were similar to those produced by *D. hafniense*, but only a 10-fold increase in biomass above inoculation was measured for *M. thermoacetica*, while there was a 50-fold increase for *D. hafniense*. Tests for removal of Se from solution using ICP-MS found *M. thermoacetica* was able to mineralize 80% (Table 5.2). This illustrates it was less effective at selenium mineralization than *D. hafniense*, which removed 99.9% from solution.

Studies with *M. thermoacetica* in ferric citrate yielded no precipitate or biomass production above levels attributable to inoculation. These results along with lack of Fe(III) reduction indicate that *M. thermoacetica* was unable to grow with soluble Fe(III) as the sole electron acceptor with lactate. This greatly contrasts the profuse biomass

production coupled to iron reduction observed with *D. hafniense*, and is surprising as the formate dehydrogenase of *M. thermoacetica* possesses 30% amino acid homology to corresponding subunits of the soluble Fe(III) reductase of *Geobacter sulfurreducens* (Kaufmann 2001). The profuse amount of biomass production by *D. hafniense* in cultures with Fe(III) is likely attributable to a combination of carbon substrates supporting growth, such as lactate with citrate, CO₂ fixation, and acetate (Chapter 2).

DISCUSSION

M. thermoacetica was determined to have depressed growth with Cd(II) and Se(VI). Extracellular vesicles similar to those of *D. hafniense* were seen when grown in the presence of Se(VI), but growth was depressed. Vesicle production by *M. thermoacetica* (Table 5.2) and in other studies with *D. hafniense* (Chapter 4), *Sulfospirillum barnesii*, *Sulfospirillum shriftii*, and *Bacillus selenitireducens* (Oremland 2004) do suggest that this method may be a general approach for cells to mineralize and detoxify selenium. Despite having a higher optimum growth temperature, *M. thermoacetica* was unable to produce the increase in biomass observed with *D. hafniense* in medium with As(V), Se(VI), Cd(II), and Fe(III). It appeared that with the considerably slower generation time and significantly lower biomass yields of *M. thermoacetica* in CBF with As(V) and lactate, fermentation with pyruvate is a preferred mode of growth. *M. thermoacetica* is typically cultivated with yeast extract to produce greater than 30% more in biomass yields, despite being able to ferment molecules such as oxalate and pyruvate (Daniel 1993). From our study, using yeast extract, peptone, tomato juice, and other complex nutrients in medium are unnecessary, which is important as they can affect metal reduction results.

This study discovered new metabolic capabilities in *M. thermoacetica* by comparing it to known abilities in a species from the same family (*D. hafniense*) that possessed a homologous major carbon pathway. Large similarities exist [e.g. acetogenic ability, reduction of As(V) and Se(VI), and altered ligand binding with Cd(II)] as do stark contrasts [e.g. growth yields with metals, and reduction of soluble Fe(III)]. These comparisons can help to determine the role of these bacteria in the environment. The findings may also have impacts for bioremediation of thermophilic environments, particularly with Fe(III) and As(V) since As(V) adsorbs to Fe(III).

ACKNOWLEDGEMENTS

Use of the Advanced Photon Source was supported by the U.S. Department of Energy, Office of Science, Office of Basic Energy Sciences, under Contract No DE-AC02-06CH11357. The assistance of Dr. Shelly Kelly was greatly appreciated during beamline studies and performing XAS analyses at Argonne National Laboratory (Argonne, IL). Dr. Ed O'Loughlin of the Molecular Environmental Science Group in the Biosciences Division at Argonne National Laboratory was gracious to collect ICP-MS data. The technical assistance of Dr. Mali Balasubramanian at Pacific Northwest Consortium Collaborative Access Team (PNC-CAT) Sector 20-BM at Argonne National Laboratory was also appreciated during beamline studies.

REFERENCES

- Andreesen, J. R., A. Schaupp, C. Neurauter, A. Brown, and L. G. Ljungdahl.** 1973. Fermentation of glucose, fructose, and xylose by *Clostridium thermoaceticum*; effect of metals on growth yield, enzymes, and the synthesis of acetate from CO₂. J. Bacteriol. 114:743-751.
- Brumm, P. J.** 1988. Fermentation of single and mixed substrates by the parent and an acid-tolerant mutant strain of *Clostridium thermoaceticum*. Biotech. Bioeng. 32:444-450.
- Christiansen, N. and F. K. Ahring.** 1996. *Desulfitobacterium hafniense* sp. nov., anaerobic, reductively dechlorinating bacterium. Int. J. Syst. Bacteriol. 46:442-448.
- Cunningham, D. P. and L. L. Lundie Jr.** 1993. Precipitation of cadmium by *Clostridium thermoaceticum*. Appl. Environ. Microbiol. 59:7-14.
- Daniel, S. L. and H. L. Drake.** 1990. Characterization of the H₂- and CO-dependent chemolithotrophic potentials of the acetogens *Clostridium thermoaceticum* and *Acetogenium kivui*. J. Bacteriol. 172:4464-4471.
- Daniel, S. L. and H. L. Drake.** 1993. Oxalate- and glyoxylate-dependent growth and acetogenesis by *Clostridium thermoaceticum*. Appl. Environ. Microbiol. 59:3062-3069.
- Fontaine, F. E., W. H. Peterson, E. McCoy, M. J. Johnson, and G. J. Ritter.** 1942. A new type of glucose fermentation by *Clostridium thermoaceticum*. J. Bacteriol. 43:701-715.
- Gottwald, M., J. R. Andreesen, J. Legall, and L. G. Ljungdahl.** 1975. Presence of cytochrome and menaquinone in *Clostridium formicoaceticum* and *Clostridium thermoaceticum*. J. Bacteriol. 122:325-328.
- Kaufmann, F. and D. R. Lovley.** 2001. Isolation and characterization of a soluble NADPH-dependent Fe(III) reductase from *Geobacter sulfurreducens*. J. Bacteriol. 183:4468-4476.
- Kerby, R. and J. G. Zeikus.** 1983. Growth of *Clostridium thermoaceticum* on H₂/CO₂ or CO as energy source. Curr. Microbiol. 8:27-30.
- Lanthier, M., R. Villemur, F. Lepine, J-G. Bisailon, and R. Beaudet.** 2001. Geographic distribution of *Desulfitobacterium frappieri* PCP-1 and *Desulfitobacterium* spp. in soils from the province of Quebec, Canada. FEMS Micro. Ecol. 36:185-191.
- Löffler, F. E., R. A. Sanford, and J. M. Tiedje.** 1996. Initial characterization of a reductive dehalogenase from *Desulfitobacterium chlororespirans* Co23. Appl. Environ. Microbiol. 62:4982-4985.

Lovley, D. R. and E. J. P. Phillips. 1988. Novel mode of microbial energy metabolism: organic carbon oxidation coupled to dissimilatory reduction of iron or manganese. *Appl. Environ. Microbiol.* 54:1472-1480.

Madsen, T. and D. Licht. 1992. Isolation and characterization of an anaerobic chlorophenol-transforming bacterium. *Appl. Environ. Microbiol.* 58:2874-2878.

Miller, T. L. and W. J. Wolin. 1974. A serum bottle modification of the Hungate technique for cultivating obligate anaerobes. *Appl. Environ. Microbiol.* 27:985-987.

Oremland, R. S., M. J. Herbel, J. Switzer Blum, S. Langley, T. J. Beveridge, P. M. Ajayan, T. Sutto, A. V. Ellis, and S. Curran. 2004. Structural and spectral features of selenium nanospheres produced by Se-respiring bacteria. *Appl. Environ. Microbiol.* 70:52-60.

Wolin, E. A., R. S. Wolfe, and M. J. Wolin. 1963. Viologen dye inhibition of methane formation by *Methanobacillus omelianskii*. *J. Bacteriol.* 87:993-998.

Chapter VI

SUMMARY AND CONCLUSIONS

Microbial interactions with metals can alter mobility and toxicity of a metal in the environment. Studies of these interactions can aid bioremediation of metal contaminated sites. The studies conducted in this dissertation have focused on exploring this bioremediation potential in the dehalogenator *Desulfitobacterium hafniense* DCB-2. The main objective of this research was to investigate the potential of using *D. hafniense* as the first model Gram-positive organism for dissimilatory metal reduction (Chapter 1). Having been found in metal-contaminated soils, it was selected to further understand Gram-positive microbial interactions with metals as previous metal reduction research has primarily focused on Gram-negative bacteria. These are not the first studies to report metal-reducing abilities of this bacterium; however, they are the most extensive and exhaustive proving direct interactions with the metals. This is in large part due to the detail in methods and controls, which we developed to take into account both passive and active interactions, true perpetuation of cultures in experimental conditions, and limiting outside compounding factors in measurements.

Three specific objectives were addressed during this study (Chapter 1). The first objective, “to determine the spectrum of metals reduced and which metals support growth by respiratory coupling of metal reduction to energy production”, was addressed in

Chapter 2. Growth of *D. hafniense* in the presence of metals was examined both under pyruvate fermentation conditions and respiration conditions with lactate. Nine metals were provided as terminal electron acceptors, including: As(V), Cd(II), Co(III), Cr(VI), Cu(II), Fe(III), Ni(II), Se(VI), and U(VI). During pyruvate fermentation, depressed growth from metal toxicity effects were observed at the following metal concentrations: 500 μ M Cr(VI), 1 mM Cd(II), 1 mM Ni(II), 1 mM Cu(II), 2.5 mM and above Se(VI), and all concentrations tested of U(VI). Altered binding of ligands to metals was observed with cells in As(V), Cd(II), Co(III), Cu(II), Fe(III), Ni(II), Se(VI), and U(VI) (Chapter 2). Respiration of metals with lactate occurred with As(V), Fe(III), and weakly with Cu(II) using nitrate as a positive respiration control.

Four of the nine metals tested were found to be conclusively reduced by *D. hafniense* during valence state analysis at the Advanced Photon Source synchrotron at Argonne National Laboratory (Argonne, IL) (Chapter 2). Fe(III) was reduced when presented both in a soluble form (ferric citrate) and as a solid (ferric oxide). Cr(VI) was reduced as well, but the reaction was so fast upon introduction to cultures that it was unable to be determined if cells were directly involved. When XANES analysis was examined for Cd(II), Co(III), Cu(II), and Ni(II), the metals were found not to be reduced, but rather only to have alternate ligand binding partners. The potential for incomplete reduction, or reduction of some portion of the metal introduced, below detection limits of the synchrotron exists, as growth was present using Cu(II) as a sole electron acceptor with lactate and significant loss of solubility was present for Co(III). Moreover, the color changes observed for Co(III) cultures are typical of previous reports of its reduction by

bacteria. Alternate media, carbon sources, or metal complexes introduced (e.g. using Co(III) EDTA rather than Co(III) chloride) may facilitate conclusive results to determine the reduction of Co(III), Cr(VI), and Cu(II) by *D. hafniense*.

The second specific objective was “to determine whether there are differences in the cell morphology caused by reduction of different metals, and if specific adaptations occurred to aid metal reduction” (Chapter 1). This research was conducted using Fe(III), Se(VI), and U(VI), which were all conclusively reduced (Chapters 3 and 4). Using both bright-field and electron microscopy, unusual cell morphologies (that reflected gene expression) were observed in the presence of respiration with Fe(III) and fermentation with U(VI) and Se(VI) (Chapters 3 and 4). With 50 mM Fe(III), *D. hafniense* presented itself as chains of cells, while with 0.5 mM U(VI) and 1 mM Se(VI) the cell was elongated significantly as compared to growth with pyruvate fermentation alone. These chains of cells observed with Fe(III) and lactate were shorter than pyruvate fermenting cells, and were surrounded by large amounts of exopolysaccharides, which bound the reduced Fe(II) (Chapter 3). The shorter cell, and thus larger surface area of the cell indicates that *D. hafniense* may be rapidly dividing and likely thriving while reducing Fe(III), which is supported by Fe(III)-reducing cultures having roughly half the generation time as pyruvate-fermenting cultures (Chapter 2). In contrast, cultures grown with U(VI) had a significantly slower generation time than with pyruvate fermentation alone (Chapter 2). An elongation of the cell was observed and is believed to occur due to cells resisting potential metal toxicity (Chapter 3).

Extracellular vesicles were observed both free-floating and cell-associated in the presence of Se(VI) (Chapter 4). Se(VI)-reducing cultures produced two different colors (red and black) of reduced selenium, which differed by the ordering of their crystal structures. Spectroscopy techniques coupled to microscopy revealed that Se was being sequestered within these vesicles and not within the cell. Osmium, lipophilic, and live/dead® staining provided strong evidence that the vesicles were membrane-bound (Chapter 4). The vesicles were positive for Gram-staining, signifying vesicles possessed cell wall material. Live/dead® stain, which has a strong binding specificity for DNA and RNA, further implicated the presence of nucleic acids within vesicles. DAPI did not stain vesicles demonstrating DNA was not present in the vesicles. Purified vesicles were shown to contain RNA by gel electrophoresis (with and without nucleases) and by UV absorption analysis. Time-course studies revealed the formation of vesicles over time and their connection to the cell via a filament. We have proposed a model for vesicle development as it seems to occur in stages (Chapter 4). This morphological shift to produce vesicles and the reduction ability of attached and detached vesicles should be a primary focus of further research on Se(VI) reduction in *D. hafniense*.

The third research objective was “to identify genes and major pathways involved with Fe(III), Se(VI), and U(VI) reduction” when compared to pyruvate fermentation using microarray data (Chapter 1). During Fe(III) reduction, large amounts of carbon were diverted to gluconeogenesis, which corresponds to the observed cell morphology with abundant biomass production (Chapter 3). Two different nitrogenase operons were found to be up-regulated during respiration with one functioning primarily during Fe(III)

reduction and the other during nitrate reduction (Chapter 3). Several fumarate and DMSO reductases as well as cytochromes were also highly up-regulated, which indicates their involvement in Fe(III) reduction. U(VI)-reducing cultures had many similar genes expressed as during Fe(III) reduction (Chapter 3). However, U(VI) reduction appeared to highly stress cells, up-regulating DNA repair mechanisms and cell wall biosynthesis compared to pyruvate-fermenting cultures. The possibility of cells attempting to evade high concentrations of uranium exists as chemotaxis and flagellar genes were highly expressed as well. This chemotactic response to uranium could be studied further in real-time using controlled cell chambers with microscopy. Nitrate-reducing cultures unexpectedly expressed gene groups annotated as assimilatory sulfate reduction and N₂ fixation-like function by the Nifl operon. Further investigation, possibly by knock-out mutation, must be explored to conclude the role of these expression study findings with Fe(III), U(VI), and nitrate. Many questions still surround Se(VI) reduction, as most of the genes identified as highly expressed compared to pyruvate fermentation possessed unknown function (Chapter 3). None of the known Se(VI)-reducing genes found in other bacteria were up-regulated in *D. hafniense*. While some genes potentially involved in Se(VI) reduction were found, we think focus should be directed to identifying the proteins of the selenium-containing vesicles for which we have developed a protocol (Appendix C).

Genetic studies of cultures grown with these reduced metals by microarrays revealed a highly complex use of carbon. One highly expressed gene (compared to pyruvate-fermenting conditions) was carbon monoxide dehydrogenase, which is used by the

acetyl-CoA reduction pathway, or Wood-Ljungdahl pathway (Chapter 3). Acetogenic growth by *D. hafniense* was confirmed with $\text{H}_2:\text{CO}:\text{N}_2$ (30:30:40), $\text{H}_2:\text{CO}_2:\text{N}_2$ (30:30:40), and $\text{CO}:\text{CO}_2:\text{N}_2$ (30:30:40) (Chapter 3). This pathway was previously shown to be active in the phylogenetically related acetogen, *Moorella thermoacetica*, and it was therefore used as a positive control for the experiment. The use of this CO_2 fixation pathway is likely to account for the need to shuttle excess electrons produced by the reduction of the metals. This newly discovered metabolic ability of *D. hafniense* to grow acetogenically solely using the Wood-Ljungdahl pathway also has profound implications for future research on this organism.

In related studies to this work, it was discovered that *D. hafniense* can form biofilms, which can help establish and maintain it within the environment (a characteristic desirable for bioremediation) (Appendix A). These biofilms were observed to form on two distinct surfaces (silica and activated carbon beads) under both fermentation conditions with pyruvate and respiration conditions with Fe(III) and lactate. While this observation requires future quantification, it introduces the possibility of biofilm research with *D. hafniense*.

To exemplify the role of *D. hafniense* as a model Gram-positive metal-reducer, metal reduction experiments were also performed with *M. thermoacetica*. These experiments showed that Se(VI) and As(V) were reduced to similar products made by *D. hafniense*. Both bacteria also formed Cd(II) sulfide when presented with CdCl , but remained

unchanged in controls without live cells. This had previously been found with *M. thermoacetica*, and further illustrates the similar reactions both bacteria are performing in the presence of metals. In strong contrast, however, soluble Fe(III) was not reduced by *M. thermoacetica* when presented with lactate (Chapter 5).

The guiding hypothesis for this research was that *D. hafniense* is capable of reducing metals for energy gain through dissimilatory, including respiratory, metal reduction. I have found that this hypothesis is true for the metals As(V), Fe(III), Se(VI), and U(VI), and possibly true for Co(III), Cr(VI), and Cu(II). Additionally, I hypothesized that *D. hafniense* is capable of reducing the same metals as those reduced by model, Gram-negative, metal-reducing organisms *Geobacter sulfurreducens* and *Shewanella oneidensis* MR-1. Of the nine metals tested, *D. hafniense* was found to reduce the same metals as both Gram-negative model organisms. Moreover, Cr(VI) was reduced by both Gram-negative organisms, and the likelihood that *D. hafniense* reduces it is very high. Co(III) reduction was found with *S. oneidensis* MR-1 and *G. sulfurreducens* when presented as Co(III) EDTA, and judging by our color reaction and growth studies, *D. hafniense* may also reduce Co(III) EDTA effectively. As was found with *S. oneidensis* MR-1, *D. hafniense* is able to convert the ligand binding to cadmium and copper. However, further research must be done to conclude how and why this is occurring.

In this work, examination of the metal reducing abilities of *D. hafniense* was the main objective, which was facilitated by the recently released genome sequence. This organism is of particular interest to bioremediation as a spore-former capable of

halorespiration and respiration of metals, which we have coined metalorespiration. Beyond the main objective we have discovered a previously unknown acetogenic ability of *D. hafniense* with both CO and CO₂ (Chapter 3). The capability of this bacterium to form single species biofilm was also found (Appendix A). These two significant findings aid in the potential importance it can play in bioremediation.

However, the most valuable outcome from this research is that *D. hafniense* is now poised as the only model, metal-reducing, Gram-positive, organism to which we have shown other Gram-positive bacteria can effectively be compared (Chapter 5). Studies with *M. thermoacetica* show how research on *D. hafniense* can inform us about the potential biology in related bacterial species. This investigation also provides a necessary reference for interpretation of systems microbiology. Future research should continue to delve deeper into the metal-reducing abilities of *D. hafniense*, such as by discovering the proteins directly involved when it performs metal-reduction, and test its effectiveness *in situ* during metal reduction bioremediation. By studying *D. hafniense* and its interactions with metals, *D. hafniense* is poised to become the first Gram-positive dissimilatory metal-reducing model organism.

Appendix A

Biofilm-Forming Capacities of *Desulfitobacterium hafniense* DCB-2

Desulfitobacterium hafniense DCB-2 was tested for biofilm formation under conditions of fermentation (modified DCB-1 medium) and respiration (ferric citrate medium) using two different surfaces (Dupont and Siran beads) (Löffler 1996, Lovley 1988, and Chapters 2 and 4). Dupont beads are plastic coated activated carbon spheres ranging from 3 to 5 mm in diameter (Figure A.1A). Siran beads are extremely rough and pitted silica glass beads ranging from 2 to 3 mm in diameter (Figure A.1B and C). The beads were laid 2.5 cm deep with a 1 cm cover of medium in free-standing serum tubes. The medium was replaced every 2 to 3 days using a 22 G spinal needle to avoid disturbing bacteria attaching to the beads and forming biofilms.

D. hafniense growth and biofilm formation were observed under all conditions throughout 25 medium transfers (Figure A.2). The biofilm settled in amongst the beads unless disturbed, although the biofilm consistency and abundance varied for each condition (Figure A.2A and B). Ferric citrate medium demonstrated characteristic reduction coloration (burnt orange to brown to olive to yellow) with cultures on both Dupont and Siran beads (Figure A.2C and D). The largest accumulated biofilm occurred in ferric citrate medium on Siran beads (Fig A.2E). Cell morphology varied similarly depending on media and substrata. Bacteria were easily retrieved in quantity from

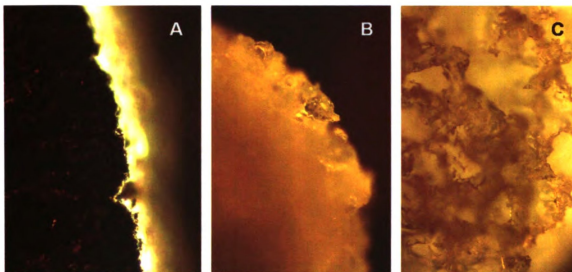


Figure A.1. Bright field microscopic images (100 \times magnification) of beads. (A) Cross-section of a Dupont activated carbon bead showing the thin white plastic surface coating. (B). Side view of a Siran glass bead illustrating its rough surface. (C) Top view of a Siran glass bead showing its deeply pitted surface.

Dupont beads. These pelagic bacteria were clustered in streptobacilli formations not typical of *D. hafniense* during growth fermenting pyruvate. Pelagic bacteria were not readily recovered from the Siran beads. However, those recovered were in streptobacilli clusters or isolated. Removal of *D. hafniense* biofilm from the highly pitted Siran beads was significantly more difficult than retrieving biofilm samples from the smoother Dupont beads. This difficult retrieval may have caused some bacteria to break out of clusters to appear as isolates. The Dupont beads may not have provided as intricate a physical support as the Siran beads. Furthermore, ferric citrate grown *D. hafniense* were significantly smaller than normal pyruvate fermenting cells despite pelagic or sessile growth. Scanning electron microscopy has confirmed the streptobacilli shape of *D. hafniense* cells grown in ferric citrate and noted their smaller size



Figure A.2. Biofilm cultures with Dupont and Siran beads after 25 medium transfers. (A) Undisturbed (left) and shaken (right) cultures on Siran beads in DCB-1 with pyruvate. (B). Undisturbed (left) and shaken (right) cultures on Dupont beads in DCB-1 with pyruvate. (C) Culture grown on Dupont beads prior to medium transfer (left) and following transfer (right) of fresh ferric citrate medium. (D) Culture grown on Siran beads prior to medium transfer (left) and following transfer of fresh ferric citrate medium. (E) Above view of the biofilm produced by a culture grown on Siran beads in ferric citrate medium.

(Chapter 3). Energy-dispersive spectroscopy (EDS) has shown that iron appears to be sequestered in the extracellular polymeric substance and not the *D. hafniense* cell during its reduction (Chapter 3).

These results conclusively show *D. hafniense* is able to produce biofilm, which is more profuse under conditions of Fe(III) reduction as the sole terminal electron acceptor. Implications for enhanced bioremediation by bacteria due to biofilm formation have been proposed (Peacock 2004 and Singh 2006). As *D. hafniense* is a dehalogenator, metal reducer, and acetogen, the effect on augmenting the bioremediation of toxic compounds could be substantial. Further research on *D. hafniense* should investigate changes in its gene expression and the efficiency of metal reduction or dehalogenation during growth as a biofilm.

REFERENCES

- Löffler, F. E., R. A. Sanford, and J. M. Tiedje.** 1996. Initial characterization of a reductive dehalogenase from *Desulfitobacterium chlororespirans* Co23. Appl. Environ. Microbiol. 62:4982-4985.
- Lovley, D. R. and E. J. P. Phillips.** 1988. Novel mode of microbial energy metabolism: organic carbon oxidation coupled to dissimilatory reduction of iron or manganese. Appl. Environ. Microbiol. 54:1472-1480.
- Peacock, A. D., Y-J. Chang, J. D. Istok, L. Krumholz, R. Geyer, B. Kinsall, D. Watson, K. L. Sublette, and D. C. White.** 2004. Utilization of microbial biofilms as monitors of bioremediation. Micro. Ecol. 47:284-292.
- Singh, R., D. Paul, and R. K. Jain.** 2006. Biofilms: implications in bioremediation. Trends Microbiol. 14:389-397.

Appendix B

Minimal Medium and Culturing Methods for *Desulfitobacterium hafniense* DCB-2

Here, the two minimal media used for culturing *Desulfitobacterium hafniense* DCB-2 are provided along with descriptions of materials used and how to grow cultures. All media are designed for making 1 l, but can be adapted for more. The first medium, a modified DCB-1 medium was used with pyruvate in my studies to provide fermentative growth conditions (Löffler 1996, Chapter 4). The second medium, carbonate-buffered freshwater medium, does not mimic freshwater but is modified from a medium described by Lovley (1988). This medium was used with lactate and an additional electron acceptor (i.e. metals or nitrate) for studies during anaerobic respiration. Culturing methods, described here, can also be adapted for use with other anaerobic organisms. While these methods describe the use of butyl rubber stoppers, alternate culturing conditions (e.g. dechlorination studies) may require the use of different stoppers (e.g. Teflon-coated rubber stoppers) to avoid possible absorption of chemicals with the stoppers. Balch (1979) provides further information for Hungate system construction and assistance with modifying these methods for other anaerobic organisms (i.e. methanogens).

Modified DCB-1 medium (DCB-1)

(modified from Löffler 1996)

MilliQ H ₂ O	964.6 ml
10% NaCl	10 ml
10% MgCl ₂	5 ml
10% KH ₂ PO ₄	2 ml
10% KCl	3 ml
10% NH ₄ Cl	3 ml
10% CaCl ₂	150 µl
SeWo (Selenite tungstate solution)	1 ml
trace elements (SL-10)	1 ml
0.1 % resazurin	250 µl
1 M HEPES, pH 7.0	10 ml

Directions for DCB-1 medium:

1. Boil all ingredients under reflux for 10 min with 95:5 of N₂:CO₂ (hence forth referred to as under gas). Be certain to have boiling chips in your media. Two sterilized mini stir bars work fine. A water bath may not be necessary during boiling under reflux; heat may be directly applied to most round bottom flasks.
2. Stand at room temperature (10-30 min) to cool glass prior to putting in ice bath to bring to room temperature (~15 min) all while under gas.
3. Stir slowly under gas while adding 0.16 g cysteine or (0.06 g cysteine and 0.12 g Na₂S)
4. Continue stirring slowly under gas while adding 2.52 g NaHCO₃
5. Measure pH (~7.15). This is easiest with a portable pH meter. Adjust pH with ~3 pellets of NaOH if necessary.
6. Under gas dispense media and cap bottles (e.g. with butyl rubber stoppers and

aluminum tear-off seals for serum bottles).

7. Autoclave DCB-1 media for 40 min on dry/ fast exhaust for serum bottles.

*A liquid/ slow exhaust may be preferred for bottle integrity of containers over 100 ml.

8. Store at room temperature.

SeWo (selenite tungstate solution)

(from Tschech 1984)

NaOH	0.5 g
Na ₂ SeO ₃ × 5 H ₂ O	3 mg
Na ₂ WO ₄ × 2 H ₂ O	4 mg
MilliQ H ₂ O	1 liter

Final pH of the solution should be 6.9 - 7.1.

Store at room temperature.

Trace element solution SL-10:

(from Widdel 1983)

HCl (25%; 7.7 M)	10.00 ml
FeCl ₂ × 4 H ₂ O	1.50 g
ZnCl ₂	70.00 mg
MnCl ₂ × 4 H ₂ O	100.00 mg
H ₃ BO ₃	6.00 mg
CoCl ₂ × 6 H ₂ O	190.00 mg
CuCl ₂ × 2 H ₂ O	2.00 mg
NiCl ₂ × 6 H ₂ O	24.00 mg
Na ₂ MoO ₄ × 2 H ₂ O	36.00 mg
MilliQ H ₂ O	990.00 ml

First dissolve FeCl₂ in the HCl, and dilute in water. Add and dissolve the other salts in order. Finally, bring volume up to 1 l. Store at 4°C away from light.

Carbonate-Buffered Freshwater medium (CBF)

(modified from Lovley 1988)

MilliQ H ₂ O	981.5 ml
10% NH ₄ Cl (or 0.25 g)	2.5 ml
10% KCl (or 0.1 g)	1 ml
Mineral Mix	10 ml
NaH ₂ PO ₄ × H ₂ O	0.6 g
NaHCO ₃	2.5 g
Resazurin (depending on use)	

Directions for CBF medium:

1. Bring water to boil using reflux under 80:20 of N₂:CO₂ (hence forth referred to as gas).
2. Allow water to boil 10 min per liter of medium made. Cool water under gas.
3. Once water is at room temperature, add NH₄Cl, KCl, and the Mineral Mix.
4. Dissolve the NaH₂PO₄ × H₂O in about 3 ml of MilliQ water. Filter this and add the dissolved NaH₂PO₄ × H₂O to the medium.
5. To achieve the optimum pH of 6.8 - 7.0, add about 5 ml of MilliQ water to the NaHCO₃ and begin to dissolve it. While monitoring the pH of the medium, add the NaHCO₃ (filtering it first) until the optimum pH is maintained.
6. Under gas dispense media and cap bottles (e.g. with butyl rubber stoppers and aluminum tear-off seals for serum bottles).
7. Autoclave the medium for at least 20 min on dry/ fast exhaust for serum bottles.
8. Store at room temperature.

*For 50 mM ferric citrate medium, ferric citrate is first dissolved in the water. This is

then boiled under reflux with all components except $\text{NaH}_2\text{PO}_4 \times \text{H}_2\text{O}$ and NaHCO_3 , which are slowly added to cooled medium to adjust the pH. (One may also need to use 10 N NaOH to achieve optimum pH.) Care must be taken to not exceed the optimum pH as Fe can fall out of solution.

Mineral Mix for CBF medium

(from Lovley 1988)

Nitrilotriacetic acid	1.5 g
$\text{FeSO}_4 \times 7 \text{H}_2\text{O}$	100 mg
ZnCl_2	130 mg
$\text{MnSO}_4 \times \text{H}_2\text{O}$	500 mg
H_3BO_3	10 mg
$\text{CoCl}_2 \times 6 \text{H}_2\text{O}$	100 mg
$\text{CuSO}_4 \times 5 \text{H}_2\text{O}$	10 mg
$\text{NiCl}_2 \times 6 \text{H}_2\text{O}$	24 mg
Na_2MoO_4	25 mg
$\text{MgSO}_4 \times 7 \text{H}_2\text{O}$	3 g
NaCl	1 g
$\text{CaCl}_2 \times 2 \text{H}_2\text{O}$	100 mg
$\text{AlK}(\text{SO}_4)_2 \times 12 \text{H}_2\text{O}$	10 mg
$\text{Na}_2\text{WO}_4 \times 2 \text{H}_2\text{O}$	25 mg
MilliQ H_2O	990 ml

Nitrilotriacetic acid (NTA) must be added and dissolved first to 900 ml MilliQ water. As NTA can be used as a carbon source by some microbes, it can be substituted with HCl. When using HCl as a substitute for NTA, use only enough to keep the metals dissolved. Add the ingredients in the order they are listed above. Do not add the next ingredient until the previous ingredient has fully dissolved. Bring the final volume to 1 l with

MilliQ water after all ingredients have been added. Store at 4°C away from light.

Wolin vitamin solution: (1000×)

(from Wolin 1963)

Biotin	2 mg
Folic acid	2 mg
Pyridoxine-HCl	10 mg
Thiamine-HCl × 2 H ₂ O	5 mg
Riboflavin	5 mg
Nicotinic acid	5 mg
D-Ca-pantothenate	5 mg
Vitamin B ₁₂	0.1 mg
p-Aminobenzoic acid	5 mg
Lipoic acid	5 mg
MilliQ H ₂ O	1 liter

Add all ingredients in order to 900 ml of MilliQ water. Wait for the previous ingredient to dissolve prior to adding the next ingredient. Once all ingredients have dissolved, bring the final volume to 1 l. Dispense the 1 l of 1000× vitamin solution into tubes and store at -20°C away from light. This maintains vitamin integrity and allows you to unthaw only as necessary.

Prior to use, dilute the 1000× vitamin solution 1/10, filter it through a 0.22 µm filter, and then gas it (100× final concentration). Vitamins should not be autoclaved. Store at 4°C away from light.

Carbon sources for *Desulfitobacterium hafniense*

The stock carbon source for DCB-1 medium is 2 M sodium pyruvate (pyruvate), and for CBF medium it is 2 M sodium lactate (lactate). These carbon source stocks should be filtered through a 0.22 µm filter, and then gassed out to become anaerobic (described below). The final concentration desired for carbon stocks is 100× (2 M) for easy dispensing to 20 mM in culture bottles. The carbon stocks are not autoclaved. Store carbon stocks at 4°C. Note: growth in DCB-1 medium with pyruvate is fermentative, while respiration conditions are provided in CBF medium with lactate.

Gassing out items that can not be autoclaved.

(i.e. vitamins and carbon sources).

1. Filter sterilize the liquid (i.e. dissolved nutrient) through a 0.22 µm filter into a clean sterile serum bottle.
2. Gas the solution at least 10 min for 100 ml of liquid at 95:5 of N₂:CO₂ (or the desired gas ratio) being sure that the gas needle is fully submerged and bubbling through the liquid at all times. The length of time will vary on the flow rate of your gas; however, to alleviate this problem I typically gas 15-20 min per 100 ml. The gas is considered sterilized as it passes through the hot copper catalyst of the Hungate gas station.
3. Cap the bottles (butyl rubber stoppers and crimp closed with aluminum seals), and these newly anaerobic liquids are ready for use.

Making anaerobic gas bottles

Bottles containing only sterile anaerobic gas are made for transfers of any anaerobic material not performed in an anaerobic chamber. (For use see below “Culturing *D. hafniense* in DCB-1 Medium”).

1. Put clean gas canulas/ needles running gas at 95:5 of N₂:CO₂ (or desired gas ratio) into a clean, sterile serum bottle to be capped.
2. Allow gas to circulate about 3 min.
3. Holding the butyl rubber stopper over the top and canula try to create a back pressure of gas in the bottle for about 30 sec with the canula about half an inch remaining in the bottle.
4. In one swift move, plunge in the stopper while removing the canula (maintain gas pressure).
5. Crimp on aluminum seal and autoclave the bottles 40 min on dry/ fast exhaust and use.
6. Store at room temperature.
7. Dispose of bottle after about fifteen 1 ml syringe withdrawals of gas from the bottle or until it feels difficult to draw gas from the bottle (whichever comes first).

Feeding *Desulfitobacterium hafniense*

As *Desulfitobacterium hafniense* is a spore-former, old cultures may be revitalized by adding vitamins and a source of carbon. Cultures at 37°C may also be maintained in a state of constant growth by feeding once every 5-7 days with a carbon source and once a month with vitamins. To do this, simply follow steps 2 through 16 (skipping step 15) in “Culturing *Desulfitobacterium hafniense* in DCB-1 medium” (below); however, instead of using fresh DCB-1 medium, you will add pyruvate and vitamins to your culture you wish to feed.

Culturing *Desulfitobacterium hafniense* in DCB-1 medium

You will need the following: DCB-1 medium, 2 M pyruvate, 100× vitamins, anaerobic gas, and stock culture (your inoculum). These should all be anaerobic prior to starting. Other materials include (per 100 ml culturing bottle): three 1 ml syringes, three 22 G needles, ethanol, flame source, and weighing spatula (to open aluminum crimp tops) (Figure B.1A).

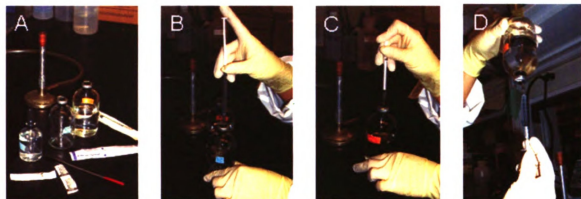


Figure B.1. Anaerobic inoculation process. (A) The materials necessary for culturing into sterile medium. Only DCB-1 medium is pictured with an anaerobic gas bottle and a bottle dropper of ethanol. The vitamin and carbon source stock bottles are not shown. (B) The position of the hand just prior to removal of the needle from the anaerobic gas bottle is shown. The index finger is on the syringe plunger ready to expel gas to prevent oxygen from coming in the needle. (C) The expelling of the needle contents into a serum bottle. (D) The mixing and measuring of the liquid from a serum bottle for subsequent transfer. The serum bottle is held upside down to obtain the liquid.

Assume inoculating a 100 ml bottle of DCB-1 medium.

1. To inoculate a sealed serum bottle of DCB-1 medium, tear back a portion of each seal using the perforated circular top furthest from the tear off edge to expose the butyl rubber

stopper. This is where you will enter the bottle with your needle. (I use a weighing spatula to open them.)

2. Put three to four drops of ethanol on the tops of all bottles to be involved in the inoculation process, and flame the ethanol off to sterilize the tops. For our purposes we will start with anaerobic gas, 2 M pyruvate and DCB-1 medium.

3. Repeat step 2 two times for a total of 3 ethanol burnings on each bottle top.

4. During your last time of flaming the tops (tops should be hot by now), unwrap the syringe barrel and quickly attach the needle (touching no part of the barrel and fitting not the needle). (If in doubt about having touched the needle at all or syringe barrel junction then discard the unit into a sharps container. Do not reuse it.)

5. Just as ethanol flames are extinguished, plunge needle into anaerobic gas bottle and take up gas (Fig B.1B). (Anaerobic gas is always the first bottle in order to exchange the oxygen from the syringe barrel.)

6. Remove the needle and slowly void the gas into the air while plunging into the next bottle's stopper (in this case, 2 M pyruvate) (Figure B.1B and C).

7. Expel all gas, flip the bottle over and pull out pyruvate while shaking bottle to mix contents (Fig B.1D).

8. Flick the syringe barrel to get all bubbles to go to the needle and expel bubbles back into the pyruvate bottle.

9. Measure out 1ml of 2 M pyruvate (1/100 dilution).

10. Remove the needle from the pyruvate bottle (do not expel the liquid as you did the gas) and plunge the needle into the DCB-1 medium bottle's stopper. (Be sure the stopper is still hot or it should be reflamed before removing the needle from the pyruvate bottle.)

11. Expel the needle contents into the DCB-1 medium bottle and remove the needle (Figure B.1C).
12. Discard the used needle and syringe barrel into a sharps container.
13. Reflame the tops of all bottles used with ethanol.
14. Repeat step 2 through 13 using 100× vitamins instead of 2 M pyruvate (use same volumes) for a 1/100 dilution of the anaerobic vitamin stock.
15. Repeat step 2 through 13 using the stock culture (your inoculum) instead of 2 M pyruvate (use same volumes) for a 1/100 dilution of the stock culture.
16. Mix and incubate the newly inoculated culture (optimum growth at 37°C; slower growth at lower temperatures).

*Do not expect cell densities as high as to *Escherichia coli*.

**For CBF medium follow the same procedure substituting 2 M lactate for 2 M pyruvate. Additionally, a step 14a should be added, in which the electron acceptor (i.e. metals or nitrate) is added by repeating steps 2 through 13. Thus, a fourth needle and syringe barrel are needed.

***For CBF medium using ferric citrate as the electron acceptor no additional step 14a is required as the Fe is added during the process of making the CBF medium.



Figure B.2. Black butyl rubber stoppers with crimped aluminum seals on a specially designed 3-port 1 l flask. These 3-port flasks were used to hold maximally 500 ml anaerobically.

MATERIAL SOURCES

Source for black butyl rubber stoppers (13 × 20 mm): Geo-Microbial Technologies Inc., P.O. Box 132, East Main Street, Ochelata, OK 74051. Catalog# 1313.

Source for tear-off aluminum crimp top seals (20 mm): distributed by VWR. Catalog# 16171-851. Manufactured by Wheaton Science Products, 1501 N. 10th Street Millville, NJ 08332-2093. Catalog# 224193-01

REFERENCES

- Balch, W. E., G. E. Fox, L. J. Magrum, C. R. Woese, and R. S. Wolfe.** 1979. Methanogens: reevaluation of a unique biological group. *Microbiol. Rev.* 43:260-296.
- Löffler, F. E., R. A. Sanford, and J. M. Tiedje.** 1996. Initial characterization of a reductive dehalogenase from *Desulfotobacterium chlororespirans* Co23. *Appl. Environ. Microbiol.* 62:4982-4985.
- Lovley, D. R. and E. J. P. Phillips.** 1988. Novel mode of microbial energy metabolism: organic carbon oxidation coupled to dissimilatory reduction of iron or manganese. *Appl. Environ. Microbiol.* 54:1472-1480.
- Madsen, T. and D. Licht.** 1992. Isolation and characterization of an anaerobic chlorophenol-transforming bacterium. *Appl. Environ. Microbiol.* 58:2874-2878.
- Miller, T. L. and W. J. Wolin.** 1974. A serum bottle modification of the Hungate technique for cultivating obligate anaerobes. *Appl. Microbiol.* 27:985-987.
- Tschech, A., and N. Pfennig.** 1984. Growth yield increase linked to caffeate reduction in *Acetobacterium woodii*. *Arch. Microbiol.* 137:163-167.
- Widdel, F., G.-W. Kohrin, and F. Mayer F.** 1983. Studies on dissimilatory sulfate-reducing bacteria that decompose fatty acids. *Arch. Microbiol.* 134:286-294.
- Wolin, E. A., R. S. Wolfe, and M. J. Wolin.** 1963. Viologen dye inhibition of methane formation by *Methanobacillus omelianskii*. *J. Bacteriol.* 87:993-998.

Appendix C

Protocols for Selenium Vesicles Isolation from Se-Reducing Cultures of *Desulfitobacterium hafniense* DCB-2 with RNA and Protein Analyses

The development of selenium-filled vesicles by *Desulfitobacterium hafniense* DCB-2 was found during growth with selenate and selenite (Chapter 4). The following is a protocol developed to isolate the vesicles from the cells for further downstream analyses, such as RNA analyses or the identification of proteins in the vesicular membrane (also described below). Proteomics of cells (isolated from the Se vesicles) may also be desired in future work, and a protocol is described below.

Se vesicles isolation. *D. hafniense* cultures grown in 1 mM Se(VI) using strict anaerobic technique (gas mixture of N₂:CO₂ (95:5)) at 37°C in a modified DCB-1 medium with pyruvate and Wolin vitamins were spun 30 min at 12,000 g (Löffler 1996, Wolin 1963, Chapter 4). The pellet was resuspended in phosphate buffered saline (PBS) and sonicated with 1 sec pulses for 20 min with 120 W output (W-385 Ultrasonics Processor, Misonix, Farmingdale, NY). The sonicated material was layered onto a step gradient column consisting of 100% and 50% Percoll® layers spun for 6 min at 2,200 g. The Percoll® gradients were fractionated into 1 ml aliquots and spun for 10 min at 12,000 g. The pellet was then washed three times with PBS and spun for 10 min at 12,000 g to remove the Percoll®.

RNA isolation and protein preparation. Replicate pellets of purified Se vesicles were used for protein and RNA studies. RNA was extracted from the Se vesicles using the RNeasy kit (QIAGEN, Valencia, CA). For protein studies of the Se vesicles, the pellet was resuspended in PBS, beta-mercapto ethanol, and two fold loading buffer containing SDS following the ReadyPrep Protein Extraction Kit (Bio-Rad Laboratories Inc., Hercules, CA). Dissolution was achieved by heating to 90°C for 10 min. This was then spun at 12,000 g for 5 min with the upper lysate being loaded for SDS-PAGE.

Proteomic preparation and analysis. Proteomic analyses should be performed against positive control cells, which for our study were pyruvate-fermenting cells. Cells harvested via centrifugation (and following the vesicle isolation protocol above if desired) are broken using a French press. Soluble and membrane proteins are then run on separate 2-D SDS-PAGE gels for each condition. Spots are selected based on gel comparisons between the test (metal-exposed) condition and the positive control for MS-DS analysis. These spots are then excised, gel purified, and run on a Thermo-Finnigan LTQ-FT mass spectrometer (Thermo Scientific, Waltham, MA) to identify the proteins.

ACKNOWLEDGEMENTS

The assistance of Dr. Sang-Hoon Kim of Michigan State University was greatly appreciated in the development of these protocols.

REFERENCES

Löffler, F. E., R. A. Sanford, and J. M. Tiedje. 1996. Initial characterization of a reductive dehalogenase from *Desulfitobacterium chlororespirans* Co23. Appl. Environ. Microbiol. 62:4982-4985.

Wolin, E. A., R. S. Wolfe, and M. J. Wolin. 1963. Viologen dye inhibition of methane formation by *Methanobacillus omelianskii*. J. Bact. 87:993-998.

MICHIGAN STATE UNIVERSITY LIBRARIES



3 1293 03063 2586